Technical University of Denmark

NKS NordRisk II: Atlas of long-range atmospheric dispersion and deposition of radionuclides from selected risk sites in the Northern Hemisphere

Smith Korsholm, Ulrik; Astrup, Poul; Lauritzen, Bent; Havskov Sørensen, Jens

Publication date:
2011

Document Version
Publisher's PDF, also known as Version of record

Nordisk kernesikkerhedsforskning
Norrænar kjarnöryggisrannsóknir
Pohjoismainen ydinturvallisuustutkimus
Nordisk kjernesikkerhetsforskning
Nordisk kärnsäkerhetsforskning
Nordic nuclear safety research

NKS-242
ISBN 978-87-7893-314-0

NKS NordRisk II: Atlas of long-range atmospheric dispersion and deposition of radionuclides from selected risk sites in the Northern Hemisphere

Ulrik Smith Korsholm[1], Poul Astrup[2],
Bent Lauritzen[2] and Jens Havskov Sørensen[1]

[1]Danish Meteorological Institute, Denmark
[2]Risø DTU, Technical University of Denmark, Denmark

April 2011

Abstract

The present atlas has been developed within the NKS/NordRisk-II project "Nuclear risk from atmospheric dispersion in Northern Europe". The atlas describes risks from hypothetical long-range dispersion and deposition of radionuclides from 16 nuclear risk sites on the Northern Hemisphere. The atmospheric dispersion model calculations cover a period of 30 days following each release to ensure almost complete deposition of the dispersed material. The atlas contains maps showing the total deposition and time-integrated air concentration of Cs-137 and I-131 based on three years of meteorological data spanning the climate variability associated with the North Atlantic Oscillation, and corresponding time evolution of the ensemble mean atmospheric dispersion.

Key words

Risk assessment; long-range transport; radionuclide; pollutants; deposition

NKS-242
ISBN 978-87-7893-314-0

Electronic report, April 2011

The report can be obtained from
NKS Secretariat
P.O. Box 49
DK - 4000 Roskilde, Denmark

Phone +45 4677 4045
Fax +45 4677 4046
www.nks.org
e-mail nks@nks.org

Atlas of long-range atmospheric dispersion and deposition of radionuclides from selected risk sites in the Northern Hemisphere

NKS NordRisk II

Ulrik Smith Korsholm[1], Poul Astrup[2], Bent Lauritzen[2], Jens Havskov Sørensen[1]

April 7, 2011

[1]Danish Meteorological Institute, Denmark
[2]Risø DTU, Technical University of Denmark, Denmark

Introduction

The NKS NordRisk II project is a continuation of the NKS project NordRisk. The purpose of the first project was to develop an atlas describing risks from long-range atmospheric dispersion and deposition of radionuclides from selected nuclear risk sites in the Northern Hemisphere. While means for practical assessment of the risk due to long-range atmospheric transport from accidental releases of radionuclides was produced in the NordRisk project, one of the objectives of NordRisk II has been to extend the applicability of the atlas. This has been done by more than doubling the number of risk sites and considering more climate regimes. For each risk site annual simulations describing long-term long-range atmospheric transport and deposition of radionuclides have been performed. The base years were selected to represent various climate regimes relevant for the Nordic countries.

As in the first NordRisk atlas, the risk indicators for the extended atlas are time-integrated activity in air and total deposition fields. The atlas is intended as a practical tool for probabilistic risk assessment. In combination with source term estimates for a particular nuclear installation, the atlas can be used in emergency preparedness planning as well as for educational purposes. For an imminent release of radionuclides, the atlas may provide a first assessment of the possible range of the atmospheric transport of radioactive material. For continuous emissions of radionuclides or other contaminants from a risk site, the atlas directly provides the expected geographical scale of contamination. In addition, the time development of the ensemble (annual) mean fields from a single release site is shown, providing the expected timescales for the atmospheric transport.

Although the main emphasis has been on atmospheric transport of radioactive materials the analysis and atlas readily applies also to nonradioactive releases.

Source term and risk sites

Sixteen different release sites in the Northern Hemisphere have been selected for the atlas.

Table 1: Geographic coordinates in decimal degrees of the nuclear risk sites selected for the atlas, with abbreviations used in the text in parenthesis and corresponding plates with figures.

Risk site	**lon** (°E)	**lat** (°N)	**plate**
Balakovo (BAL)	47.37	51.92	1-3
Belojarsk (BEL)	61.32	56.85	4-6
Bilibino (BIL)	166.45	68.05	7-9
Borssele (BOR)	3.72	51.43	10-12
Chernobyl (CHE)	30.25	51.30	13-15
Dav. Bes.[1] (DAV)	-83.09	41.60	16-18
Dukovany (DUK)	16.13	49.08	19-21
Kanupp (KAN)	66.79	24.87	22-24
Kola (KOL)	32.75	67.75	25-27
Kosloduj (KOS)	23.63	43.75	28-30
Leningrad (LEN)	29.00	59.90	31-33
Nov. Zem.[2] (NOV)	54.50	72.50	34-36
Sav. River[3] (SAV)	-81.70	33.30	37-39
Sellafield (SEL)	-3.50	54.42	41-42
Sinpo (SIN)	128.22	40.00	43-45
Tricastin (TRI)	4.73	44.33	46-48

All sites are associated with major nuclear installations: Balakovo, Belojarsk, Bilibino, Kola, Leningrad and Novaya Zemlya in Russia, Borssele in the Netherlands, Chernobyl in Ukraine, Dukovany in the Czech Republic, Davis Besse and Savannah River in the USA, Kanupp in Pakistan, Kosloduj in Bulgaria, Sellafield in the United Kingdom, Sinpo in North Korea and Tricastin in France. The sites are selected to be representative of different climates and to represent both coastal and continental regions. In Table 1 and Figure 1, the location of the release sites are shown.

Releases of three main radionuclides are considered separately for each release site, caesium embedded in aerosols (^{137}Cs), iodine in aerosols (^{131}I) and iodine in the elementary gas phase ($^{131}I_{gas}$). These species have been chosen based on their relevance in nuclear accidental releases and their span in half life (Table 2). The assumed dispersion parameters, used in the modelling part, specific to the three releases, are listed in Table 2.

[1] Davis Besse
[2] Novaya Zemlya
[3] Savannah River

Figure 1: Geographical positions of the selected risk sites considered in NordRisk II. Abbreviations can be seen in Table 1. The top map displays sites in Asia and Europe, the middle map is a zoom over Europe and the bottom one displays sites in USA. The red crosses indicate a horizontal distance of 500 km on either side of two sites.

Table 2: Dispersion and deposition parameters of released radionuclides. The nuclides ^{137}Cs and ^{131}I are in aerosols while ^{131}I$_{gas}$ is in gas phase.

	^{137}**Cs**	^{131}**I**	^{131}**I**$_{gas}$
Half life (days)	1.1×10^4	8.07	8.07
Dry deposition speed (m s^{-1})	0.0015	0.0015	0.015
Particle diameter (μm)	0.3	0.3	0

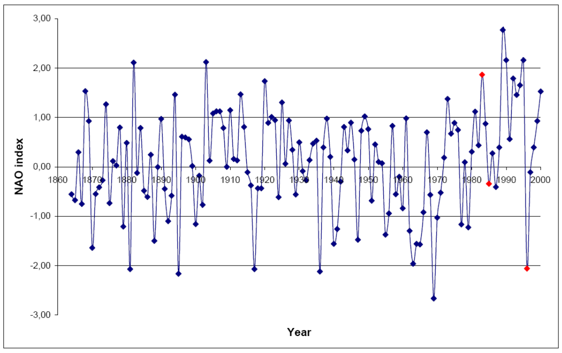

Figure 2: North Atlantic Oscillation (NAO) index for the years 1864-2000. The index measures the anomaly in sea-level pressure between the Icelandic low and Azore high-pressure systems. The base years 1983, 1985 and 1996 used in this study are marked with red dots.

For the aerosols, a typical diameter of 0.3 μm is assumed. In all cases, non-buoyant ground-level releases (cold releases) are assumed, and the radionuclides are released at a constant emission rate. The parameterization of wet deposition follows Baklanov and Sørensen (2001), and accordingly gases are not scavenged by precipitation.

Meteorological data

The meteorological fields used as input for the dispersion model simulations were taken from the European Centre for Medium-range Weather Forecasts (ECMWF) re-analysis project (ERA-40) database (http://www.ecmwf.int). A three hourly input frequency was used, the horizontal resolution of the re-analysed fields was 1.125° while 28 hybrid levels were used in the vertical.

On the annual time scales considered here, the meteorological conditions and thereby the dispersion characteristics may vary from year to year due to natural climate variability. It is, therefore, of importance to select base years which are representative of the possible changes. The main mode of variability over northern Europe is the North Atlantic Oscillation (NAO). The NAO affects the large-scale atmospheric flow from North America to northern Asia. A positive NAO index implies a stronger than usual subtropical high pressure and a deeper than normal Icelandic low. The increased pressure difference results in more and stronger winter storms crossing the Atlantic Ocean on a northerly track. This results in warm and wet winters in Europe, and in cold and dry winters in northern Canada and Greenland. The eastern USA experiences mild and wet winter conditions. A negative NAO index corresponds to a weak subtropical high and a weak Icelandic low. The reduced pressure gradient results in fewer and weaker winter storms crossing on a west-east pathway. They bring moist air into the Mediterranean and cold air to northern Europe. The North American east coast experiences outbreaks of cold air and hence snowy weather conditions. Greenland, however, will have higher winter temperatures. The NAO index varies from year to year, but exhibits a tendency to remain in one phase for intervals lasting several years (Figure 2). The years 1983, 1985 and 1996 were chosen for the simulations because they represent a large positive, an almost neutral and a large negative NAO index, respectively.

Dispersion modelling

Long-range atmospheric dispersion calculations were performed with the comprehensive atmospheric dispersion model DERMA (Danish Emergency Response Model of the Atmosphere) (Sørensen (1998); Sørensen et al. (2007)). DERMA is a three-dimensional Lagrangian stochastic puff-particle model capable of simulating plume dispersion at ranges from about 20 km and up to the global scale (Sørensen et al. (1998)). It is in use operationally in Denmark for emergency preparedness (Sørensen et al. (2000, 2001); Hoe et al. (2002); Mikkelsen et al. (2003)), and it is exercised and maintained within the EU ensemble modelling activities (Galmarini et al. (2004a,b)). DERMA has also been used for probabilistic risk assessment, generating yearly average concentration and deposition fields (Baklanov et al. (2003); Mahura et al. (2003); Lauritzen et al. (2005); Mahura et al. (2005a,b); Lauritzen et al. (2006); Baklanov et al. (2007a); Lauritzen et al. (2007)). Methodological aspects of probabilistic long-term modelling using DERMA are described by Baklanov et al. (2006, 2007a). For the present calculations the integration domain is taken as the Northern Hemisphere. During the DERMA simulations 28 levels are used in the vertical. A batch of puffs is released every 15 minutes and the atmospheric dispersion and deposition of each puff is calculated for a period of 30 days following the release. The deposition comprises both dry and wet deposition. The results of the modelling activities are evaluated on the same grid as used for the meteorological data. Based on the 1983, 1985 and 1996 meteorological data, daily and yearly averages of time-integrated air concentration and deposition density fields have been derived.

Ensemble mean dispersion

Long-range atmospheric dispersion and deposition comprise a deterministic element as well as stochastic properties. The long-term ensemble mean dispersion and deposition can be interpreted as the result of a deterministic flow of a one-particle density, while the air concentration and deposition fields resulting from a short-term release display stochastic fluctuations around the ensemble mean value (Lauritzen et al. (2006); Baklanov et al. (2007a)).

The annual averages of the radionuclide time-integrated air concentration and deposition for each of the three years considered are shown in Plates 1–48. These long-term averages constitute an approximation to the ensemble mean values. Total deposition (dry plus wet) and time-integrated concentration in ground-level air have been calculated following a unit release of ^{137}Cs, ^{131}I, and $^{131}I_{gas}$, respectively. The figures indicate that the probabilistic properties of dispersion and deposition is fairly isotropic in space and not significantly affected by the NAO on the annual time scales considered here.

In Figure 7, the total deposition following a unit release from the Leningrad release site is shown as function of the distance from the release site (1983 data). In the figure, the scatter points show the results of the atmospheric dispersion calculations for each grid point on the Northern Hemisphere, while the inserted curves are the result of a non-linear regression to the scattered data (Lauritzen et al. (2006)). For both caesium and the two forms of iodine, a strong decrease of the deposition density with distance from the release site is observed, with caesium being deposited on average at somewhat larger distances from the release site than iodine.

Time development

While plates 1–48 provide the time-integrated concentration in air and total deposition of the radionuclides after a long integration time, it is important for emergency management also to predict the short-term development of the plume dispersion and deposition. In Figures 3–4 the root-mean-square distance from the release site is displayed as function of travel time for each of the release sites. Figures 5 and 6 display the time evolution of the total deposition and integrated concentration of ^{137}Cs 1, 2, 3, 7, 14 and 30 days after the release for the Leningrad release site (1983 only).

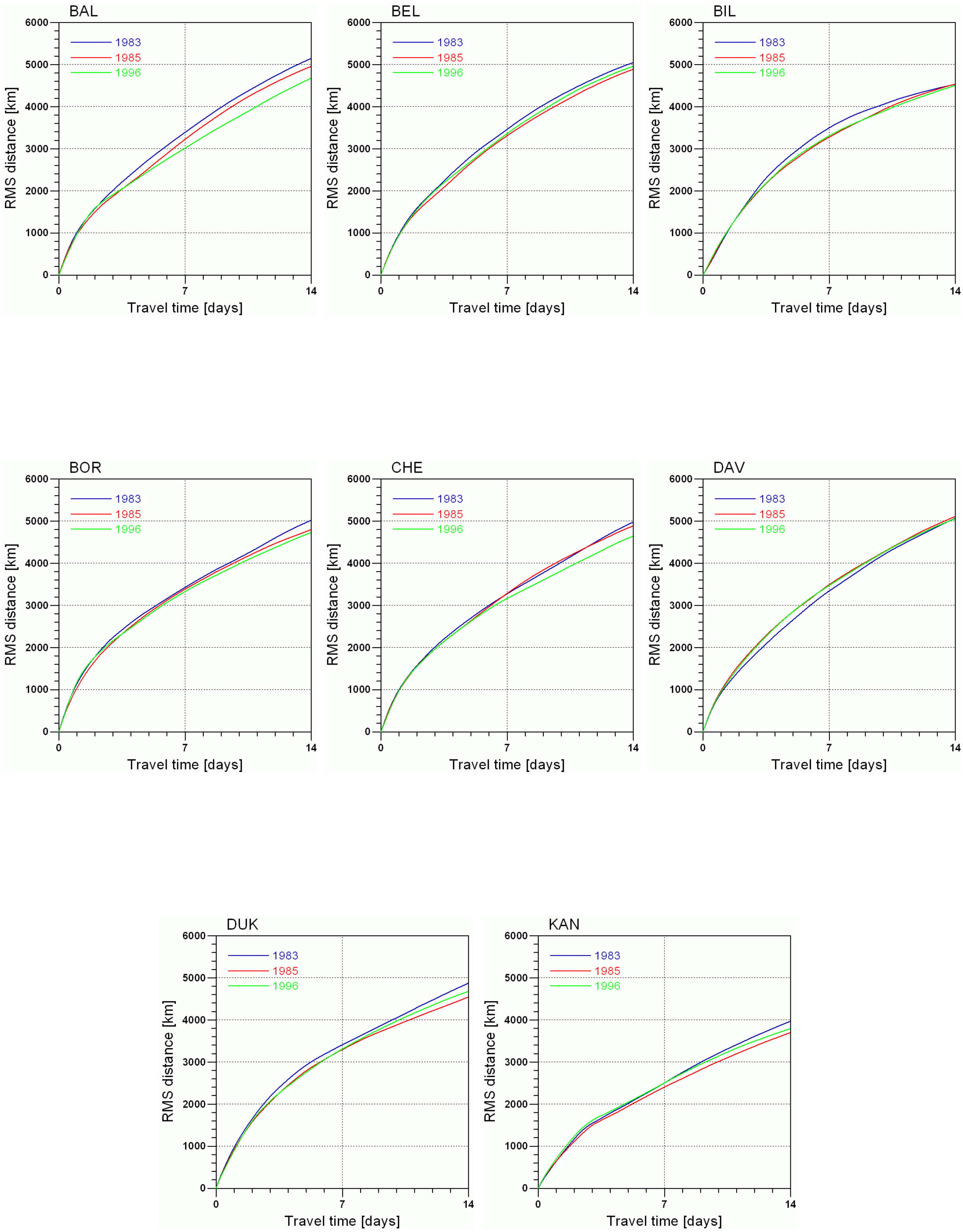

Figure 3: Root-mean-square distance from release sites, BAL, BEL, BIL, BOR, CHE, DAV, DUK and KAN (abbreviations refer to Table 1) to puff centres as function of travel time. Annual averages for 1983, 1985 and 1996.

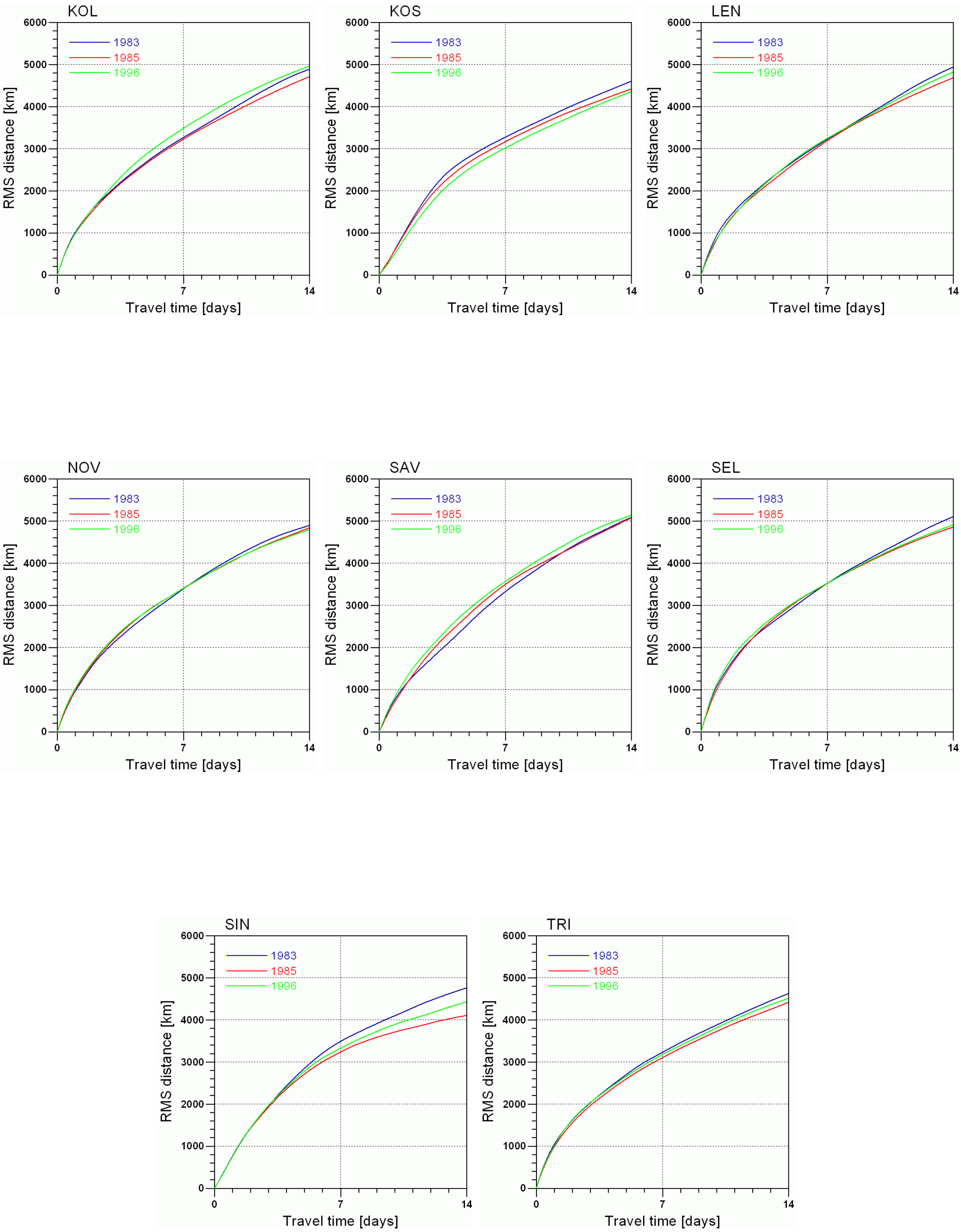

Figure 4: As in figure 3 but for release sites KOL, KOS, LEN, NOV, SAV, SEL, SIN and TRI (abbreviations refer to Table 1).

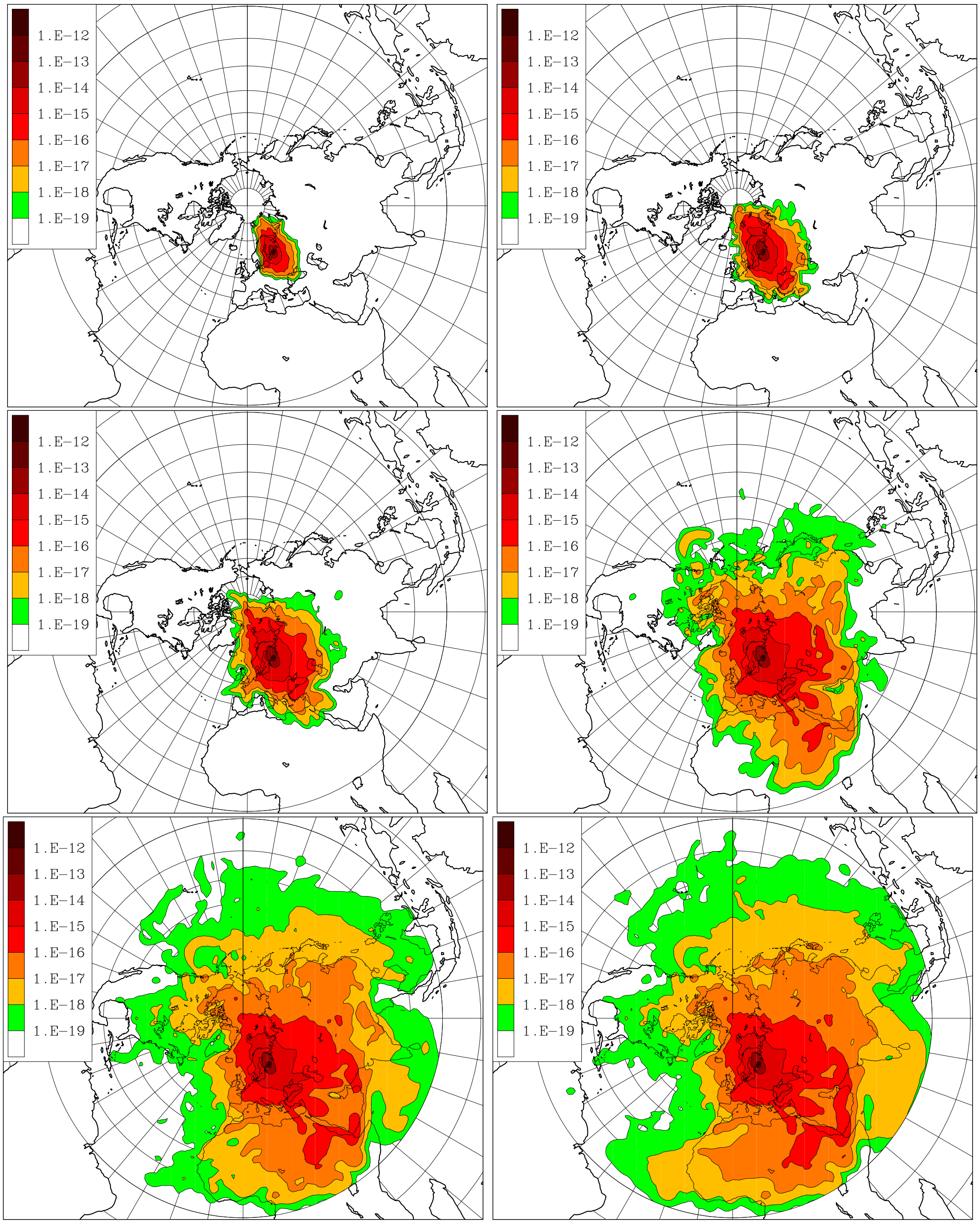

Figure 5: Time integrated surface concentration of ^{137}Cs (h m^{-3}) for the Leningrad release site with valid times 1, 2, 3, 7, 14 and 30 days, respectively, from upper left to lower right for the year 1983.

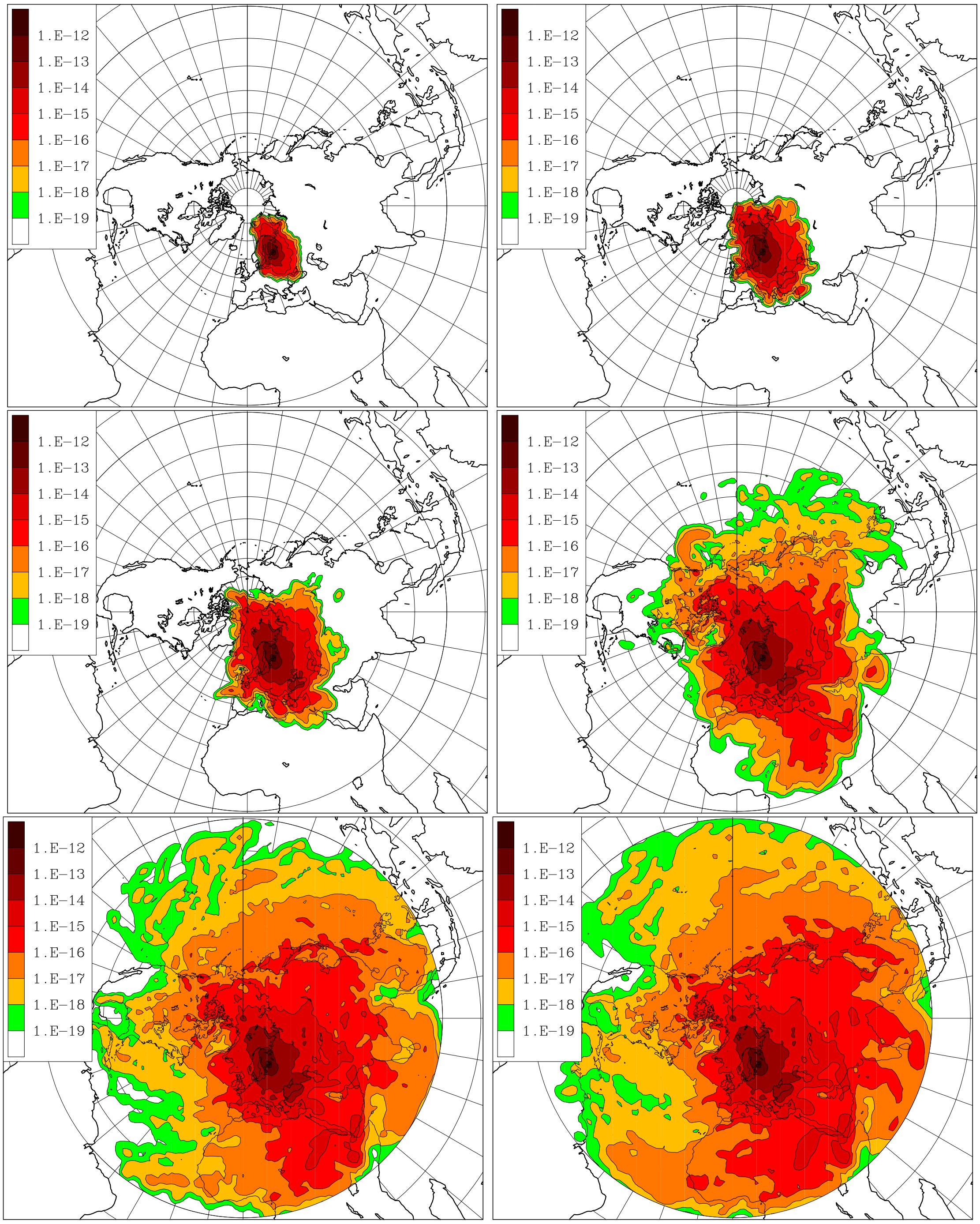

Figure 6: Total deposition of ^{137}Cs (m^{-2}) for the Leningrad release site with valid times 1, 2, 3, 7, 14 and 30 days, respectively, from upper left to lower right for the year 1983.

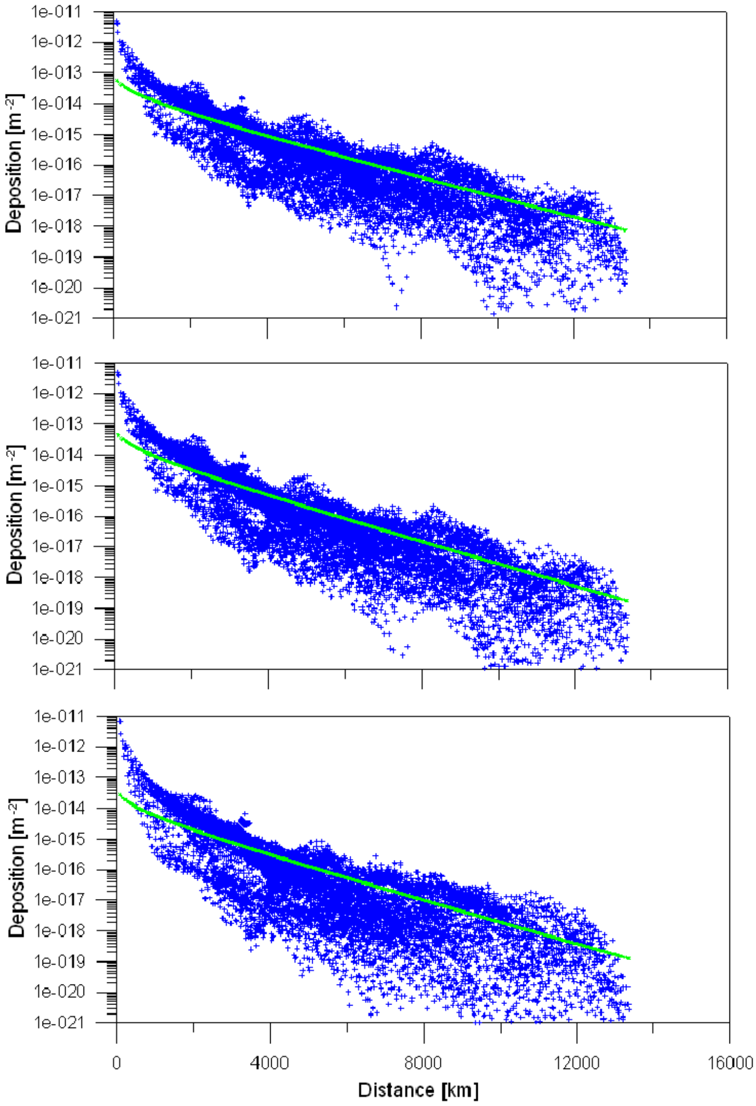

Figure 7: Annual mean deposition of ^{137}Cs (upper), ^{131}I (middle) and $^{131}I_{gas}$ (lower) as function of the distance from the release site (Leningrad, 1983 data). The averages (inserted curves) result from a non-linear regression to the deposition data.

Plate 1 Nuclear power plant: **Balakovo**; Nuclide: **Caesium-137 aerosol**

Total deposition (m^{-2}) **Time integrated conc. ($h\ m^{-3}$)**

1983

1985

1996

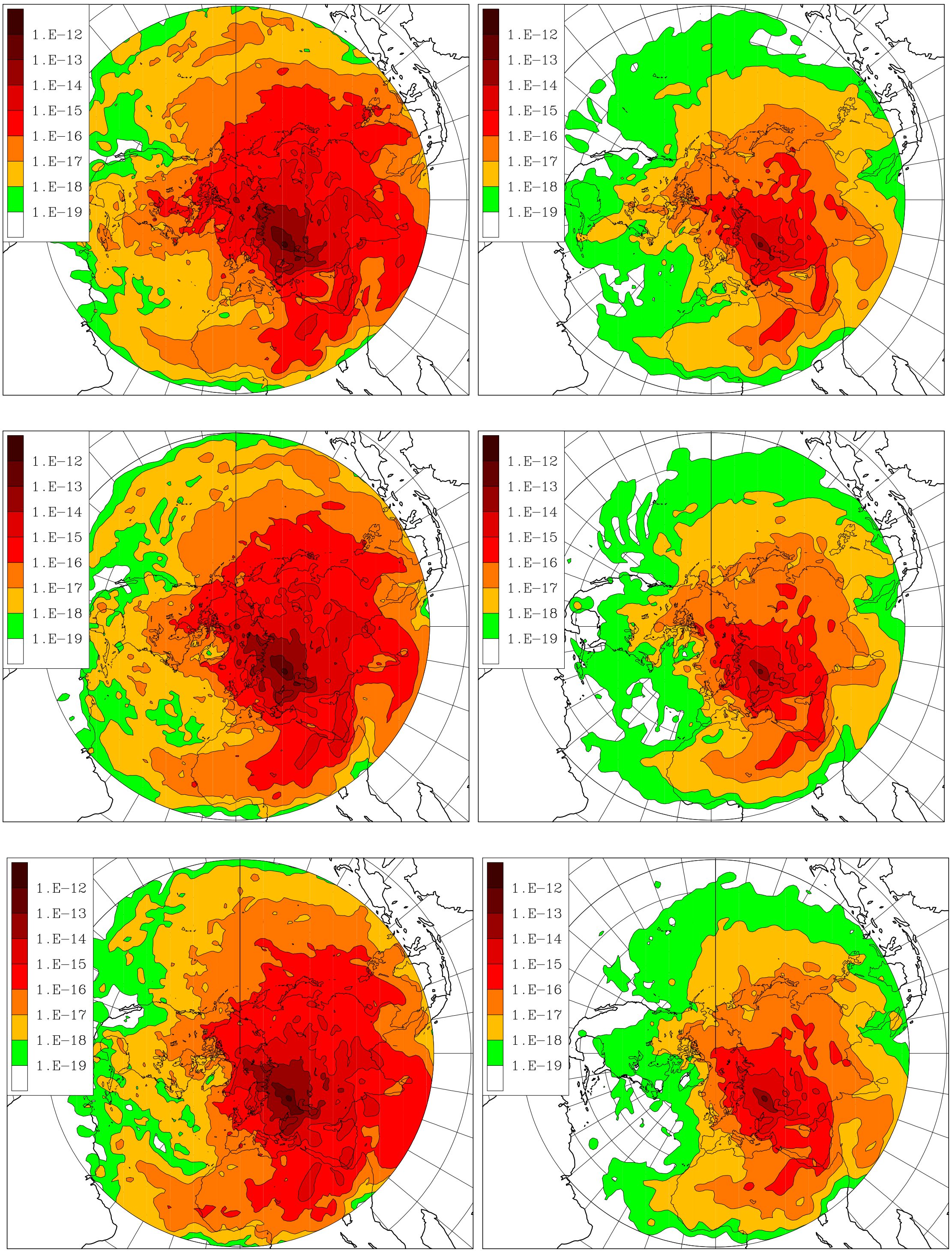

Plate 2 Nuclear power plant: **Balakovo**; Nuclide: **Iodine-131 gas**

Total deposition (m^{-2}) **Time integrated conc. ($h\ m^{-3}$)**

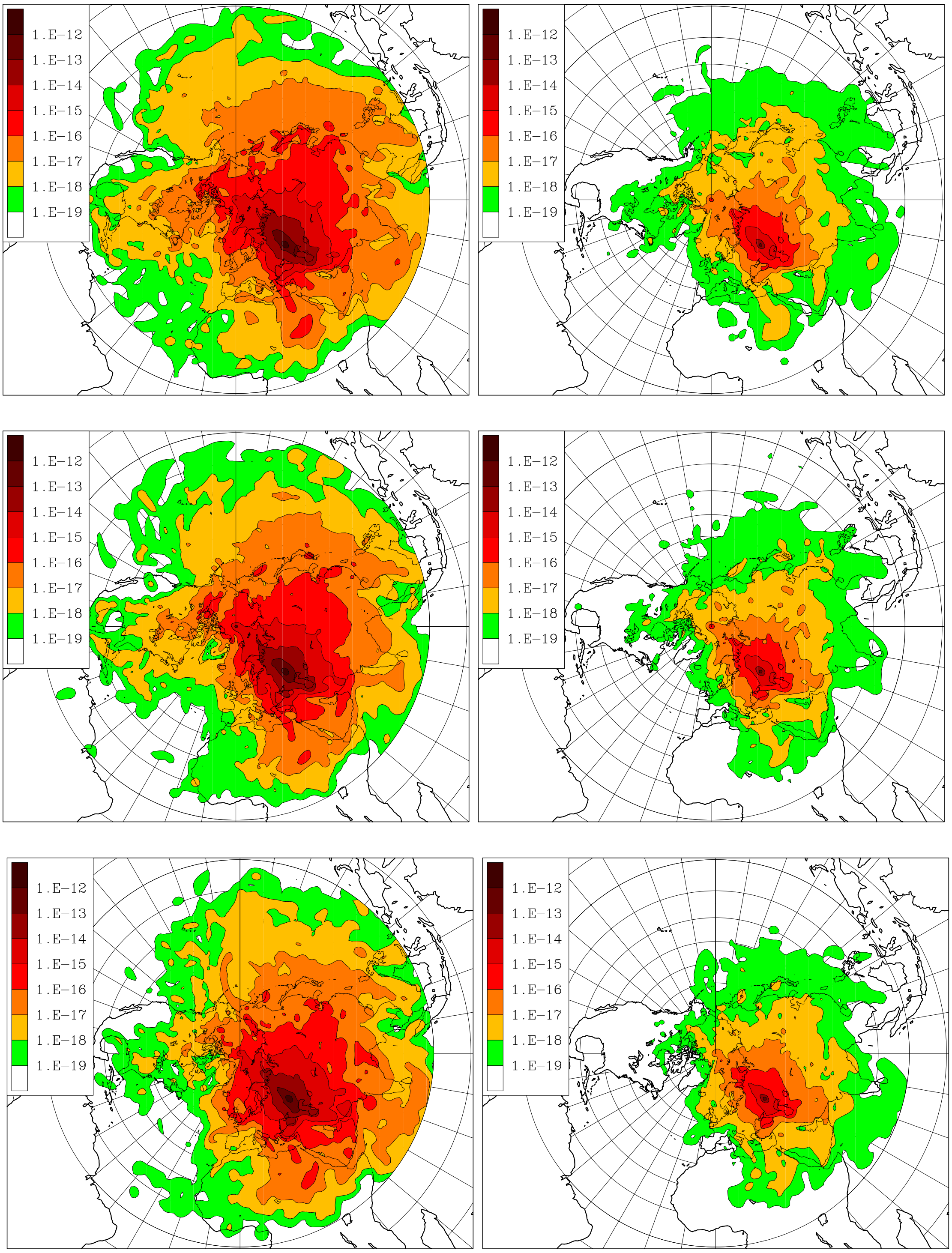

1983

1985

1996

Plate 3 Nuclear power plant: **Balakovo**; Nuclide: **Iodine-131 aerosol**

Total deposition (m^{-2}) **Time integrated conc. ($h\ m^{-3}$)**

1983

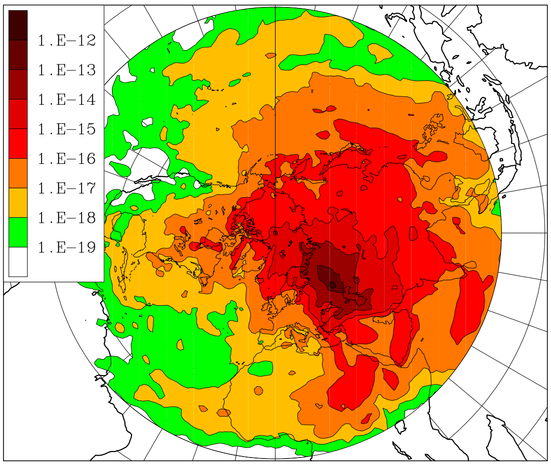

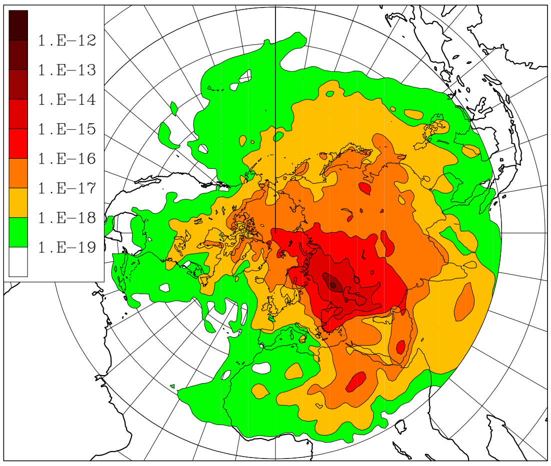

1985

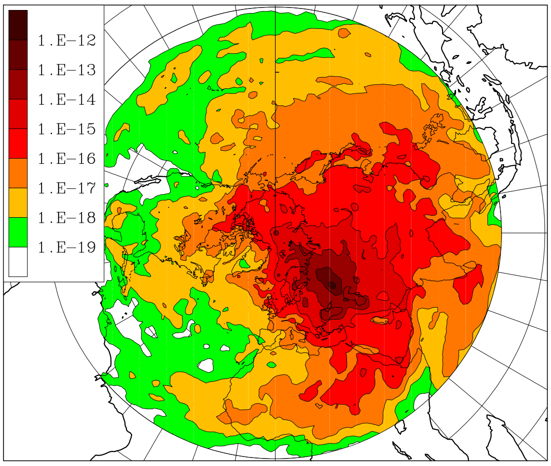

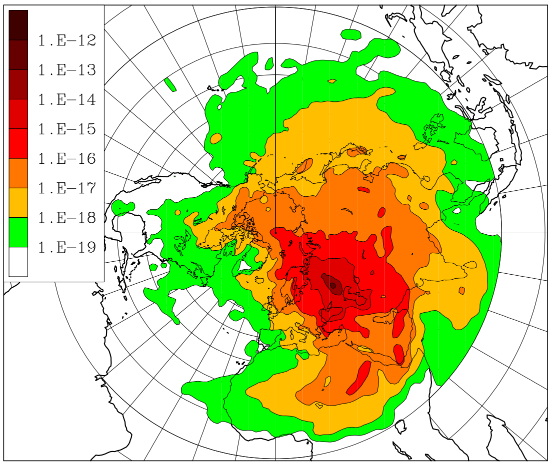

1996

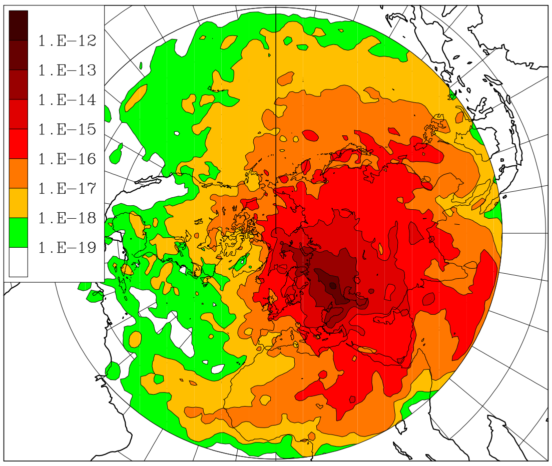

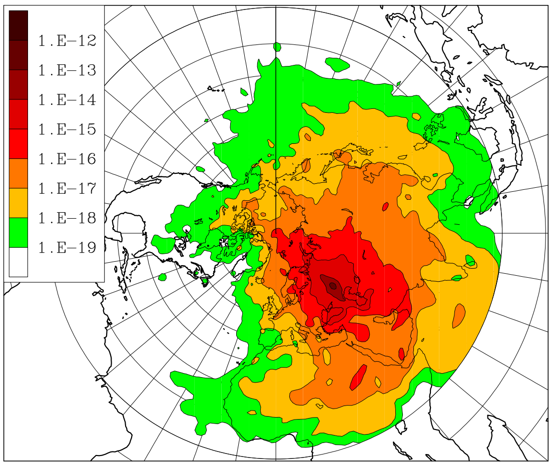

Plate 4 Nuclear power plant: **Belojarsk**; Nuclide: **Caesium-137 aerosol**

Total deposition (m^{-2}) **Time integrated conc. ($h\ m^{-3}$)**

1983

1985

1996

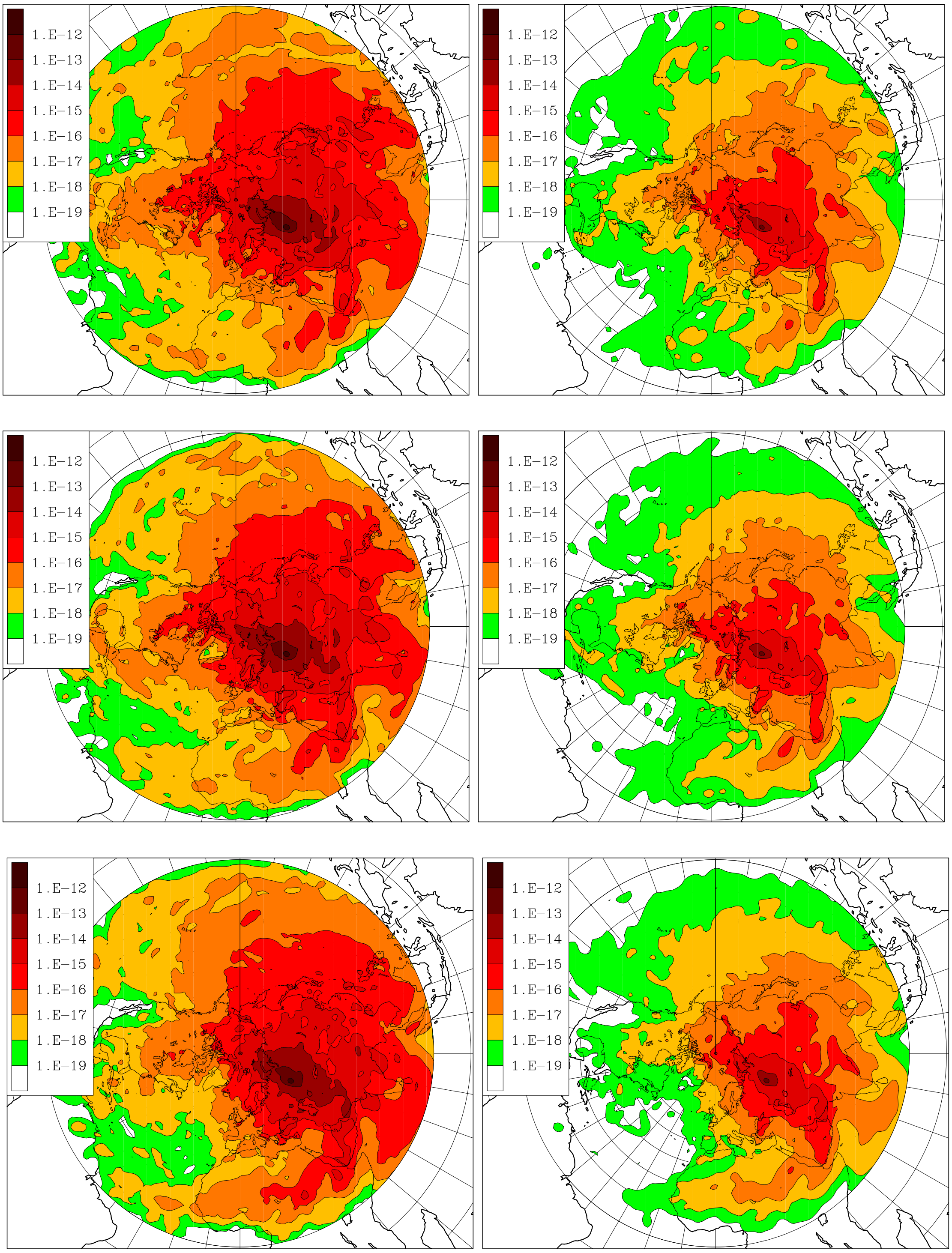

Plate 5 Nuclear power plant: **Belojarsk**; Nuclide: **Iodine-131 gas**

Total deposition (m^{-2}) **Time integrated conc. ($h\ m^{-3}$)**

1983

1985

1996

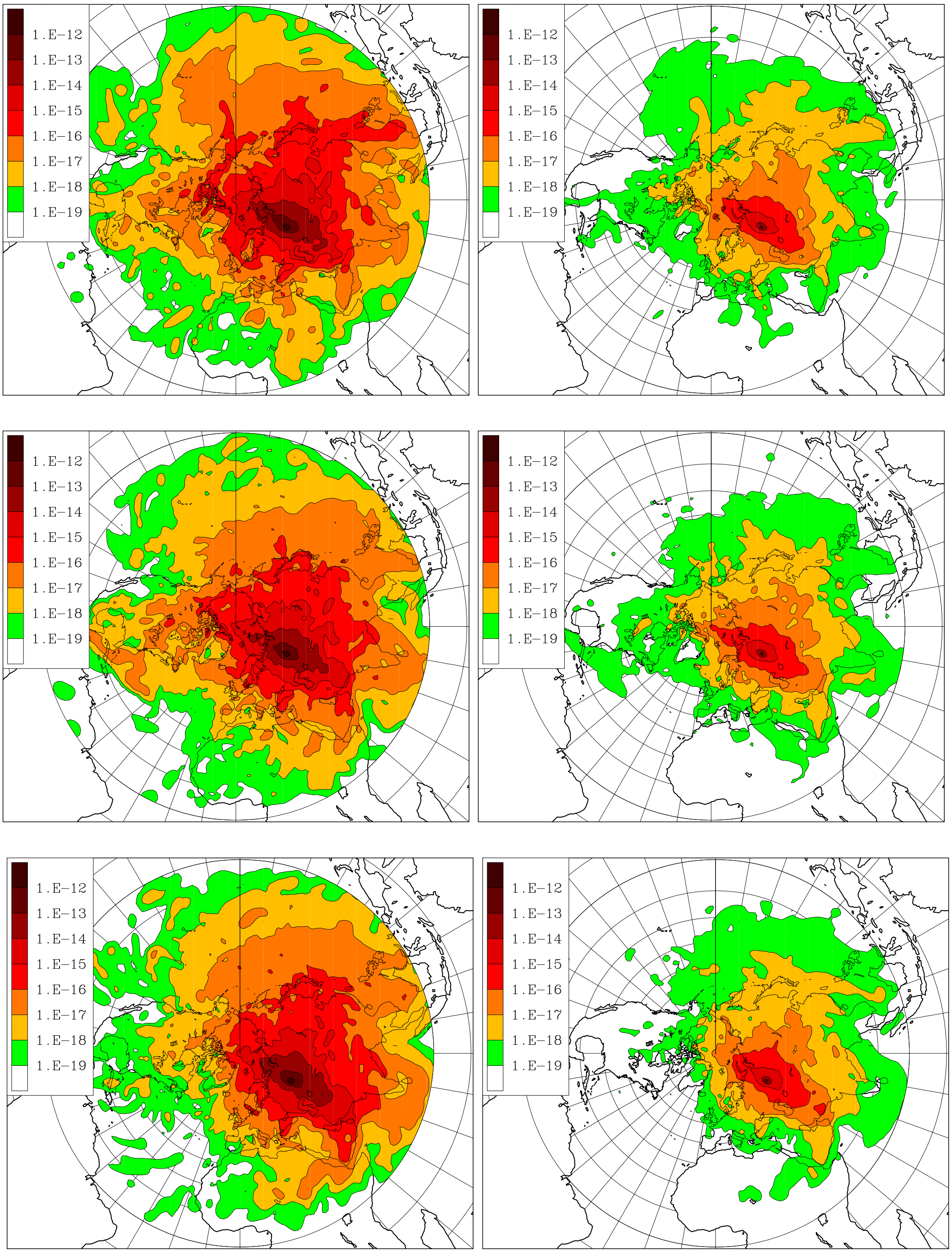

Plate 6 Nuclear power plant: **Belojarsk**; Nuclide: **Iodine-131 aerosol**

Total deposition (m^{-2}) **Time integrated conc. ($h\ m^{-3}$)**

1983

1985

1996

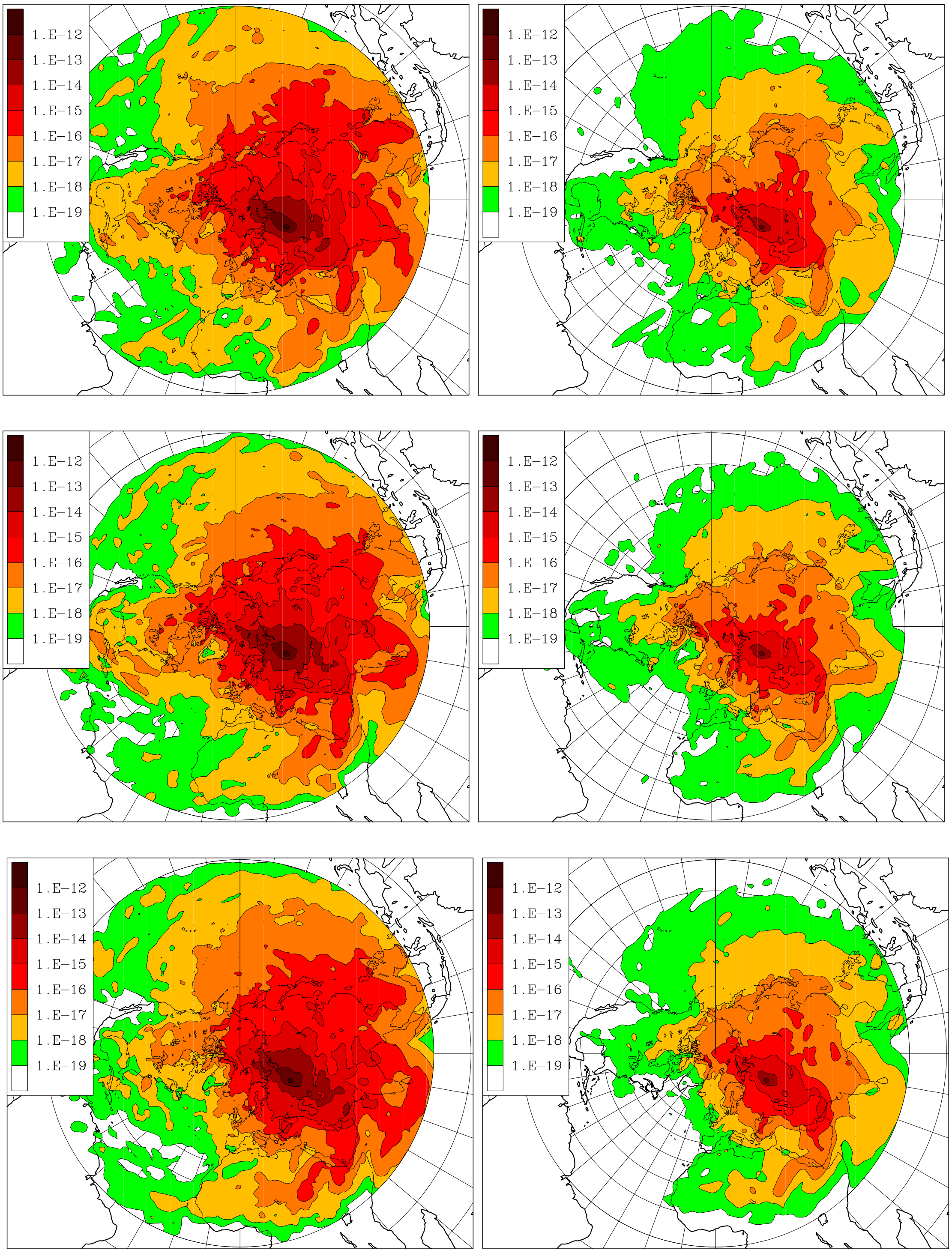

Plate 7 Nuclear power plant: **Bilibino**; Nuclide: **Caesium-137 aerosol**

Total deposition (m^{-2}) | **Time integrated conc. ($h\ m^{-3}$)**

1983

1985

1996

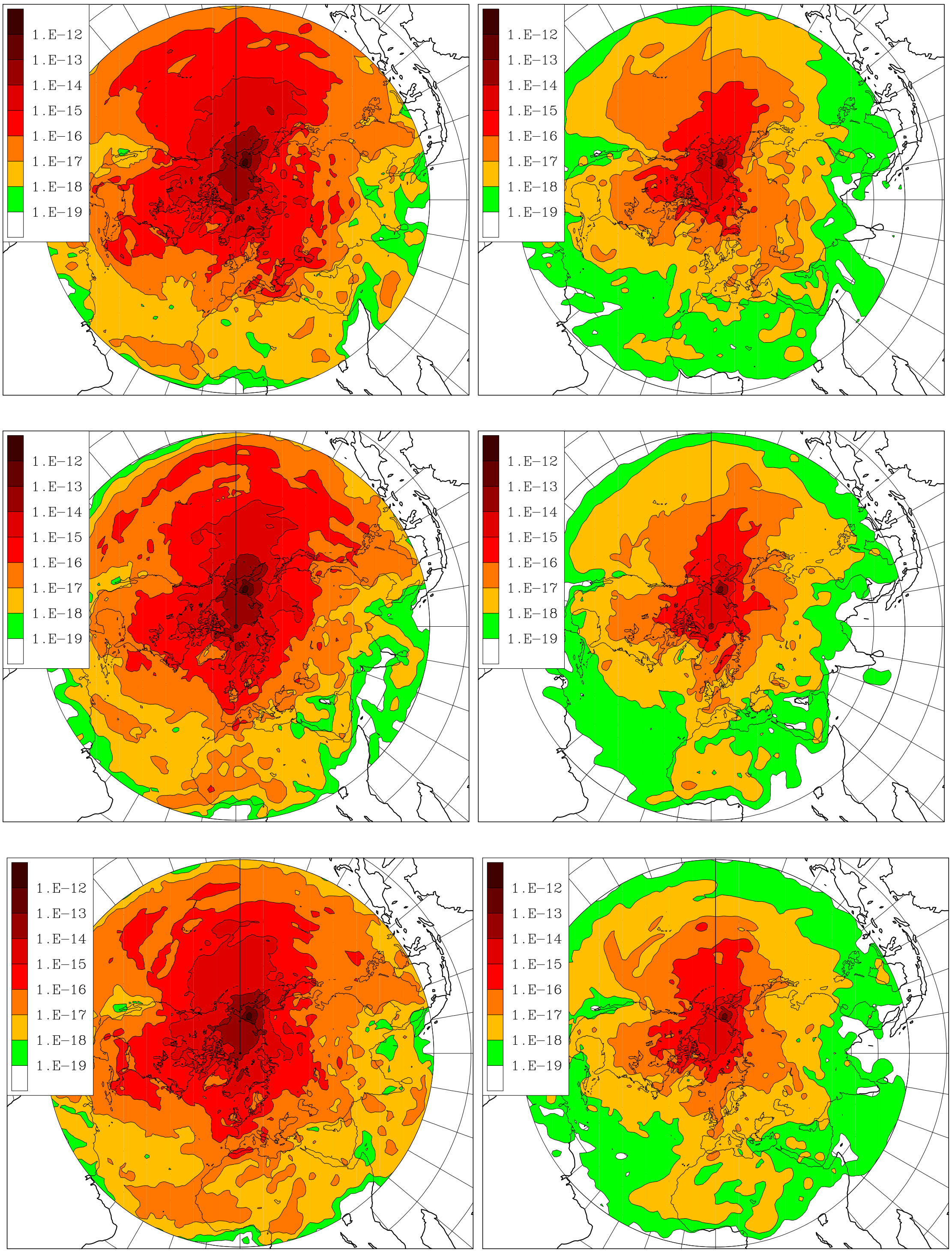

Plate 8 Nuclear power plant: **Bilibino**; Nuclide: **Iodine-131 gas**

Total deposition (m^{-2}) **Time integrated conc. ($h\ m^{-3}$)**

1983

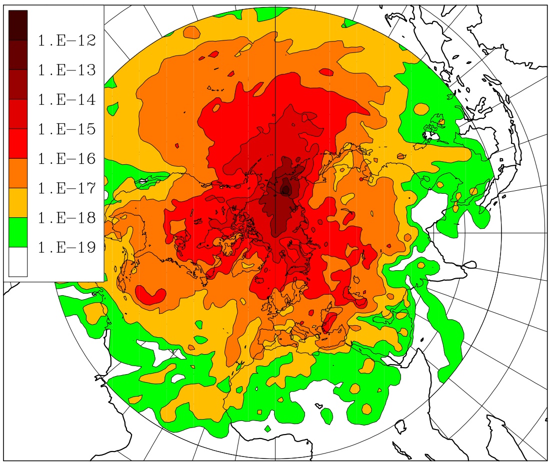

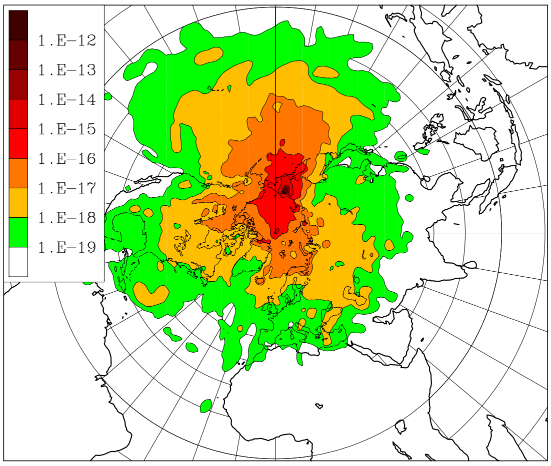

1985

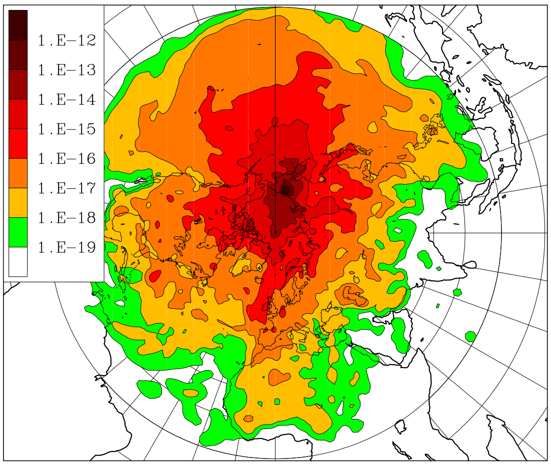

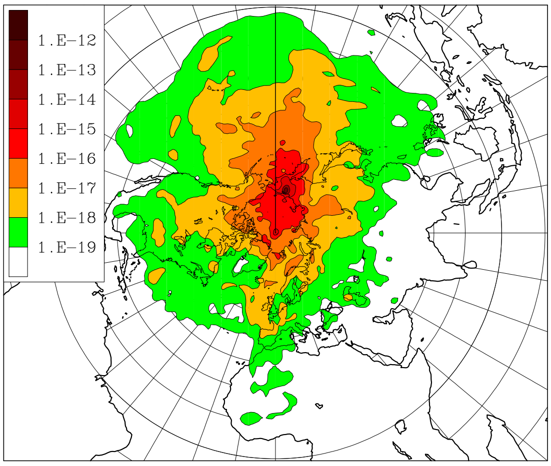

1996

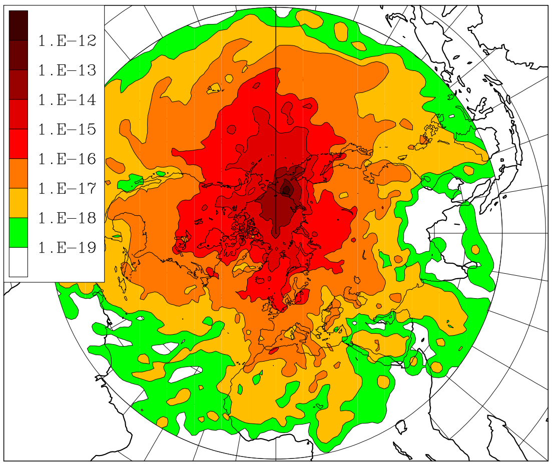

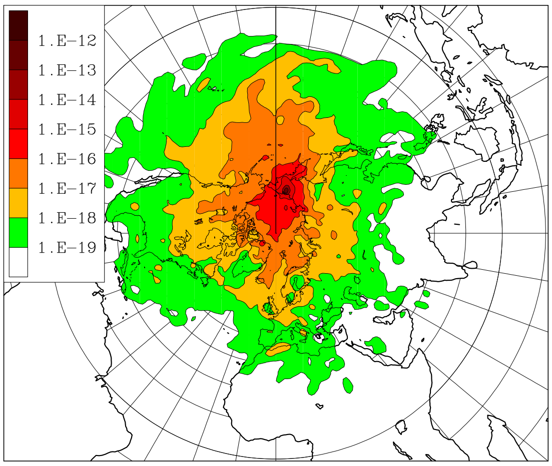

Plate 9 Nuclear power plant: **Bilibino**; Nuclide: **Iodine-131 aerosol**

Total deposition (m^{-2}) **Time integrated conc. ($h\ m^{-3}$)**

1983

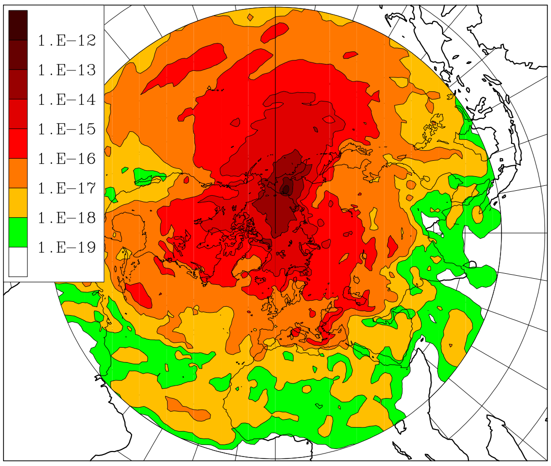

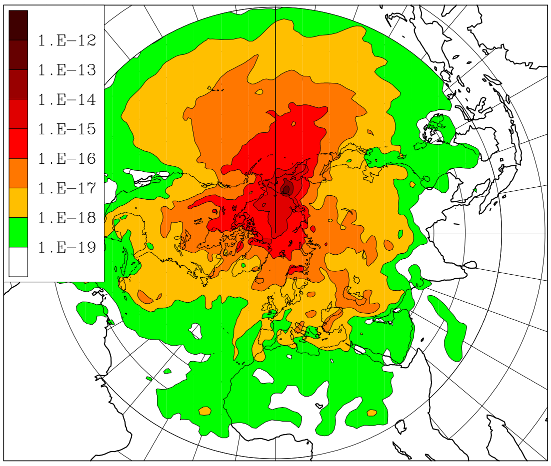

1985

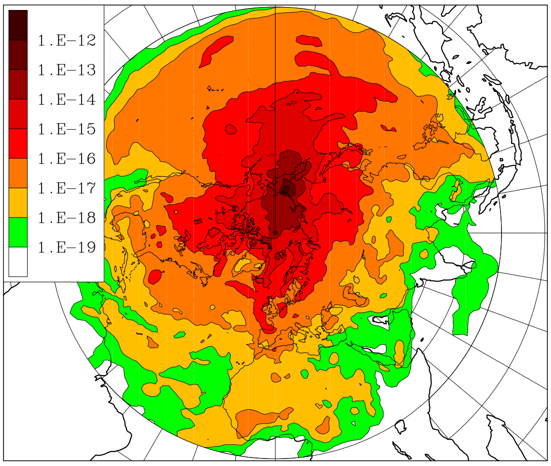

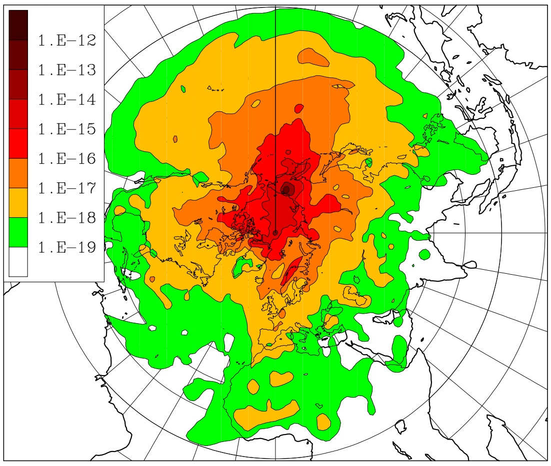

1996

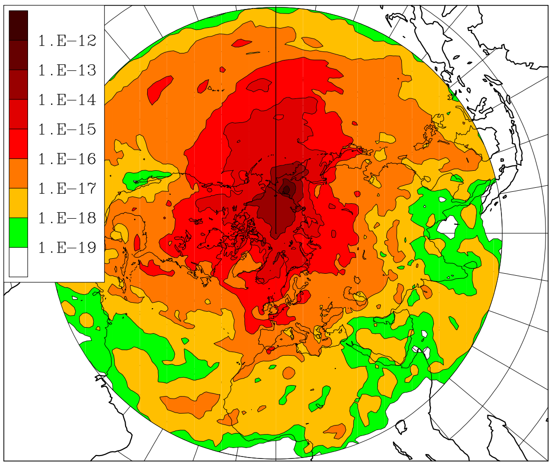

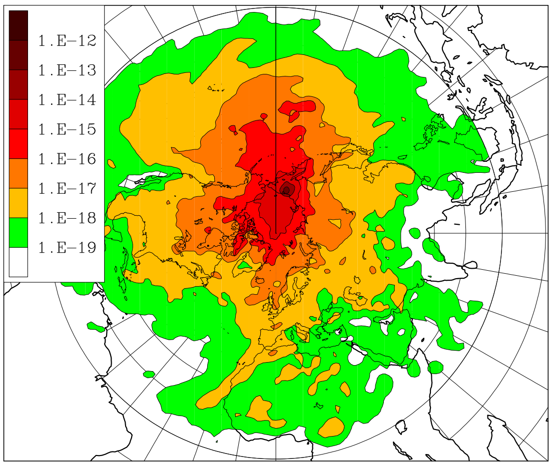

Plate 10 Nuclear power plant: **Borssele**; Nuclide: **Caesium-137 aerosol**

Total deposition (m^{-2}) **Time integrated conc. ($h\ m^{-3}$)**

1983

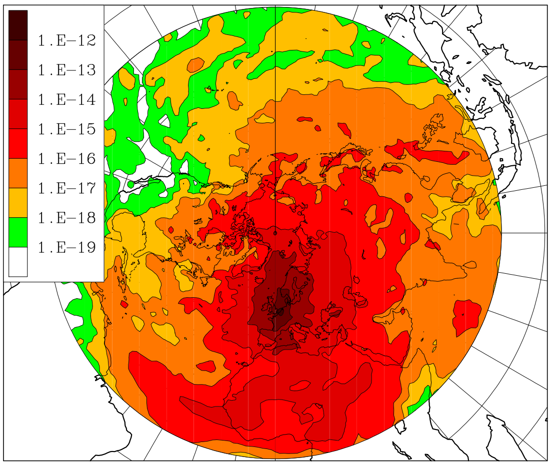

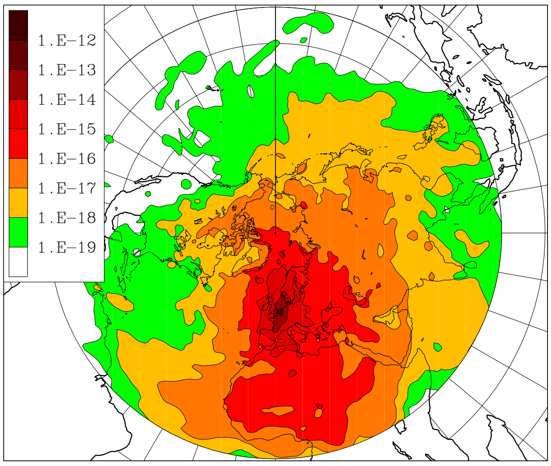

1985

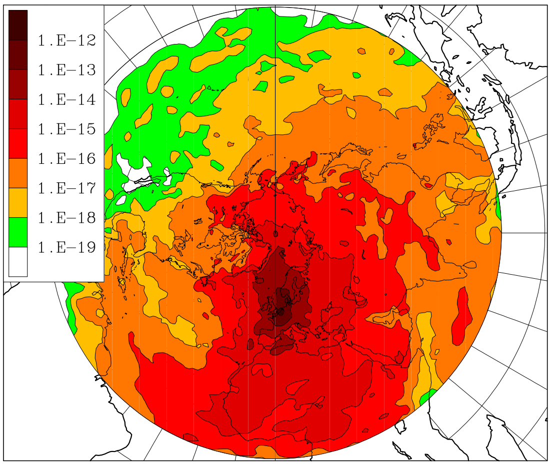

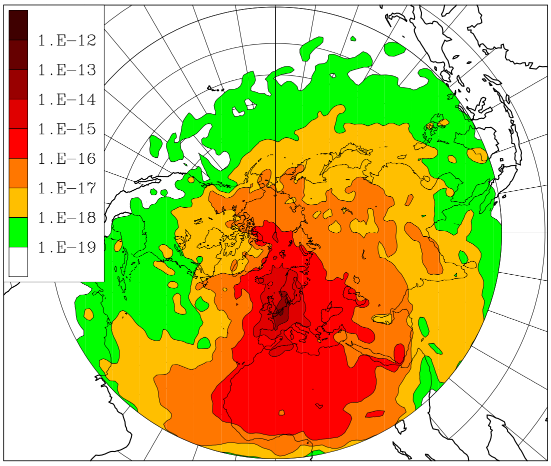

1996

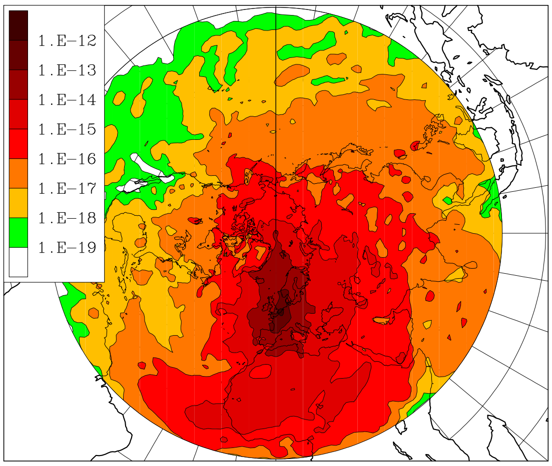

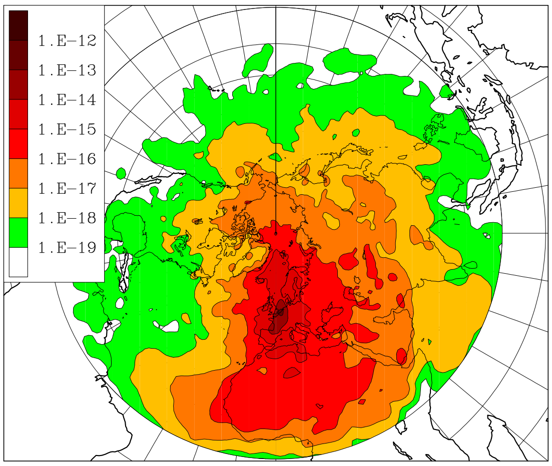

Plate 11 Nuclear power plant: **Borssele**; Nuclide: **Iodine-131 gas**

Total deposition (m^{-2}) **Time integrated conc. ($h\ m^{-3}$)**

1983

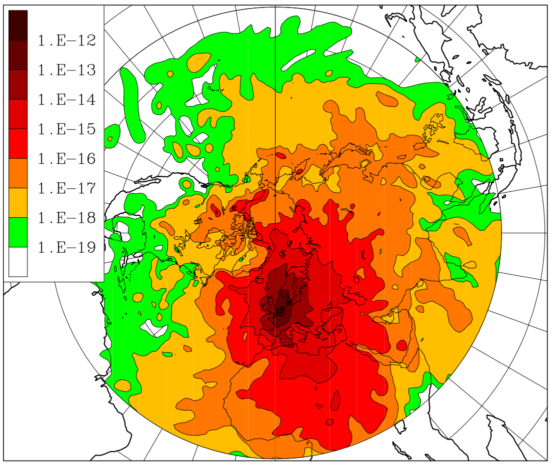

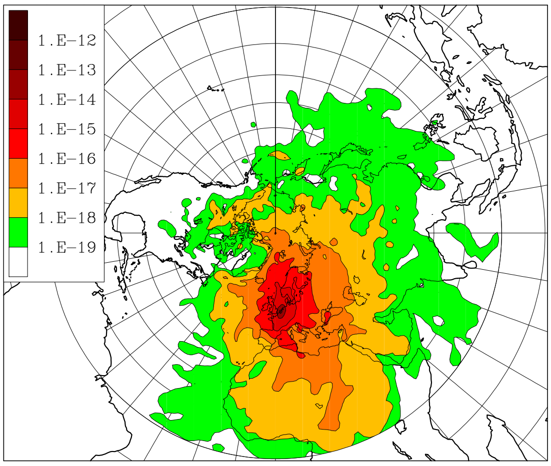

1985

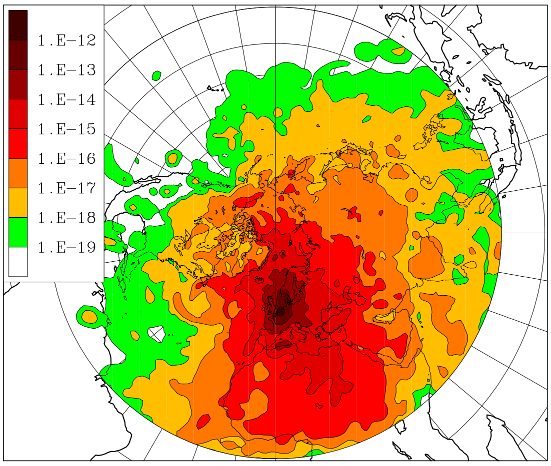

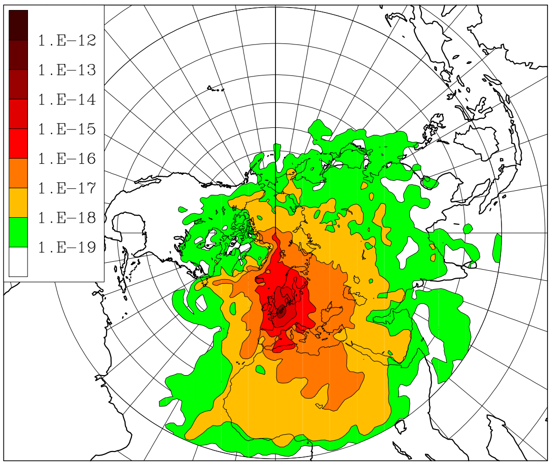

1996

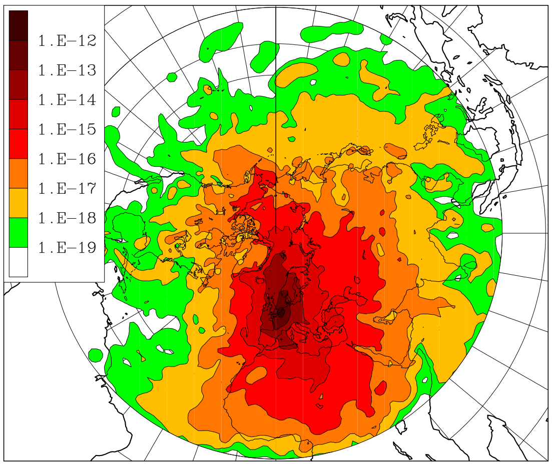

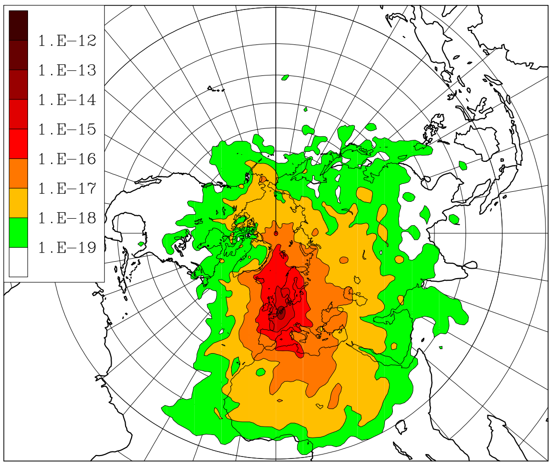

Plate 12 Nuclear power plant: **Borssele**; Nuclide: **Iodine-131 aerosol**

Total deposition (m^{-2}) **Time integrated conc. ($h\ m^{-3}$)**

1983

1985

1996

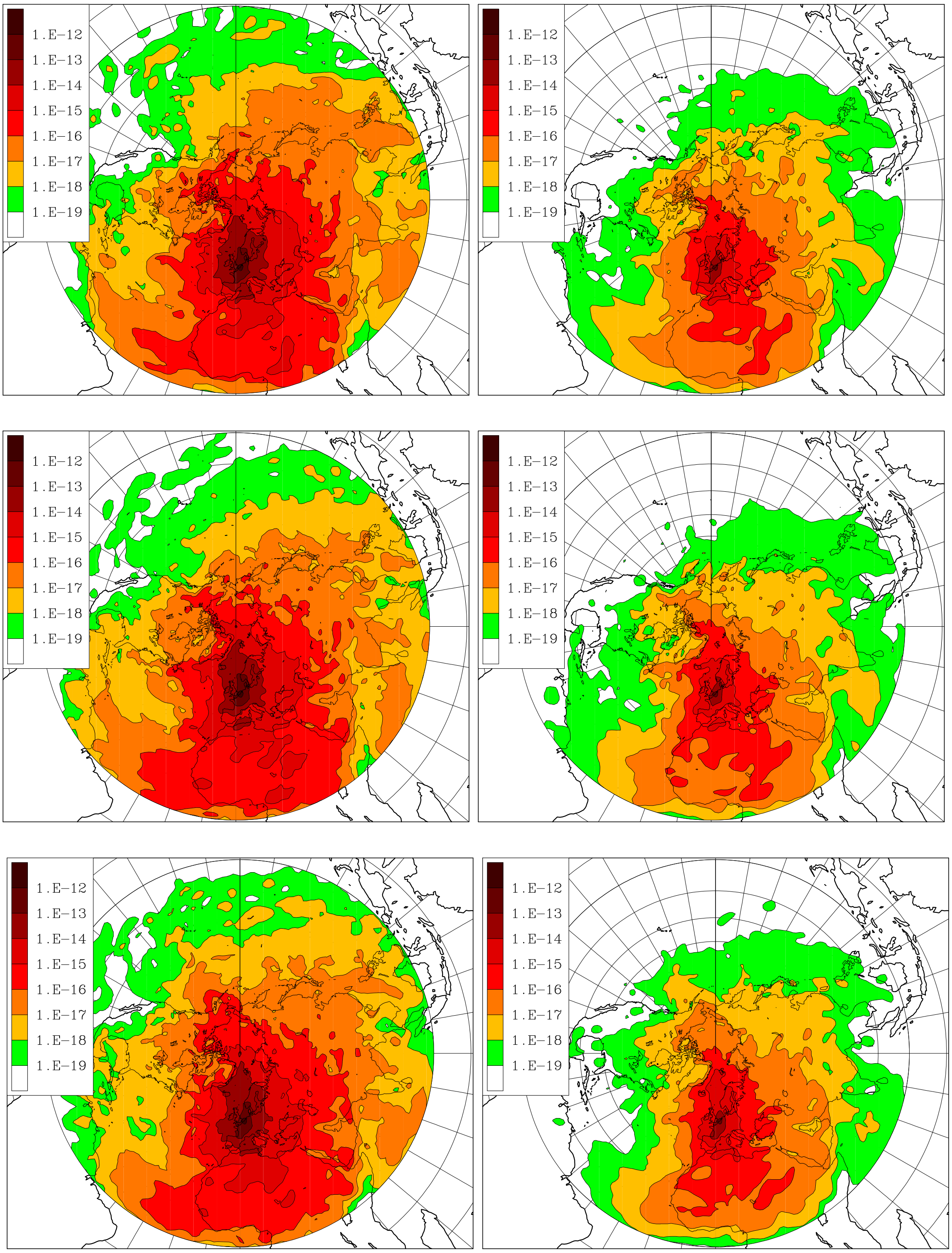

Plate 13 Nuclear power plant: **Chernobyl**; Nuclide: **Caesium-137 aerosol**

Total deposition (m^{-2}) **Time integrated conc. ($h\ m^{-3}$)**

1983

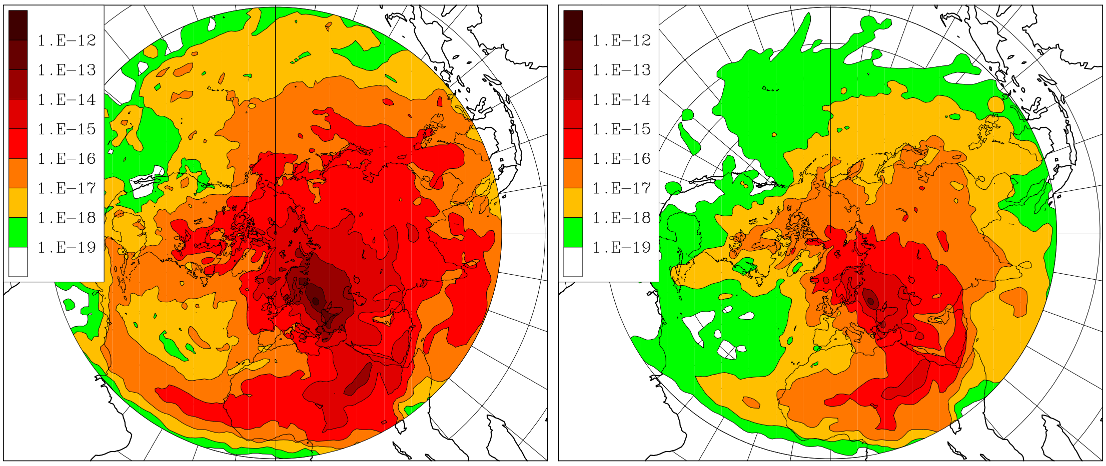

1985

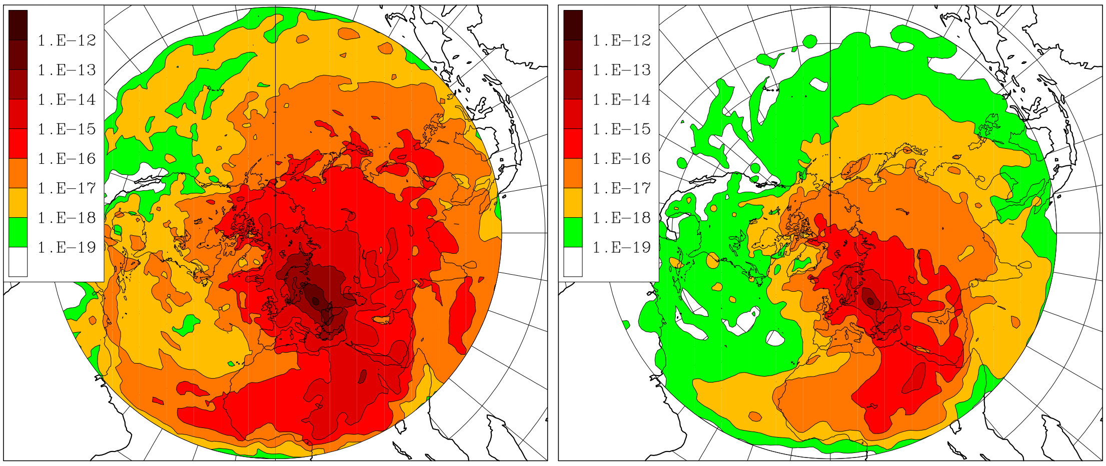

1996

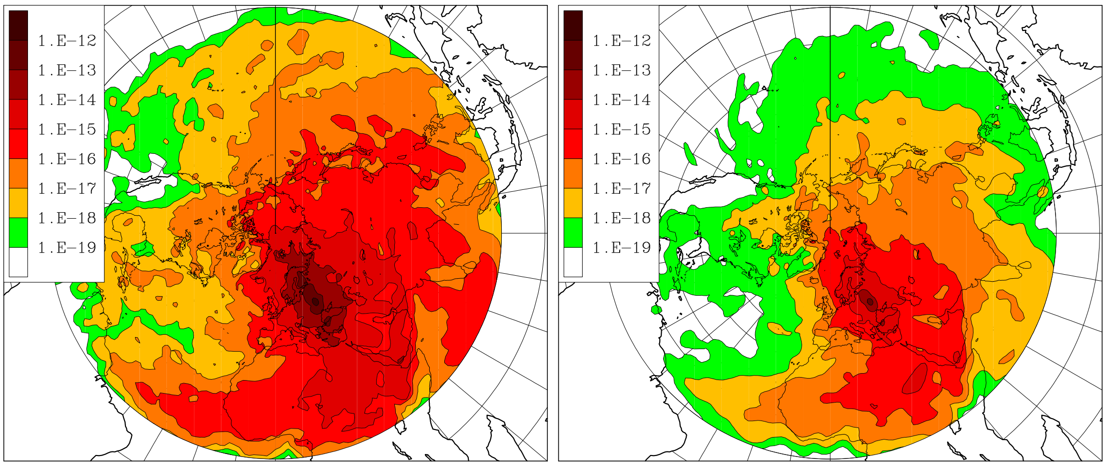

Plate 14 Nuclear power plant: **Chernobyl**; Nuclide: **Iodine-131 gas**

Total deposition (m^{-2}) **Time integrated conc. ($h\ m^{-3}$)**

1983

1985

1996

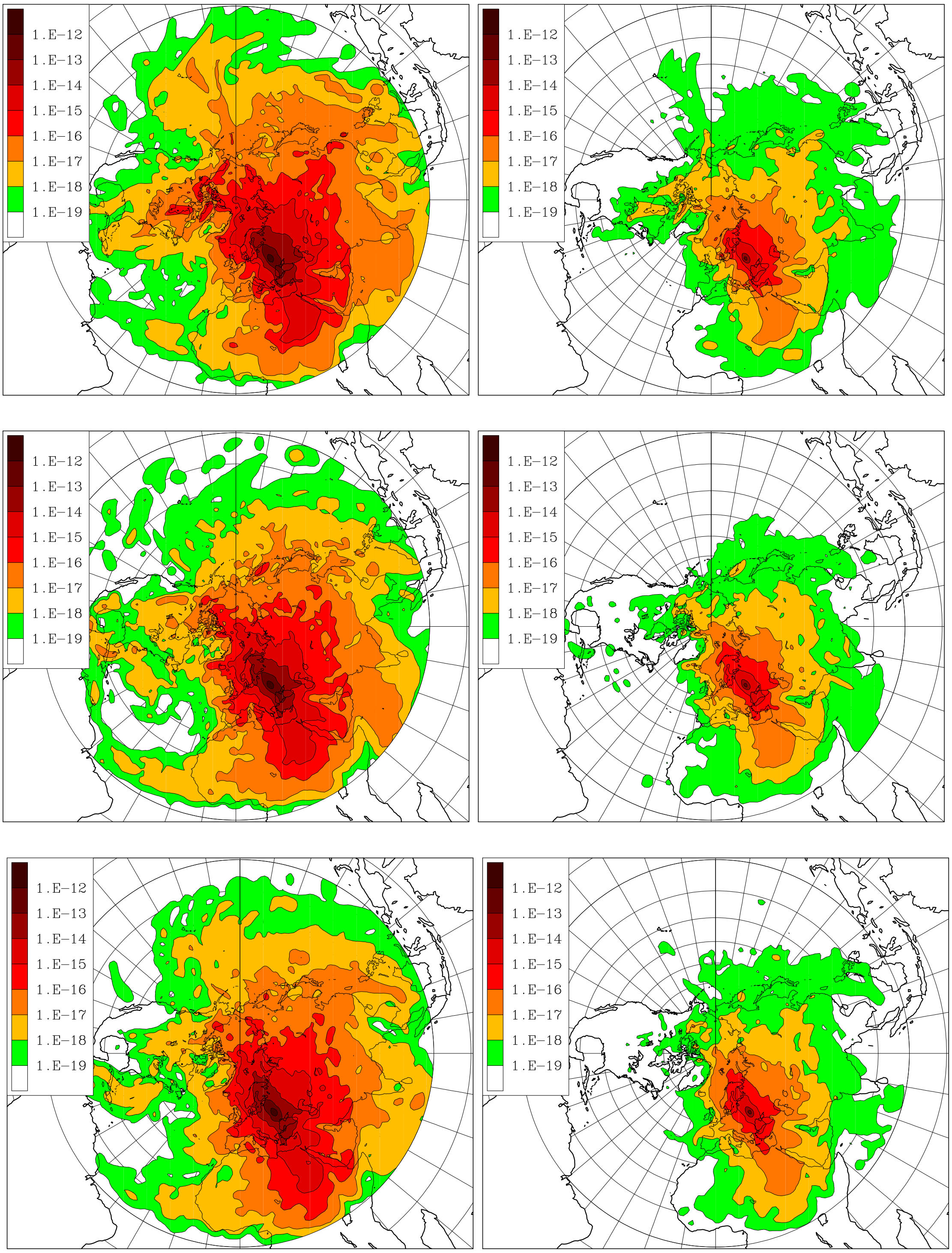

Plate 15 Nuclear power plant: **Chernobyl**; Nuclide: **Iodine-131 aerosol**

	Total deposition (m^{-2})	**Time integrated conc. ($h\ m^{-3}$)**

1983

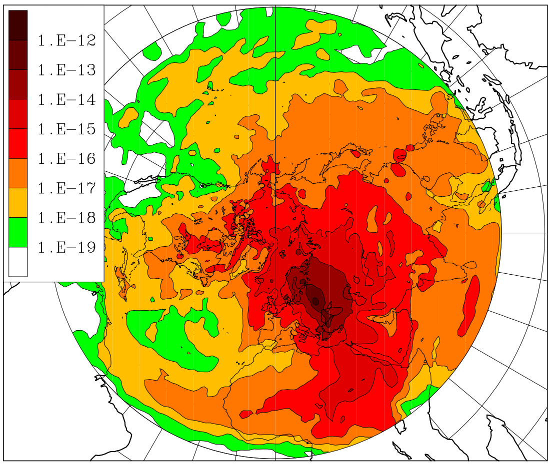

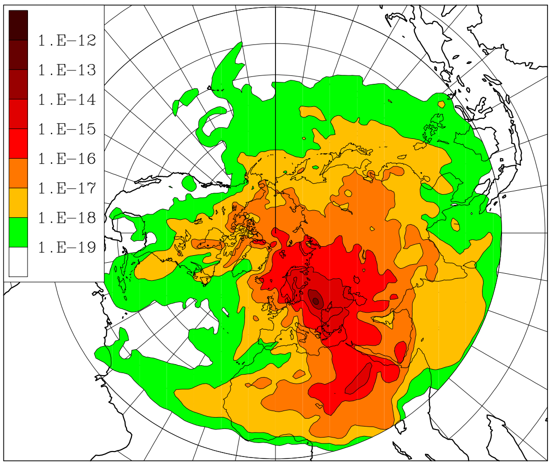

1985

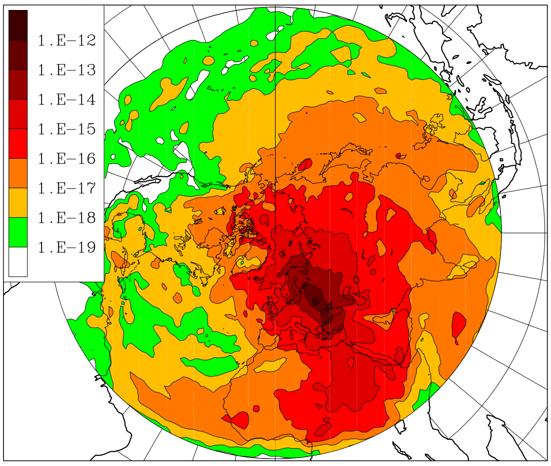

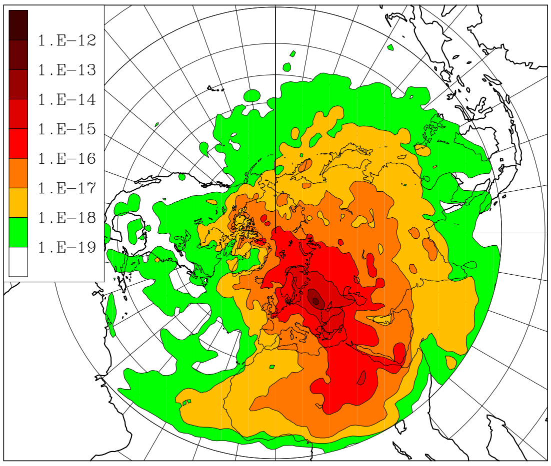

1996

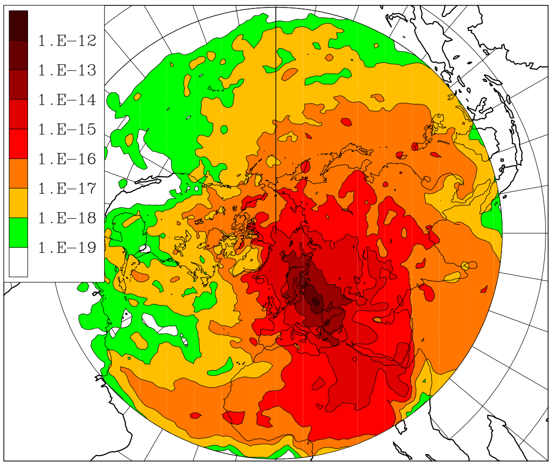

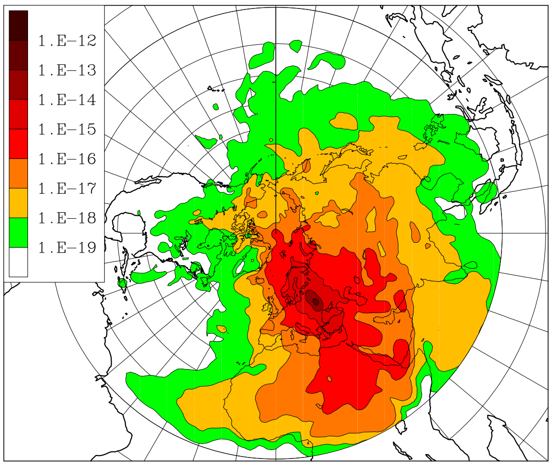

Plate 16 Nuclear power plant: **Davis Besse**; Nuclide: **Caesium-137 aerosol**

Total deposition (m^{-2}) **Time integrated conc. ($h\ m^{-3}$)**

1983

1985

1996

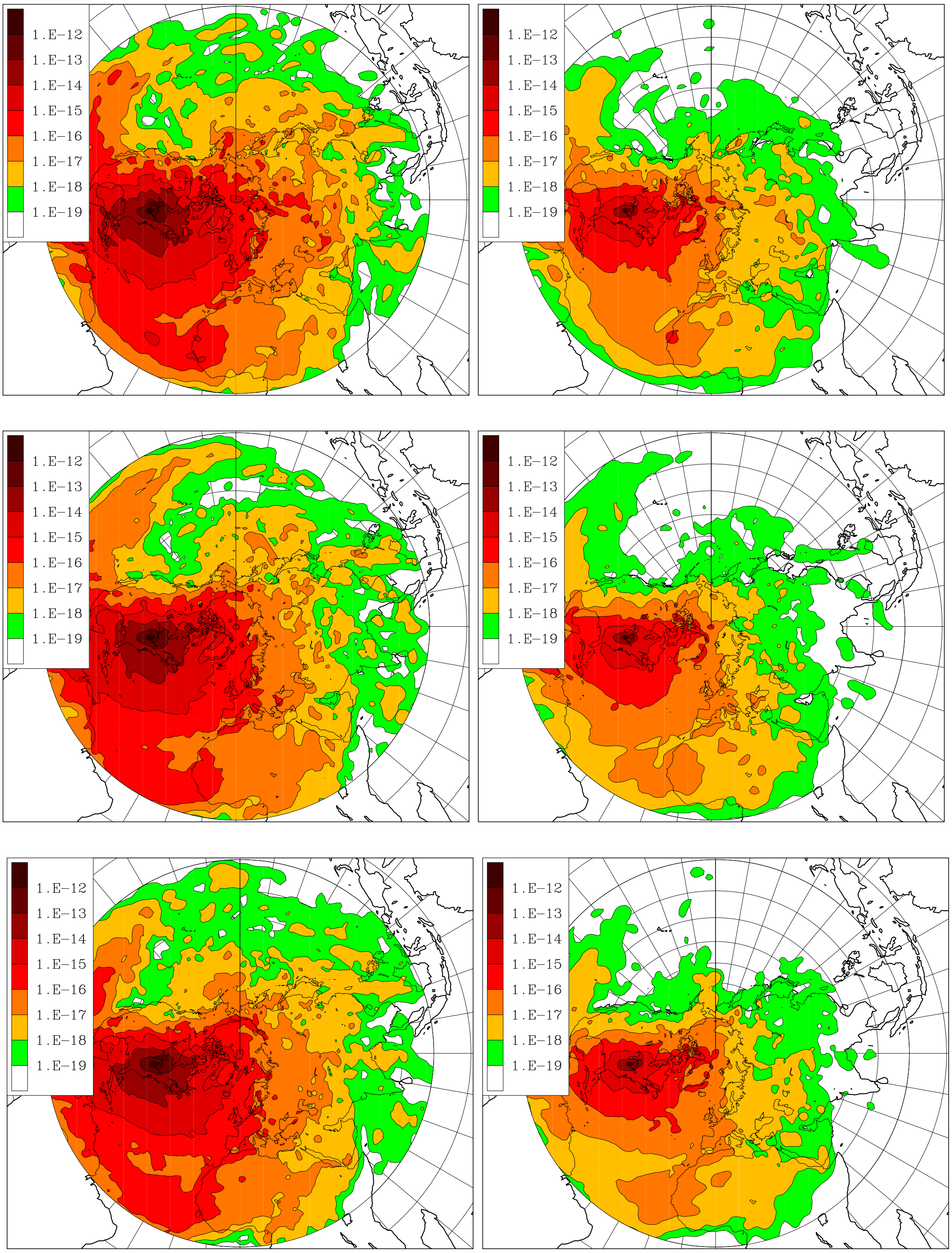

Plate 17 Nuclear power plant: **Davis Besse**; Nuclide: **Iodine-131 gas**

Total deposition (m^{-2}) **Time integrated conc. ($h\ m^{-3}$)**

1983

1985

1996

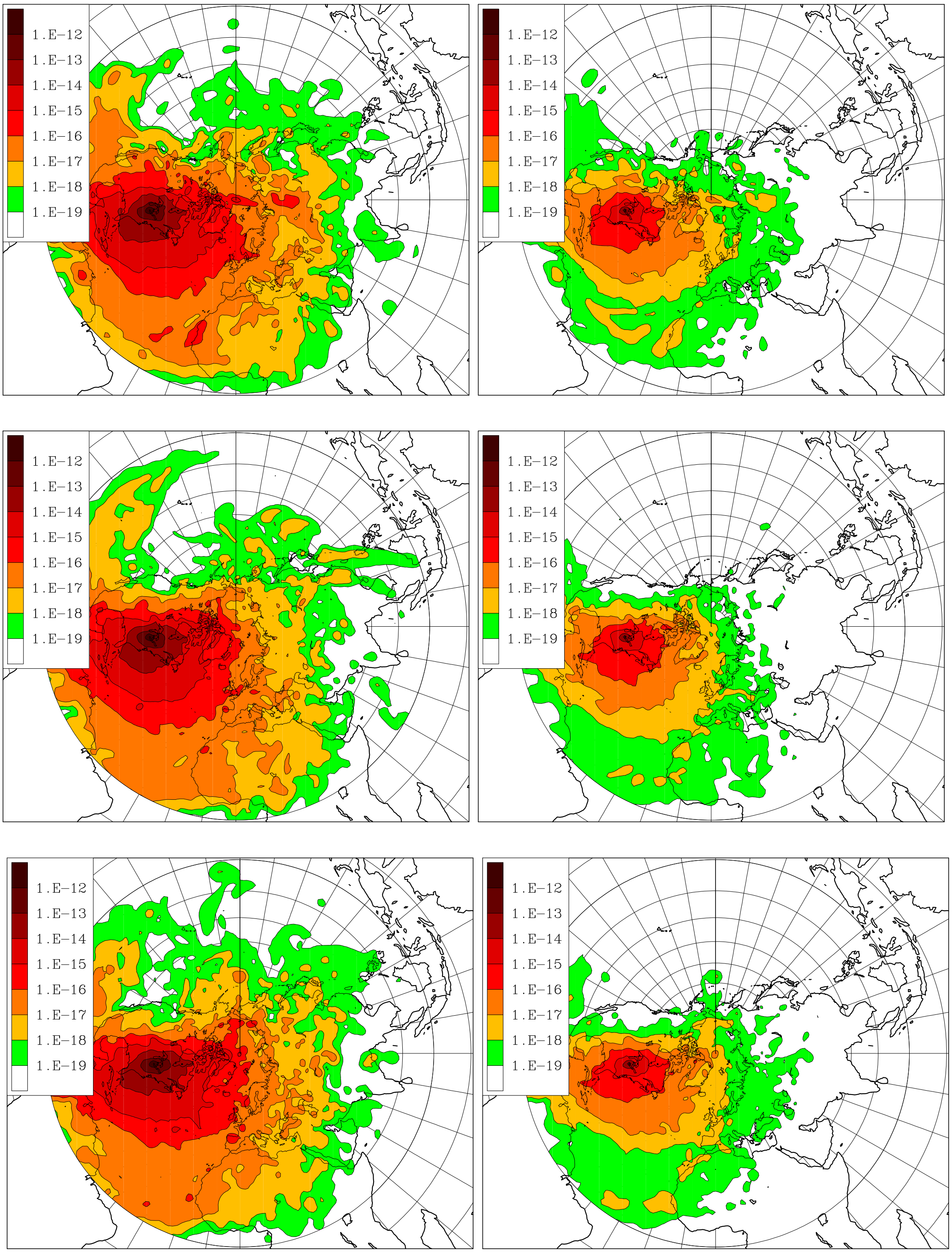

Plate 18 Nuclear power plant: **Davis Besse**; Nuclide: **Iodine-131 aerosol**

Total deposition (m^{-2}) **Time integrated conc. ($h\ m^{-3}$)**

1983

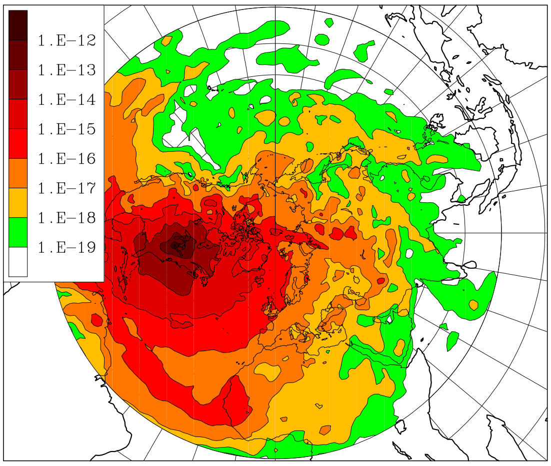

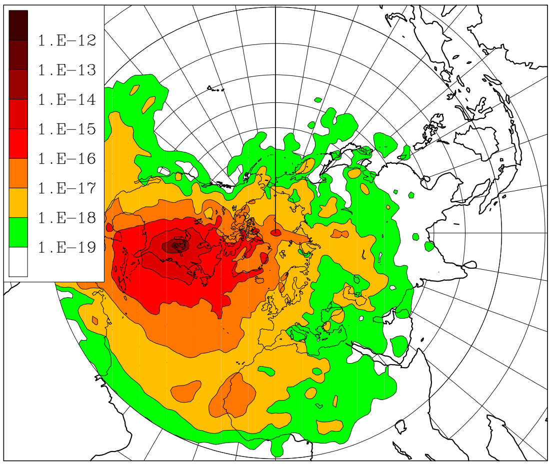

1985

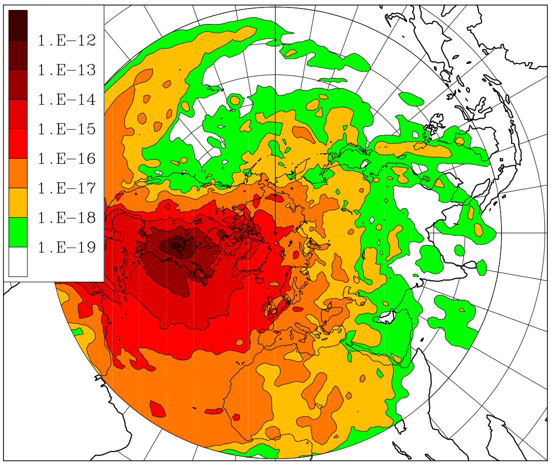

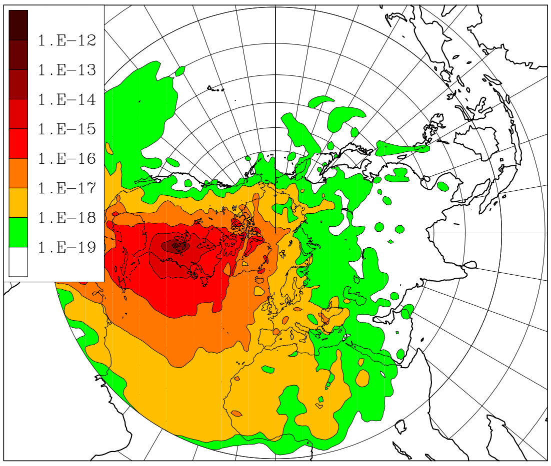

1996

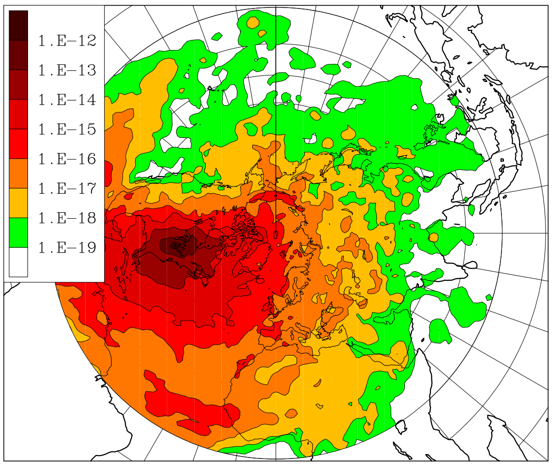

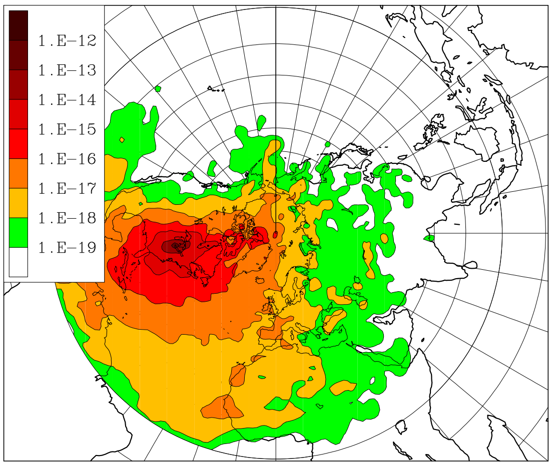

Plate 19 Nuclear power plant: **Dukovany**; Nuclide: **Caesium-137 aerosol**

Total deposition (m^{-2}) **Time integrated conc. ($h\ m^{-3}$)**

1983

1985

1996

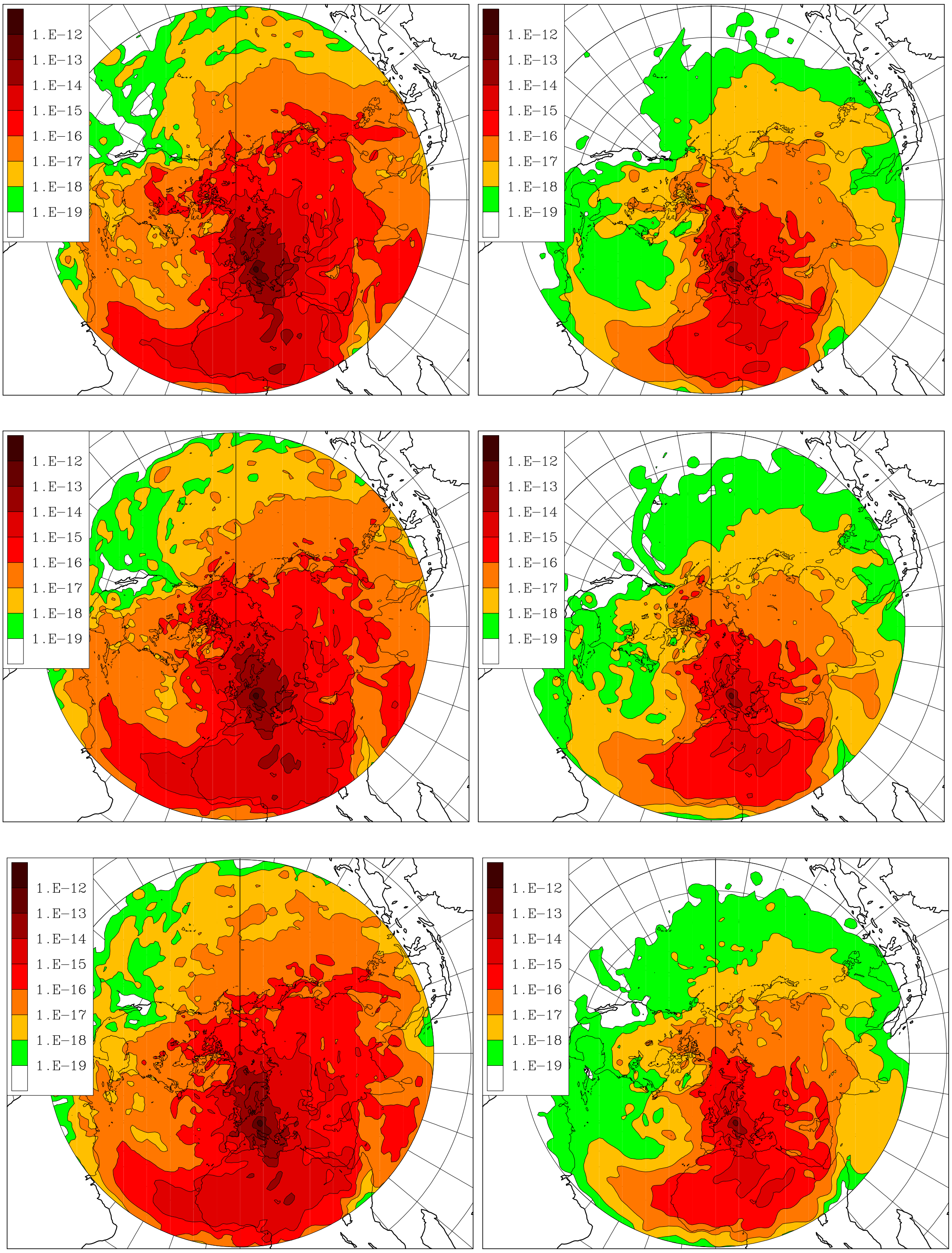

Plate 20 Nuclear power plant: **Dukovany**; Nuclide: **Iodine-131 gas**

Total deposition (m^{-2}) **Time integrated conc. ($h\ m^{-3}$)**

1983

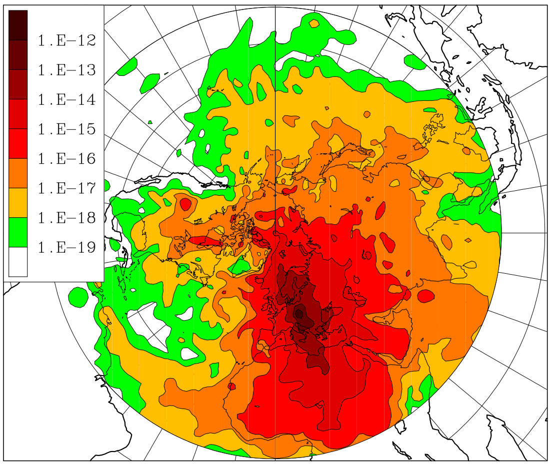

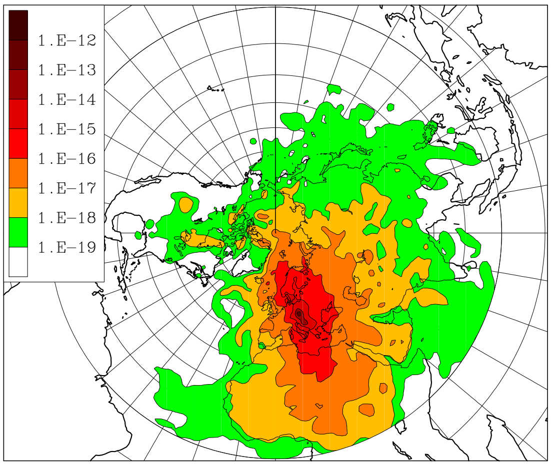

1985

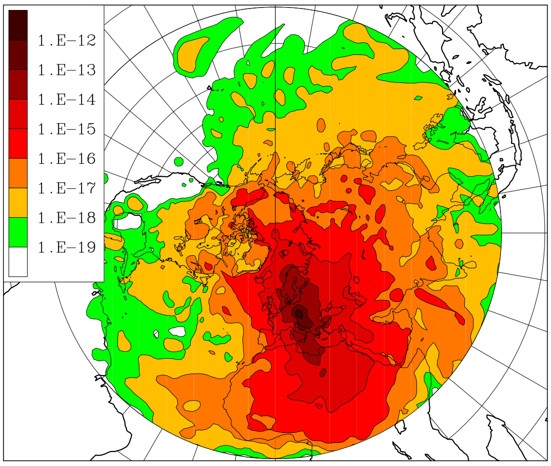

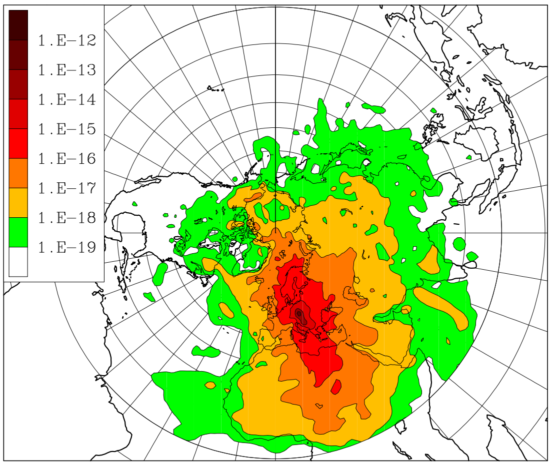

1996

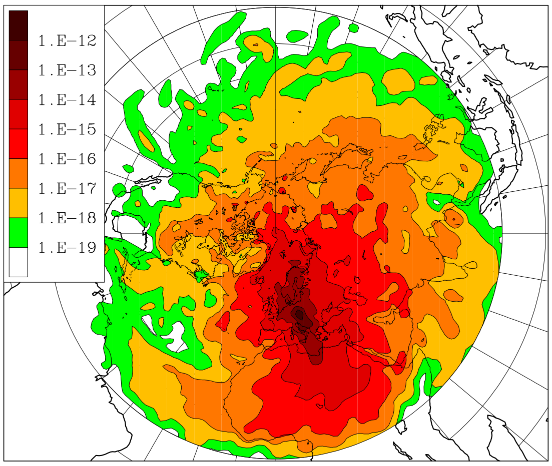

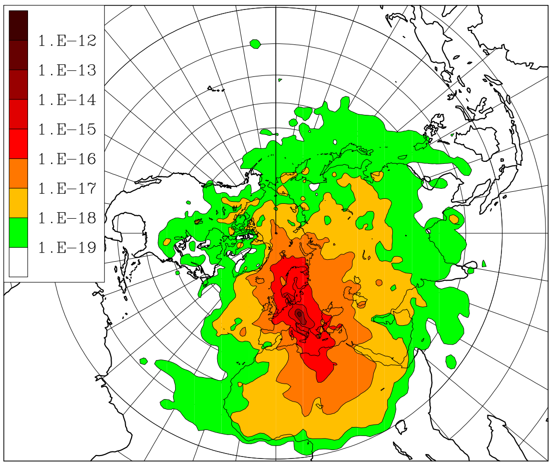

Plate 21 Nuclear power plant: **Dukovany**; Nuclide: **Iodine-131 aerosol**

Total deposition (m^{-2}) **Time integrated conc. ($h\ m^{-3}$)**

1983

1985

1996

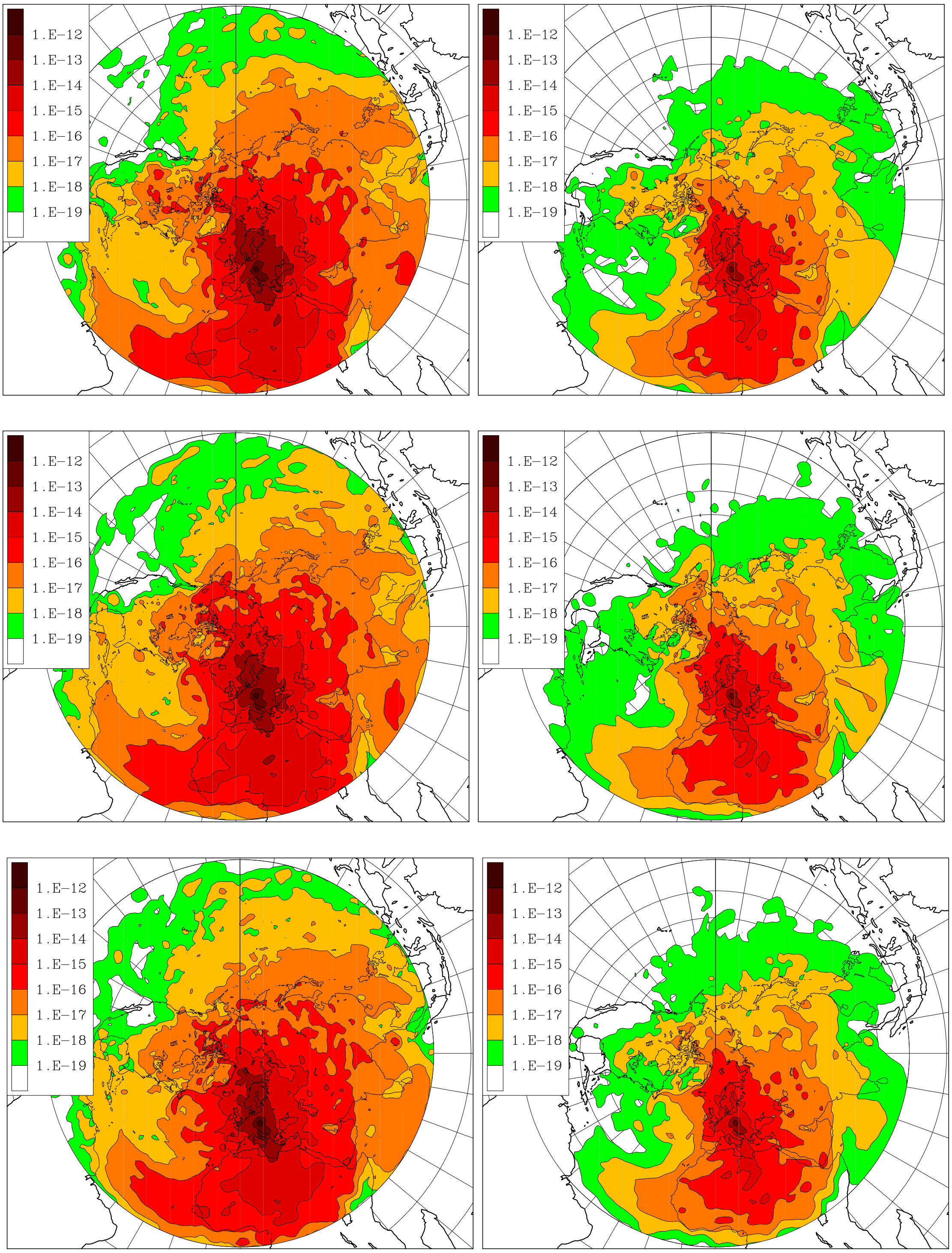

Plate 22 Nuclear power plant: **Kanupp**; Nuclide: **Caesium-137 aerosol**

Total deposition (m^{-2}) | **Time integrated conc. ($h\ m^{-3}$)**

1983

1985

1996

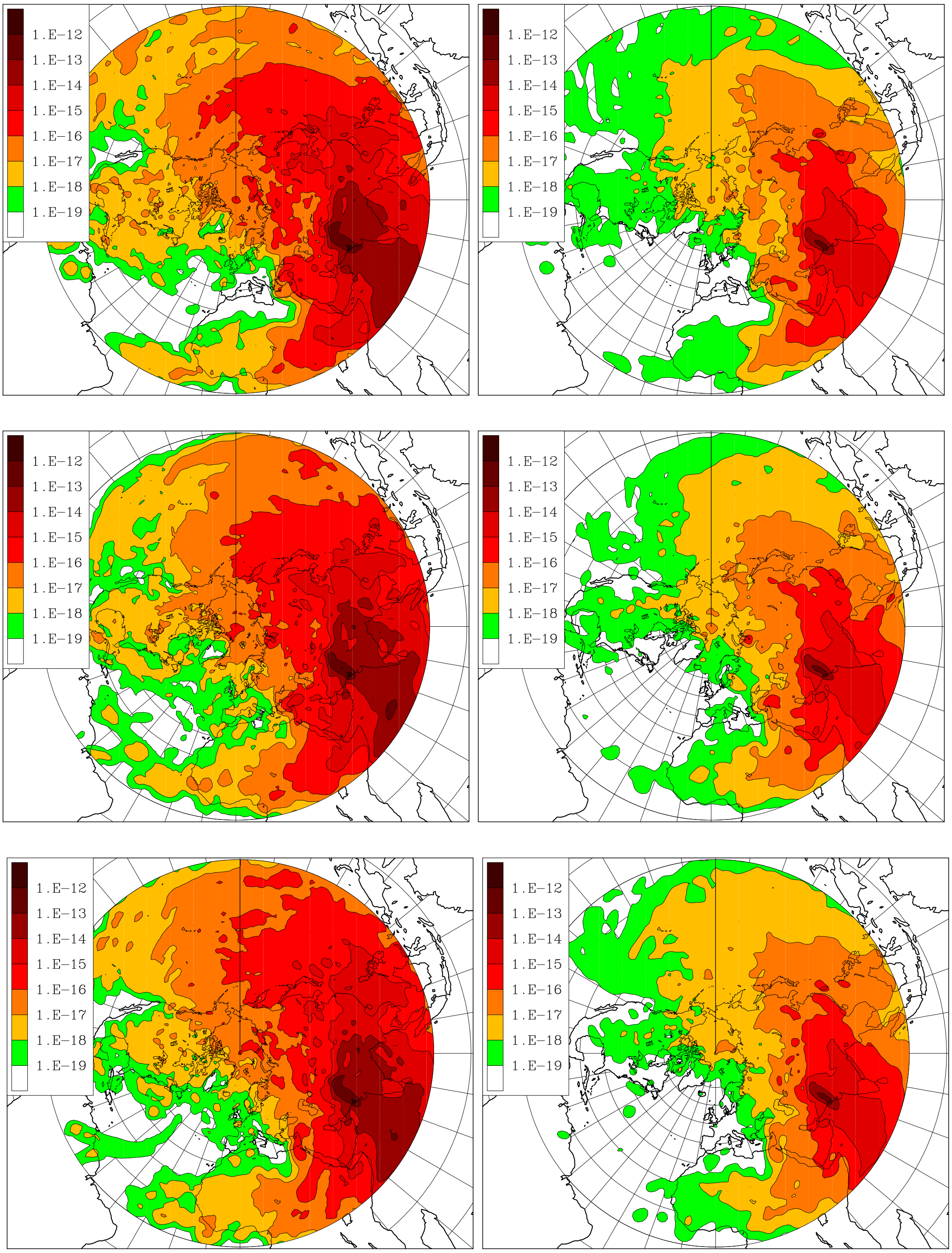

Plate 23 Nuclear power plant: **Kanupp**; Nuclide: **Iodine-131 gas**

Total deposition (m^{-2}) **Time integrated conc. ($h\ m^{-3}$)**

1983

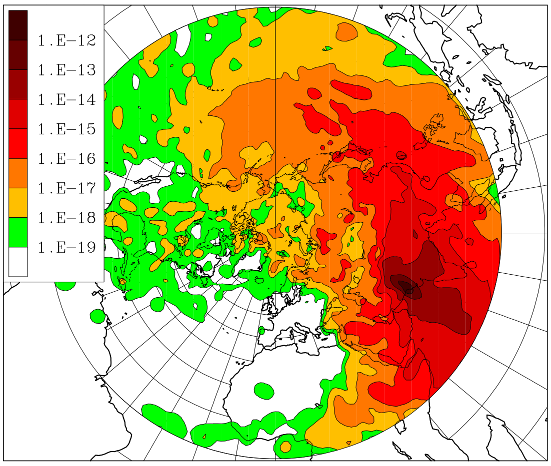

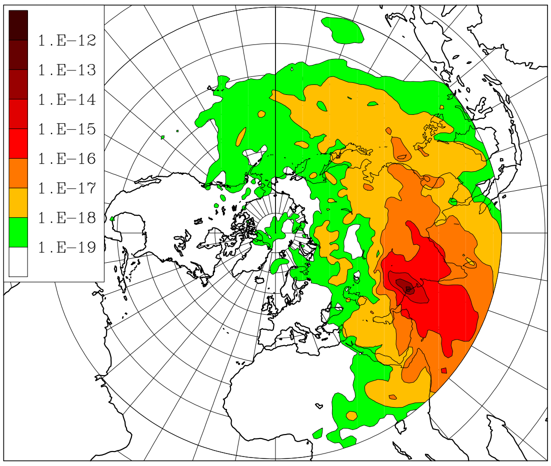

1985

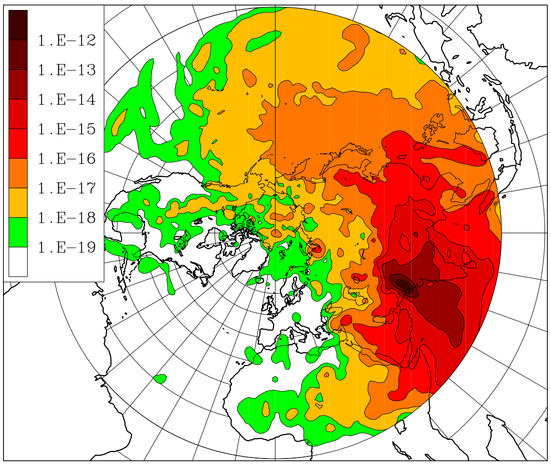

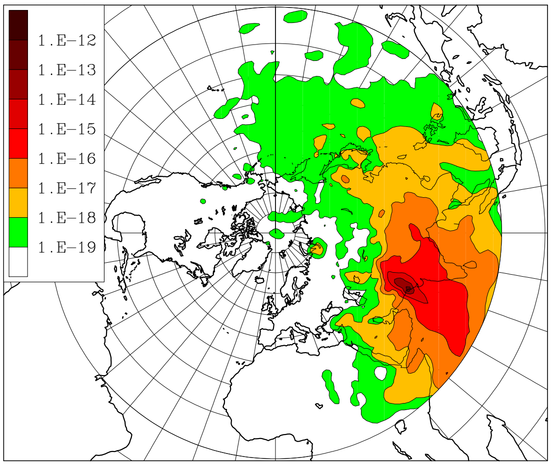

1996

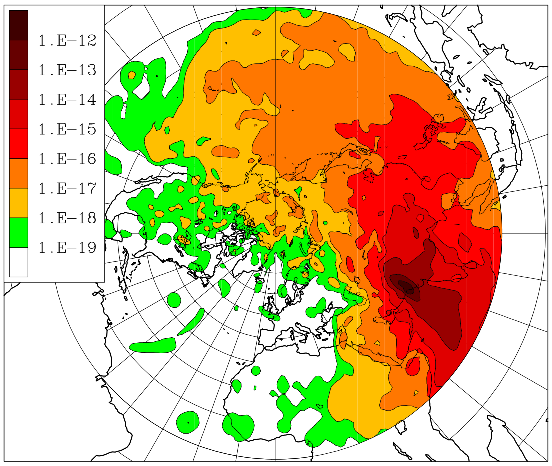

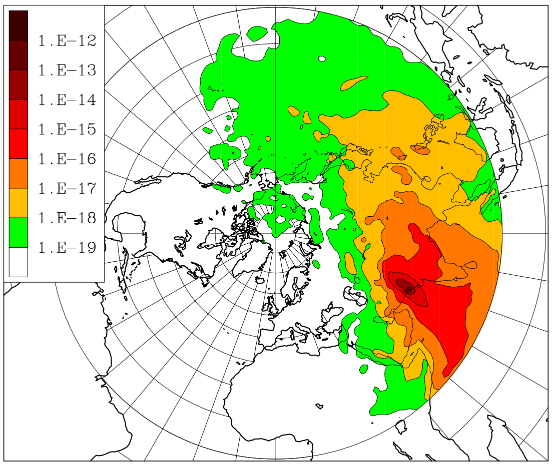

Plate 24 Nuclear power plant: **Kanupp**; Nuclide: **Iodine-131 aerosol**

Total deposition (m^{-2}) **Time integrated conc. ($h\ m^{-3}$)**

1983

1985

1996

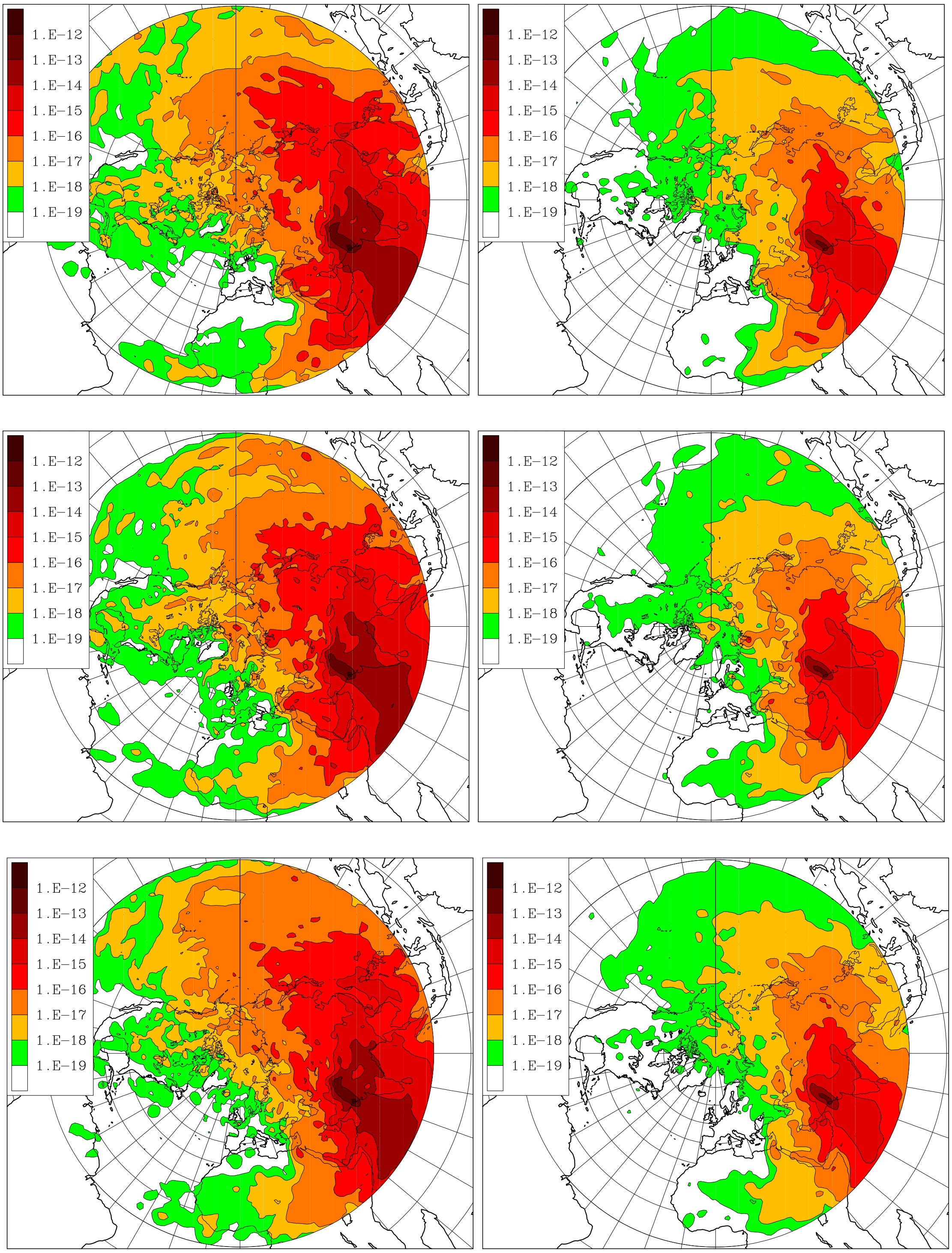

Plate 25 Nuclear power plant: **Kola**; Nuclide: **Caesium-137 aerosol**

Total deposition (m^{-2}) **Time integrated conc. ($h\ m^{-3}$)**

1983

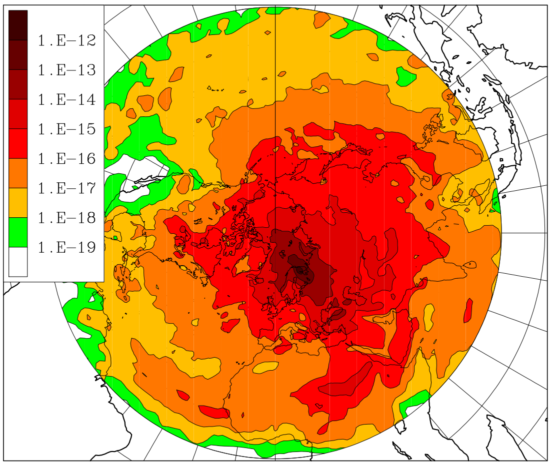

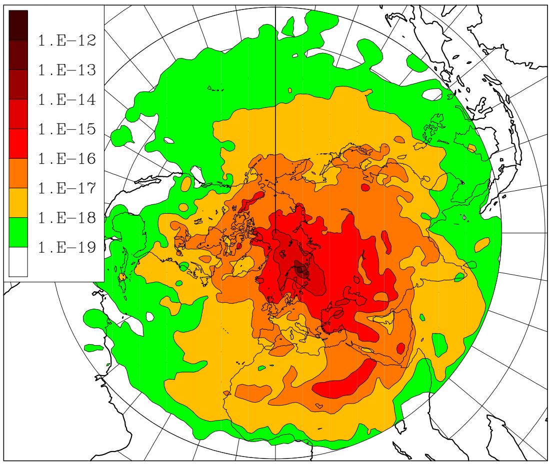

1985

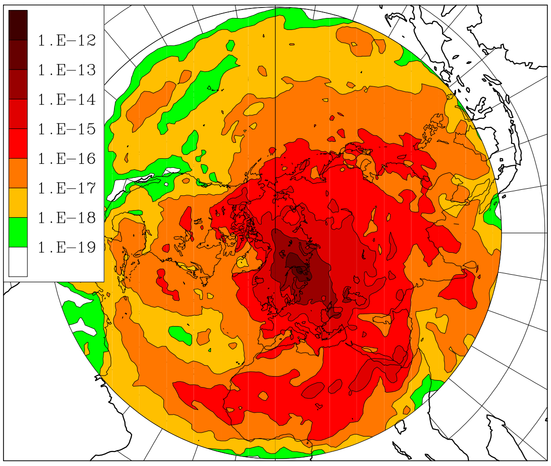

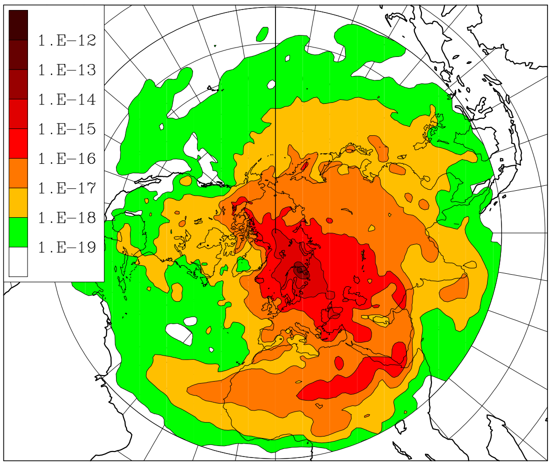

1996

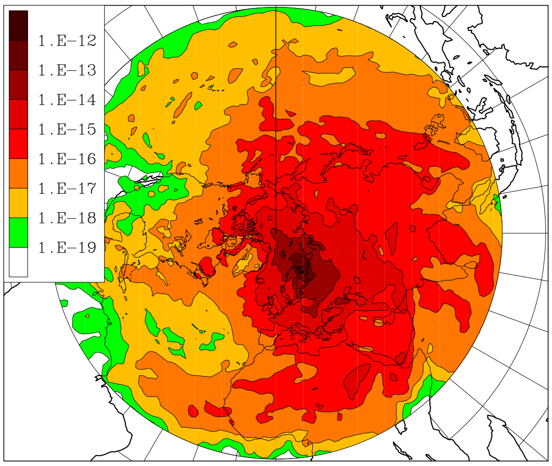

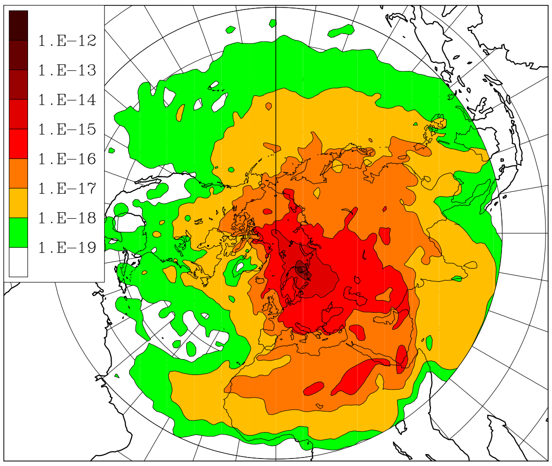

Plate 26 Nuclear power plant: **Kola**; Nuclide: **Iodine-131 gas**

Total deposition (m^{-2}) **Time integrated conc. ($h\ m^{-3}$)**

1983

1985

1996

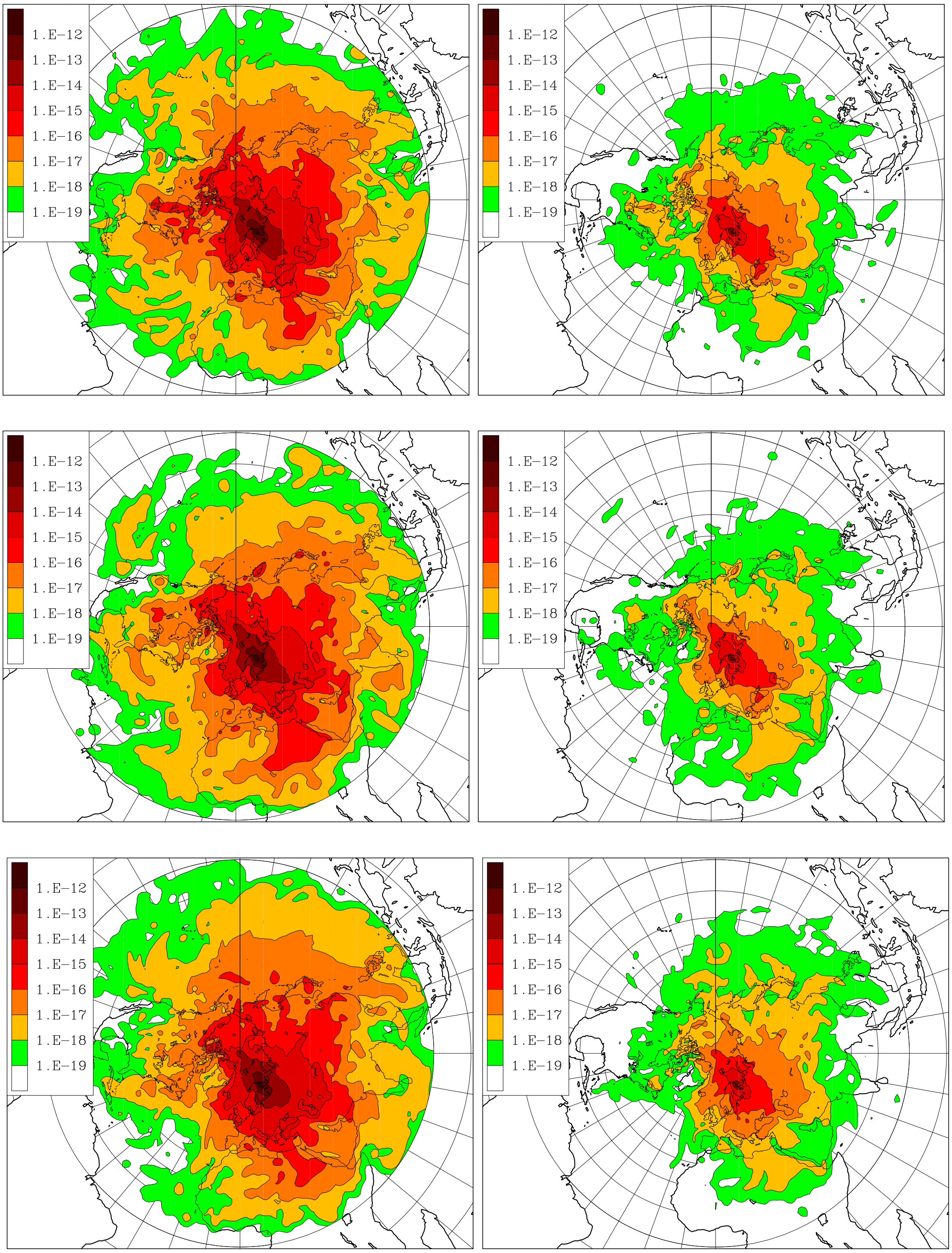

Plate 27 Nuclear power plant: **Kola**; Nuclide: **Iodine-131 aerosol**

Total deposition (m^{-2}) **Time integrated conc. ($h\ m^{-3}$)**

1983

1985

1996

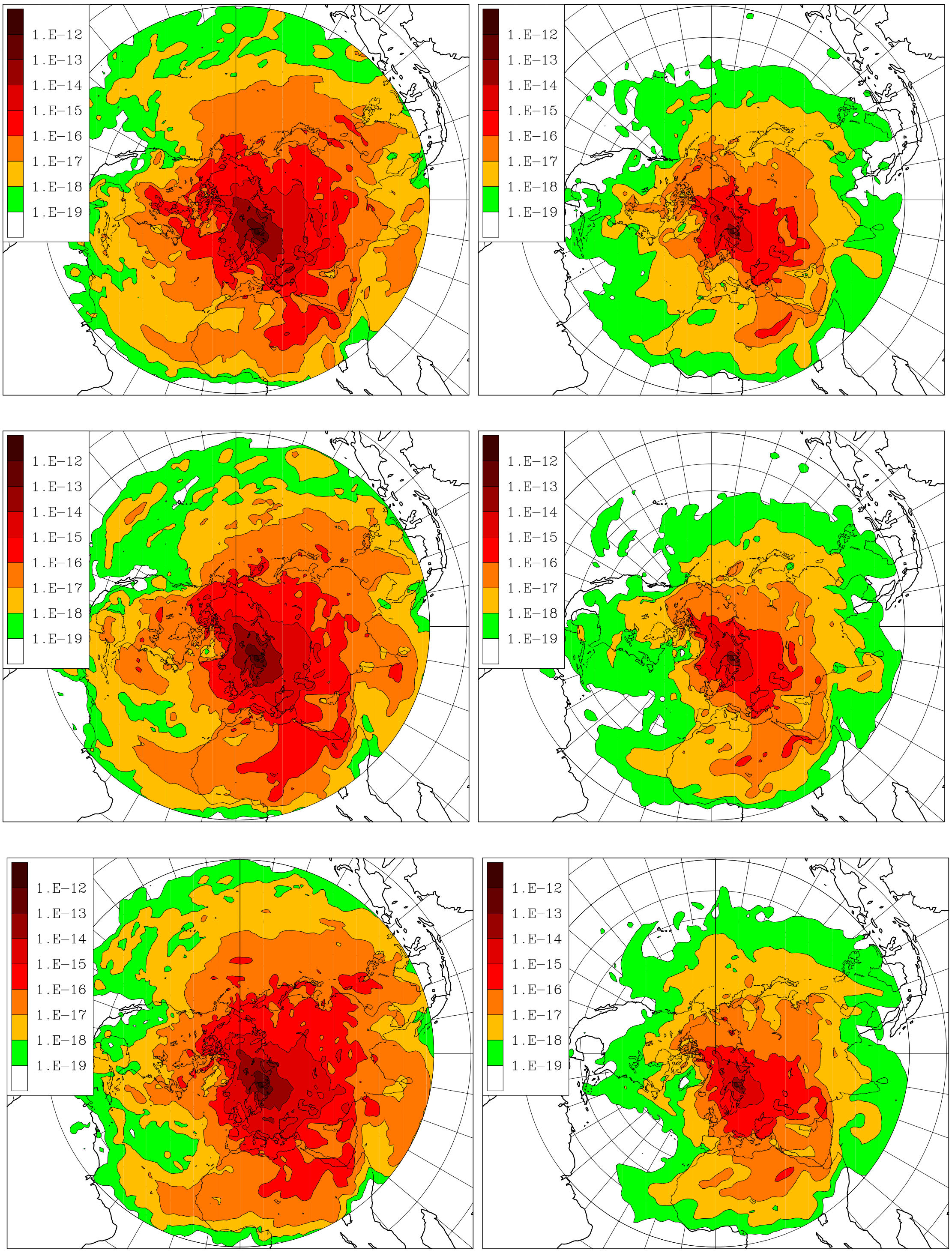

Plate 28 Nuclear power plant: **Kosloduj**; Nuclide: **Caesium-137 aerosol**

Total deposition (m^{-2}) **Time integrated conc. ($h\ m^{-3}$)**

1983

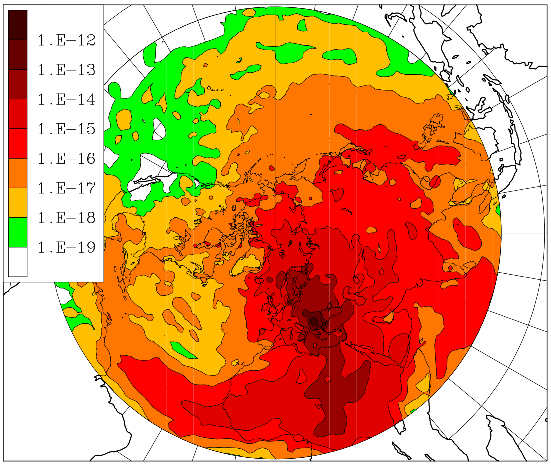

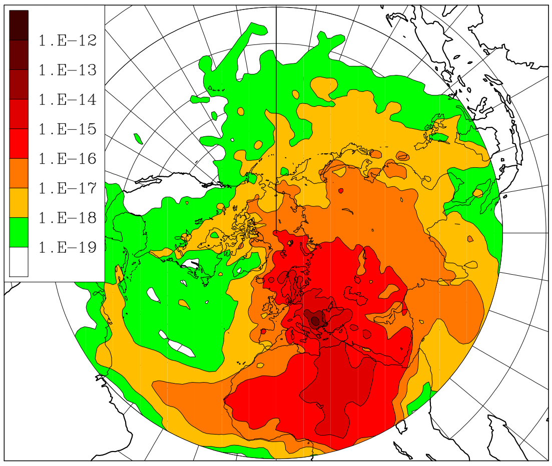

1985

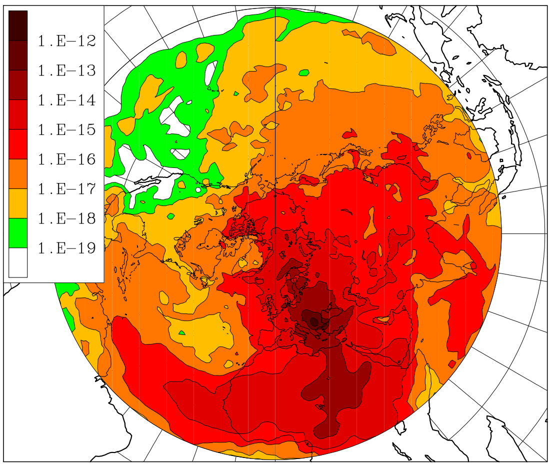

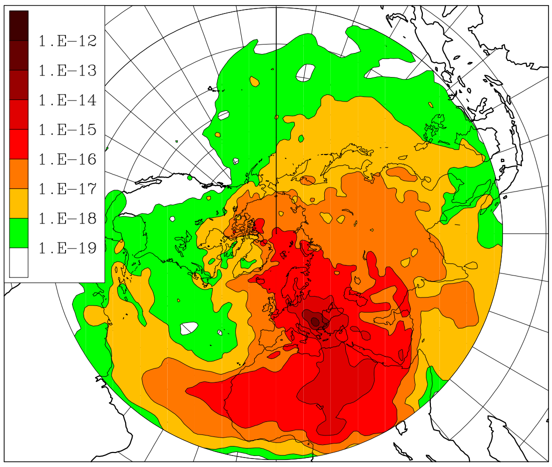

1996

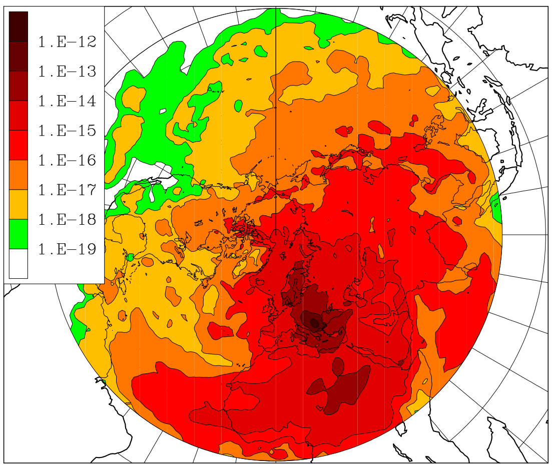

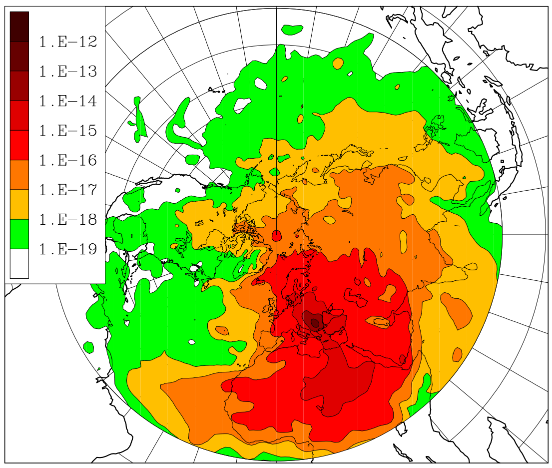

Plate 29 Nuclear power plant: **Kosloduj**; Nuclide: **Iodine-131 gas**

Total deposition (m^{-2}) **Time integrated conc. ($h\ m^{-3}$)**

1983

1985

1996

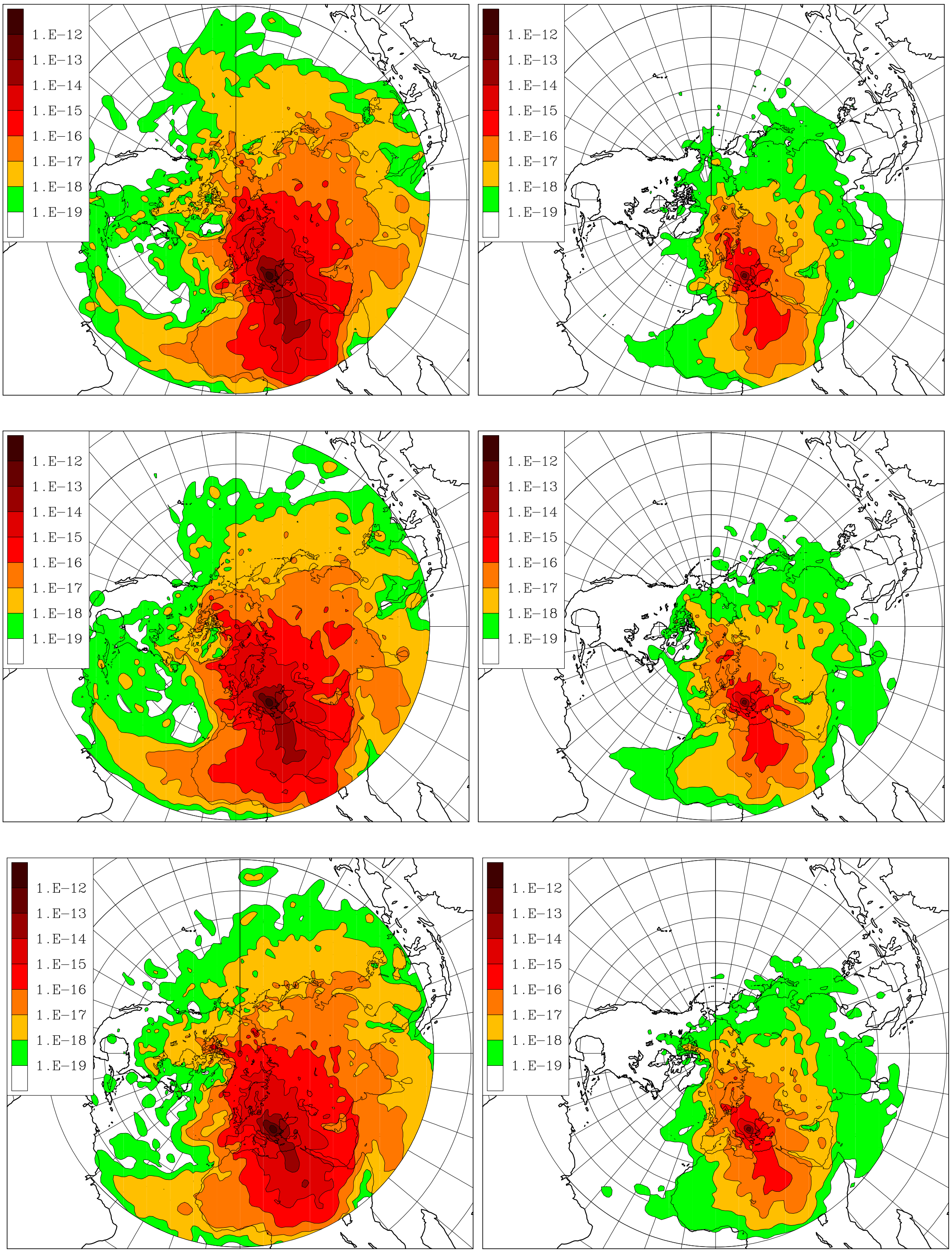

Plate 30 Nuclear power plant: **Kosloduj**; Nuclide: **Iodine-131 aerosol**

Total deposition (m^{-2}) | **Time integrated conc. ($h\ m^{-3}$)**

1983

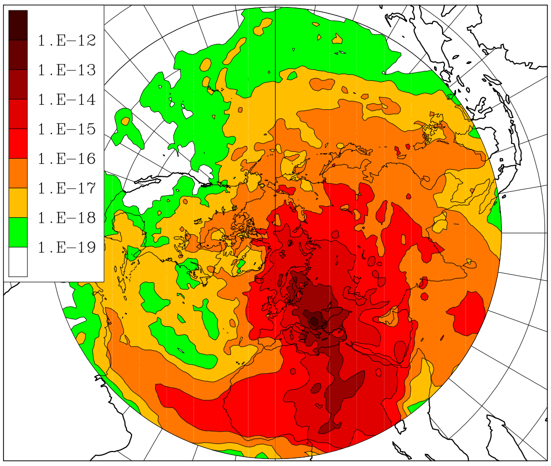

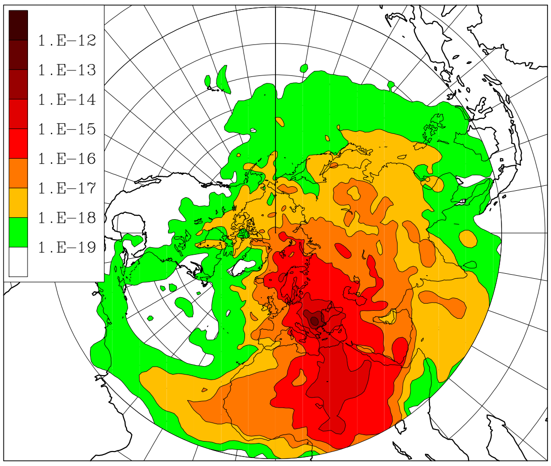

1985

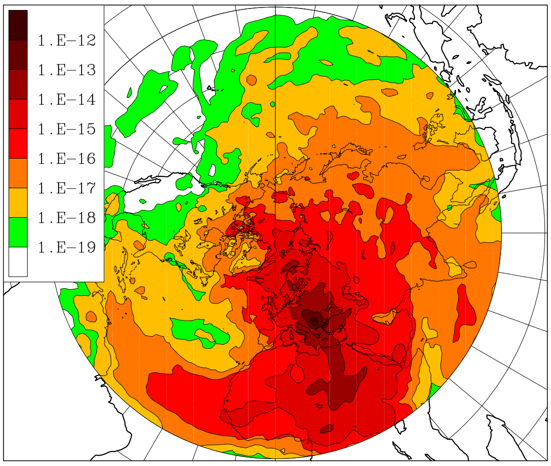

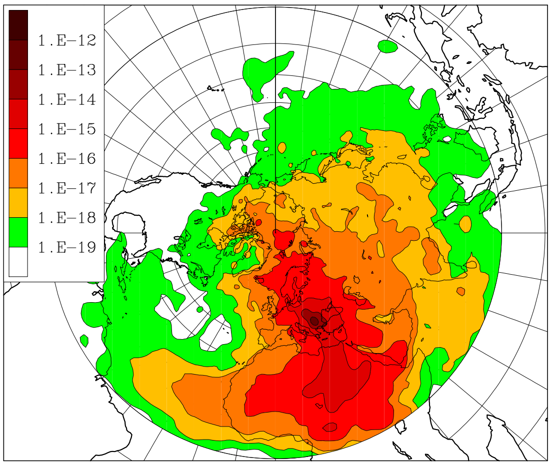

1996

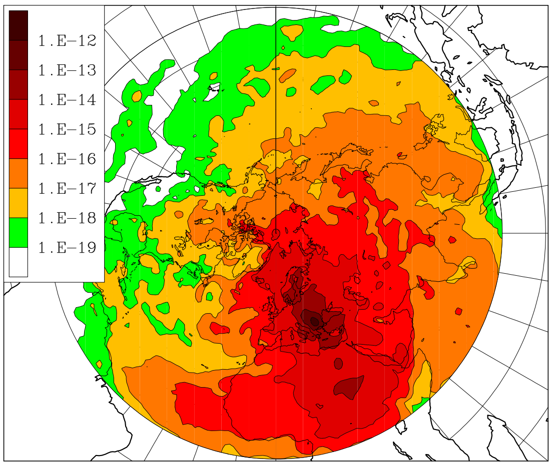

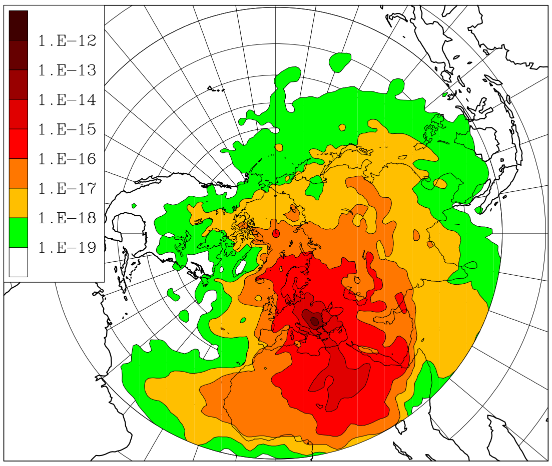

Plate 31 Nuclear power plant: **Leningrad**; Nuclide: **Caesium-137 aerosol**

Total deposition (m^{-2}) **Time integrated conc. ($h\ m^{-3}$)**

1983

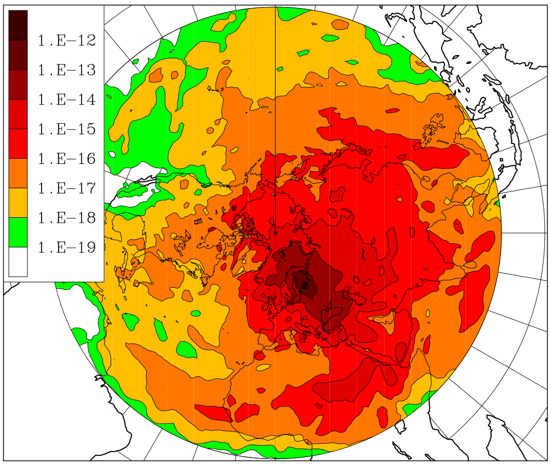

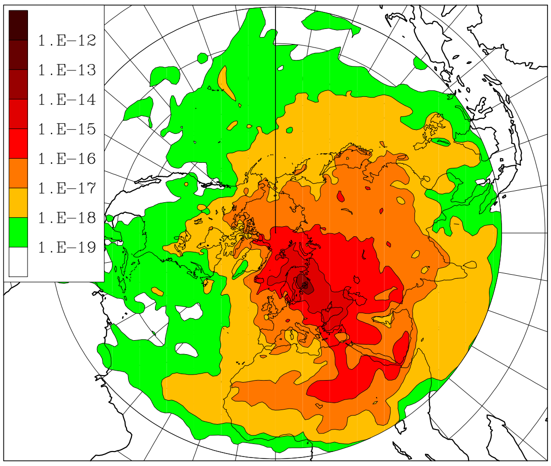

1985

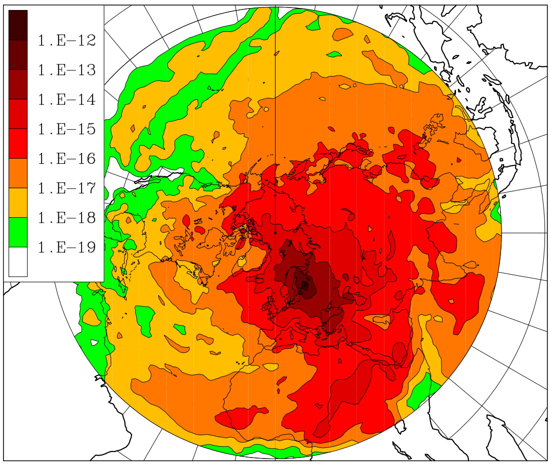

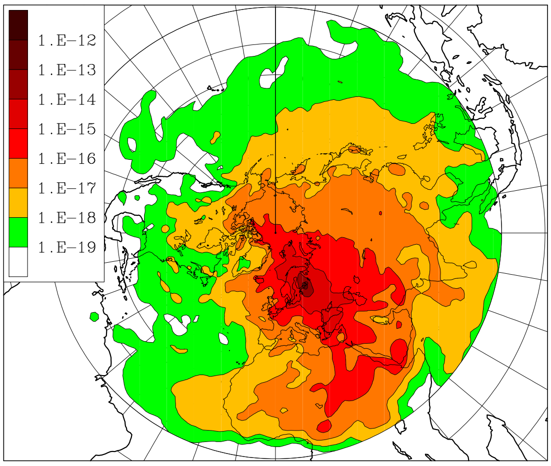

1996

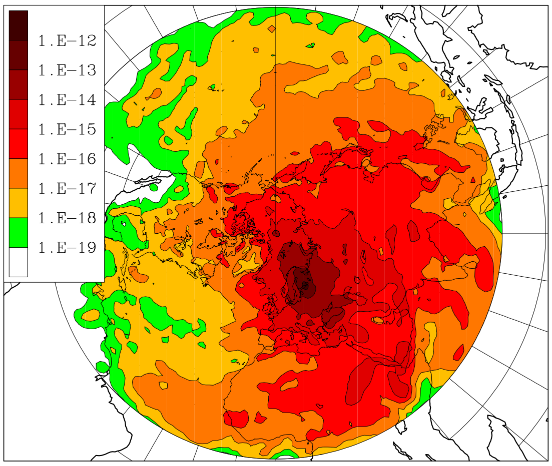

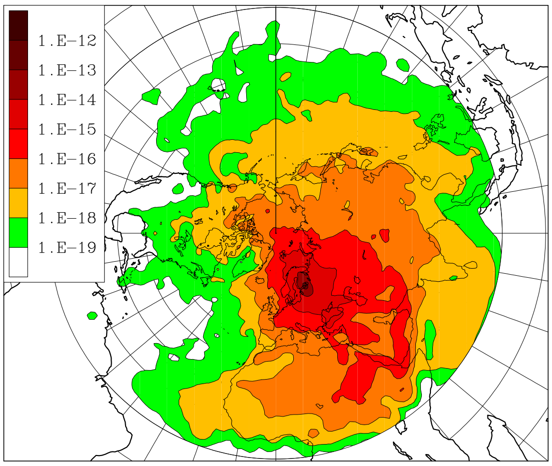

Plate 32 Nuclear power plant: **Leningrad**; Nuclide: **Iodine-131 gas**

Total deposition (m^{-2}) **Time integrated conc. ($h\ m^{-3}$)**

1983

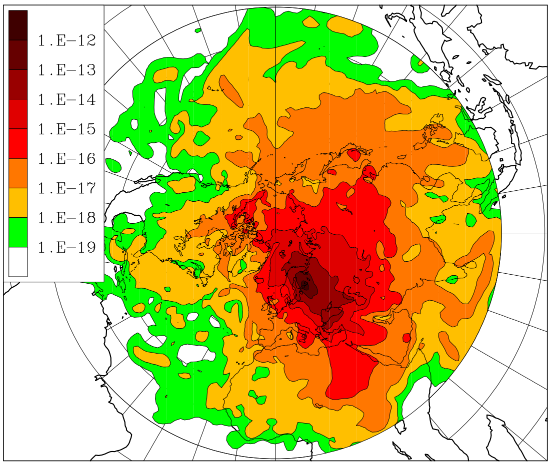

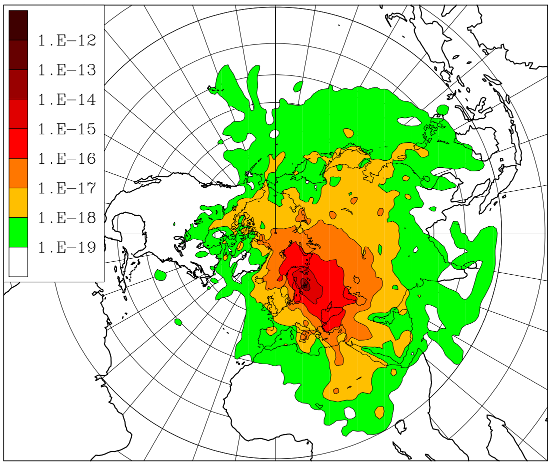

1985

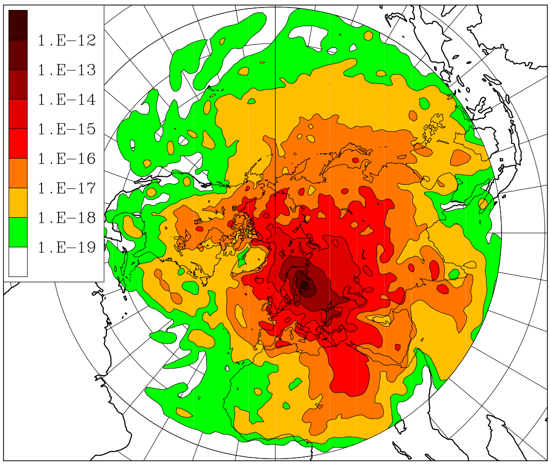

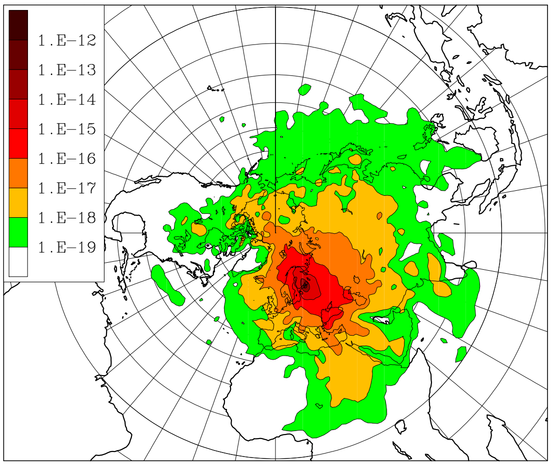

1996

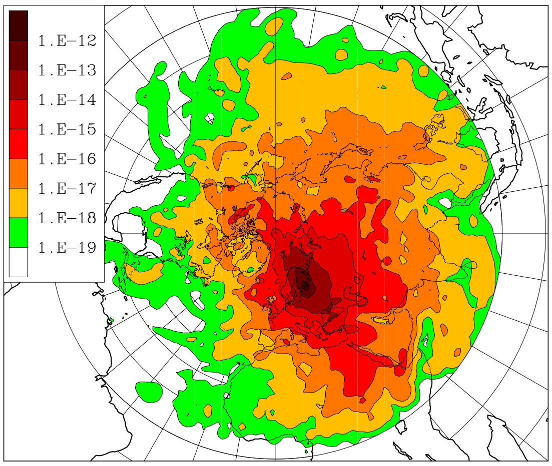

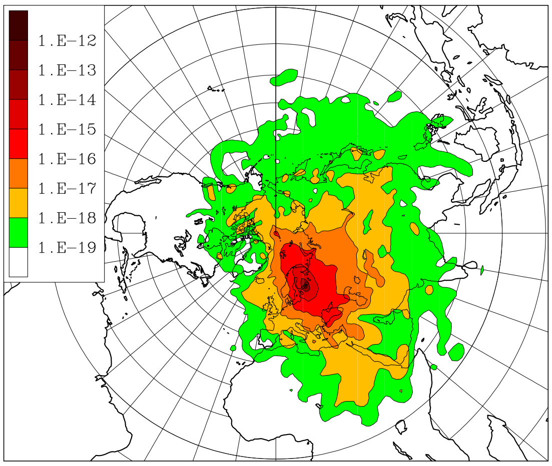

Plate 33 Nuclear power plant: **Leningrad**; Nuclide: **Iodine-131 aerosol**

Total deposition (m^{-2}) **Time integrated conc. ($h\ m^{-3}$)**

1983

1985

1996

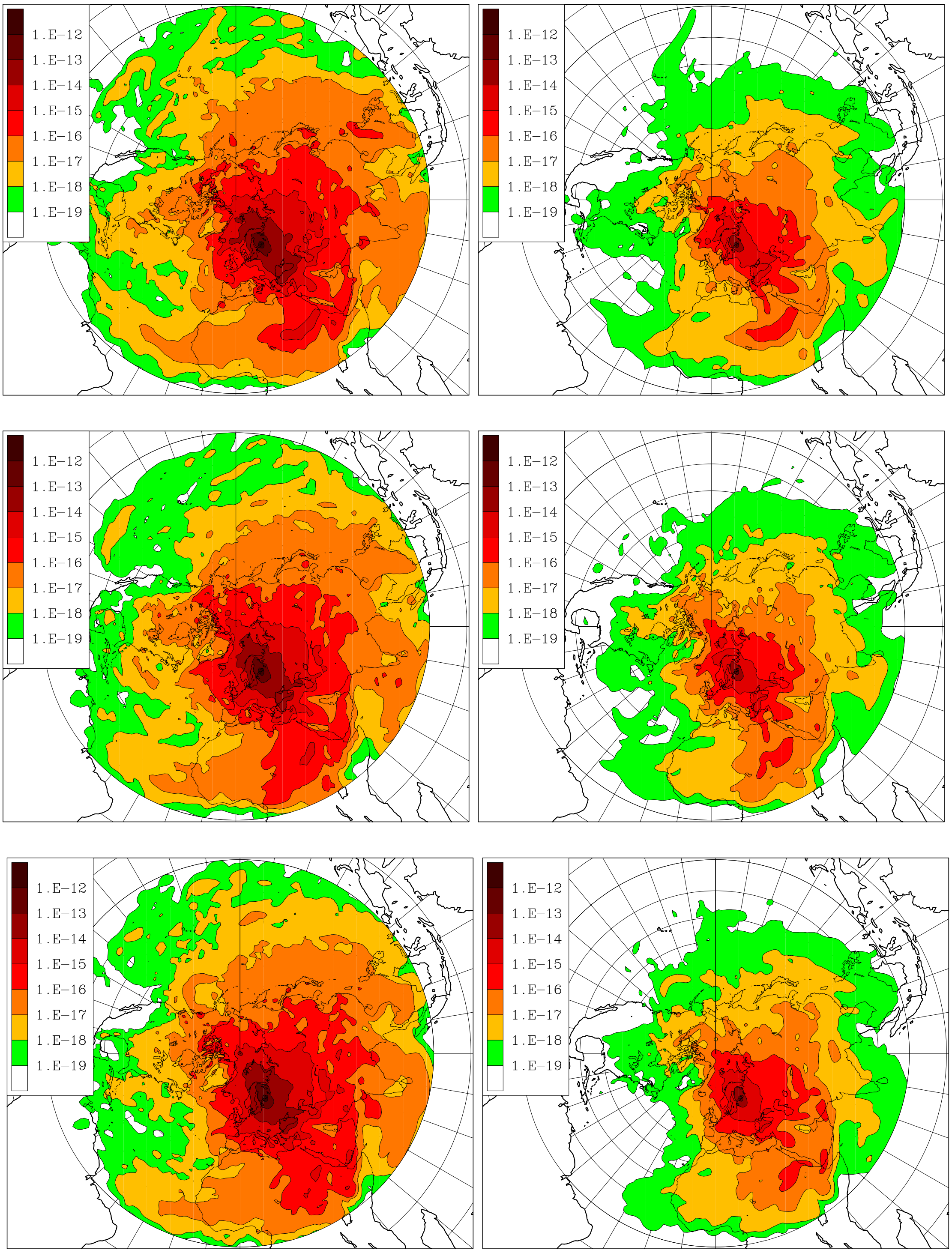

Plate 34 Nuclear power plant: **Novaya Zemlaya**; Nuclide: **Caesium-137 aerosol**

Total deposition (m^{-2}) **Time integrated conc. ($h\ m^{-3}$)**

1983

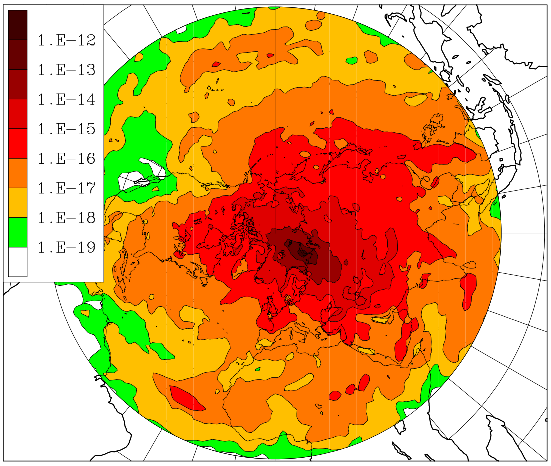

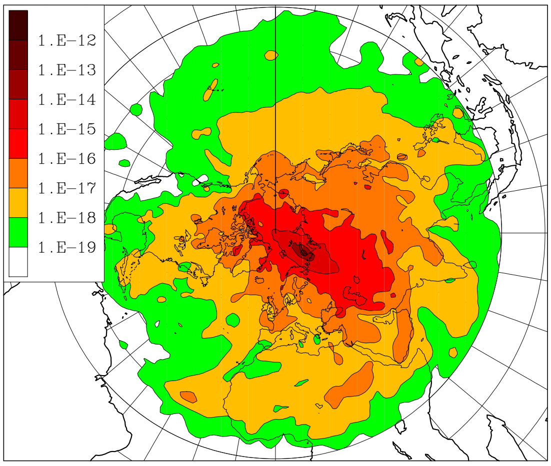

1985

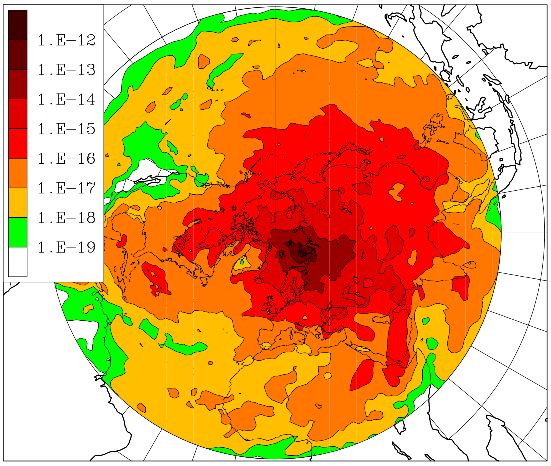

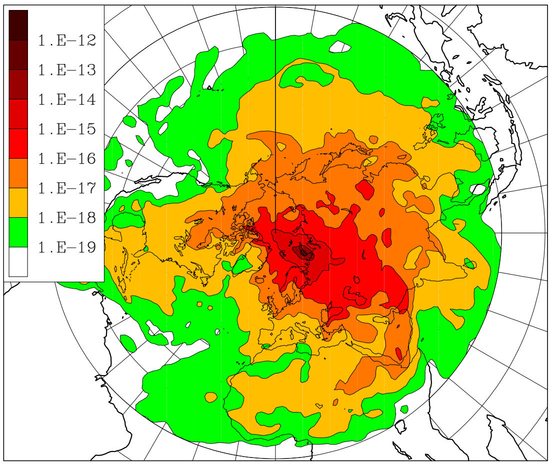

1996

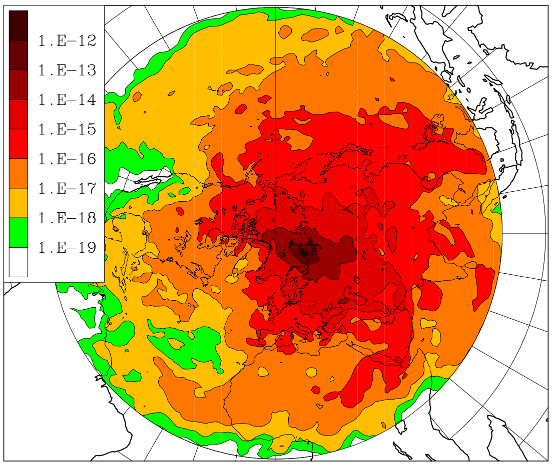

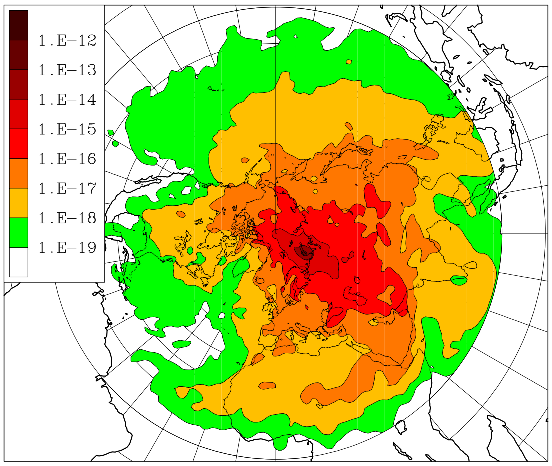

Plate 35 Nuclear power plant: **Novaya Zemlaya**; Nuclide: **Iodine-131 gas**

Total deposition (m^{-2}) **Time integrated conc. ($h\ m^{-3}$)**

1983

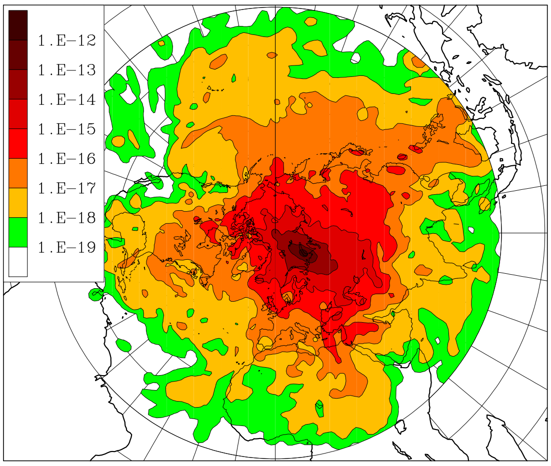

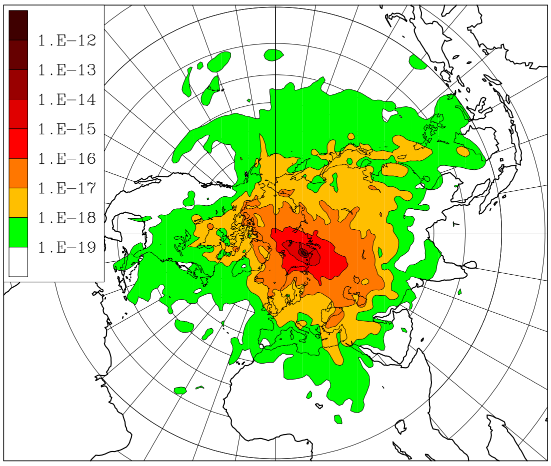

1985

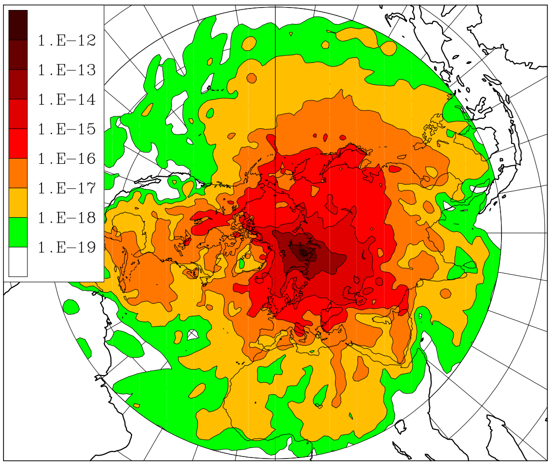

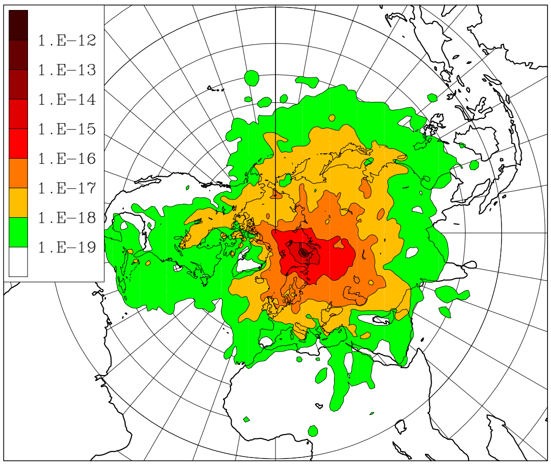

1996

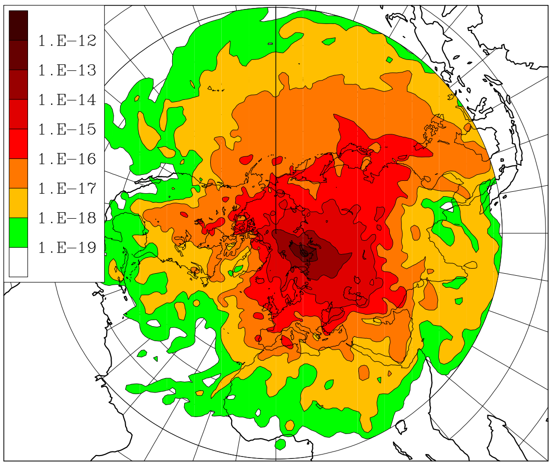

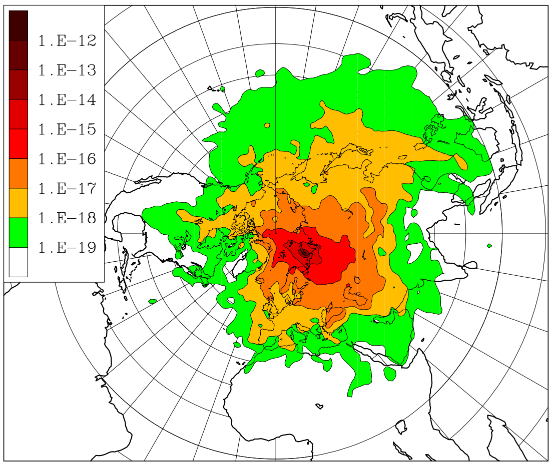

Plate 36 Nuclear power plant: **Novaya Zemlaya**; Nuclide: **Iodine-131 aerosol**

Total deposition (m^{-2}) **Time integrated conc. ($h\ m^{-3}$)**

1983

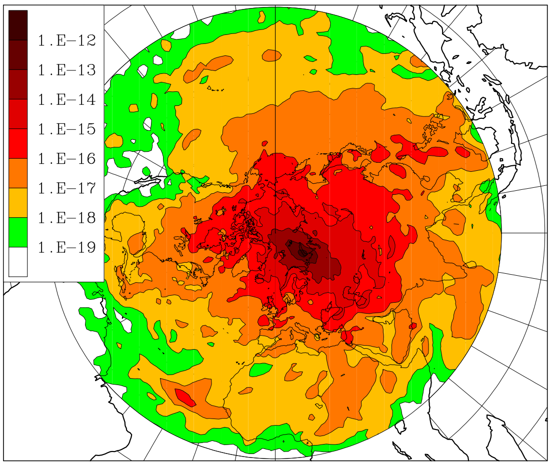

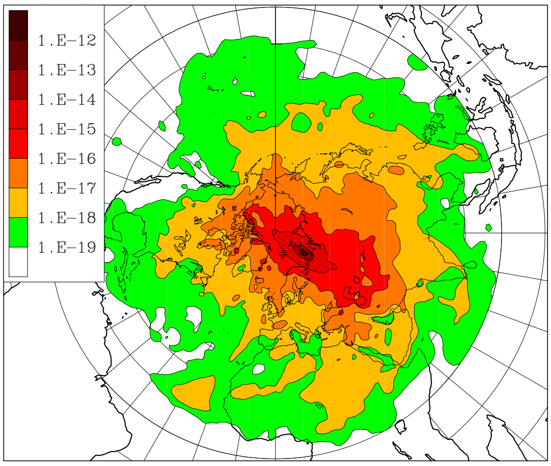

1985

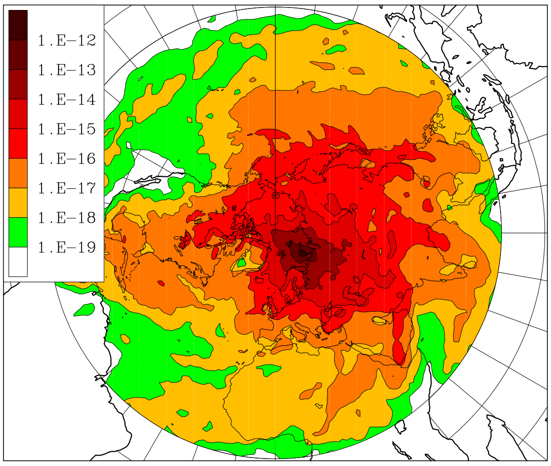

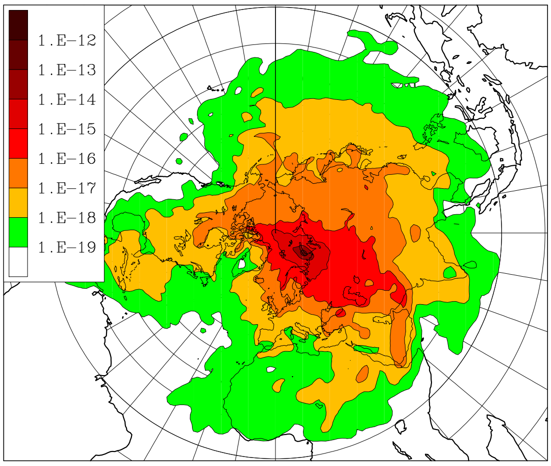

1996

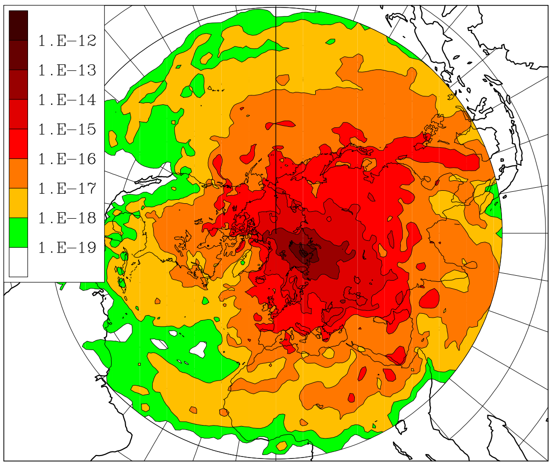

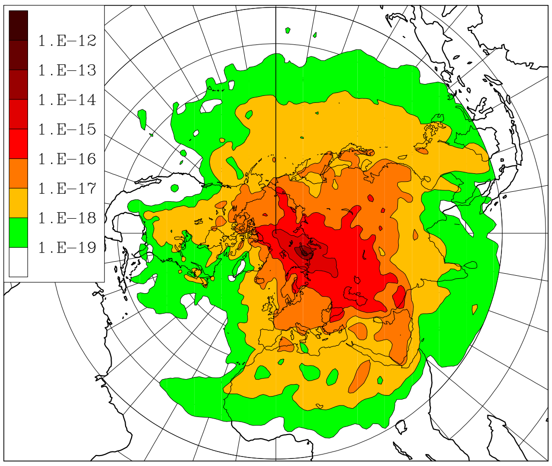

Plate 37 Nuclear power plant: **Sellafield**; Nuclide: **Caesium-137 aerosol**

Total deposition (m^{-2}) **Time integrated conc. ($h\ m^{-3}$)**

1983

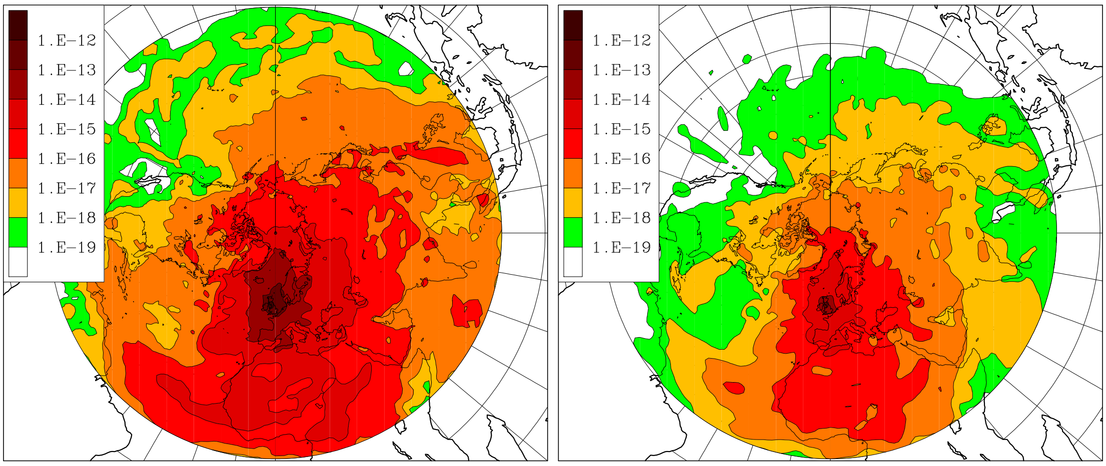

1985

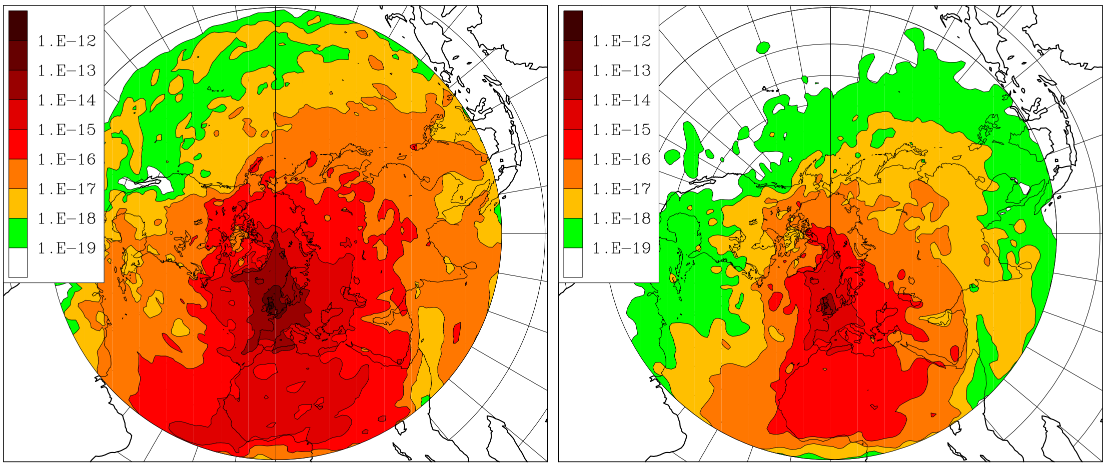

1996

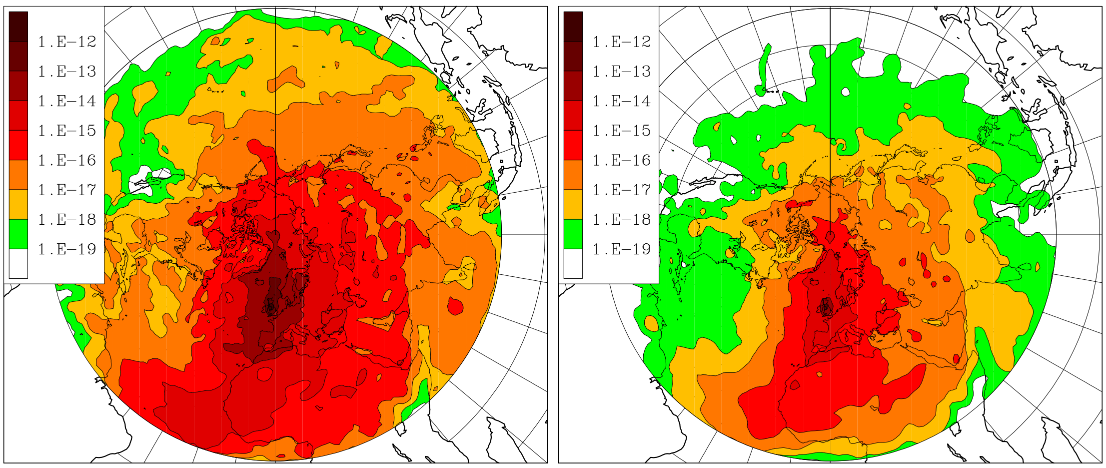

Plate 38 Nuclear power plant: **Sellafield**; Nuclide: **Iodine-131 gas**

Total deposition (m^{-2}) | **Time integrated conc. ($h\ m^{-3}$)**

1983

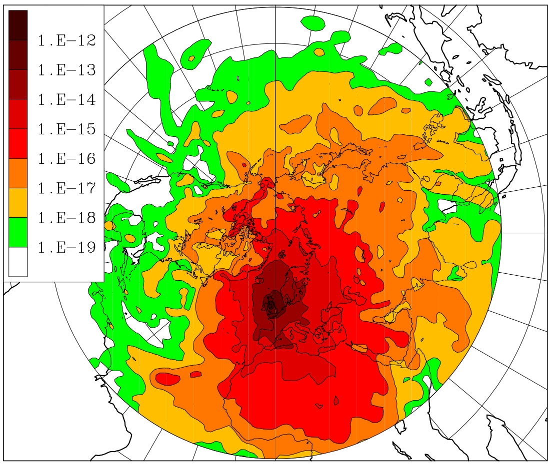

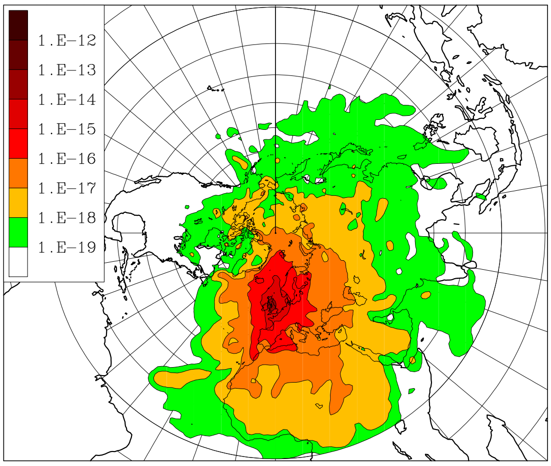

1985

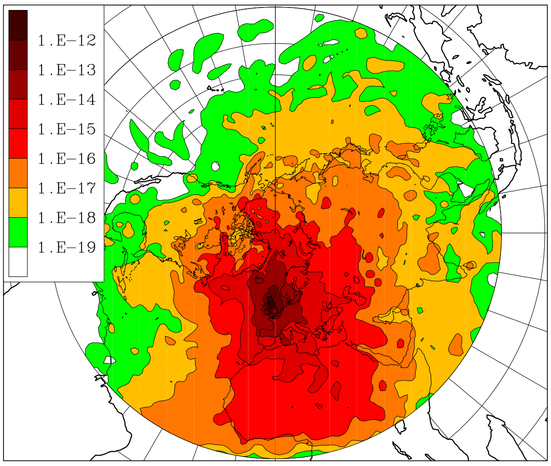

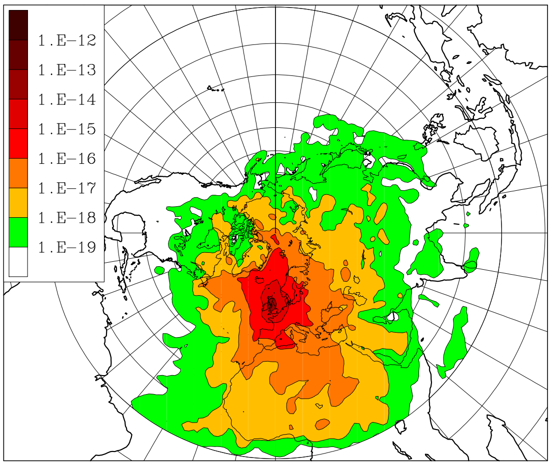

1996

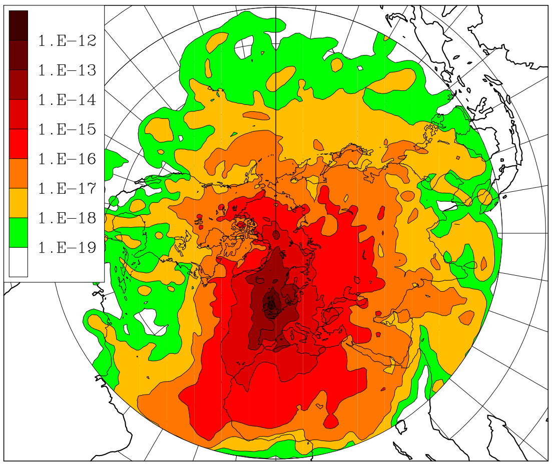

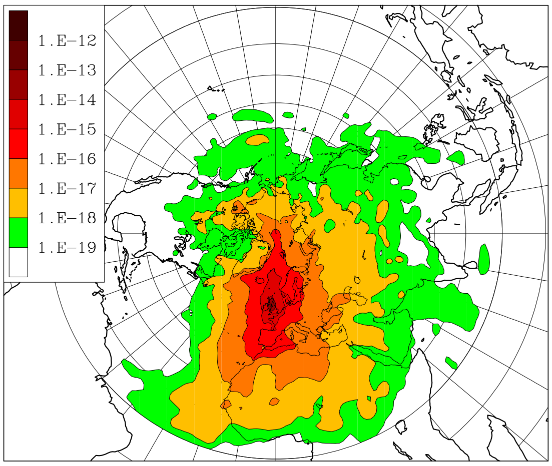

Plate 39 Nuclear power plant: **Sellafield**; Nuclide: **Iodine-131 aerosol**

Total deposition (m^{-2}) **Time integrated conc. ($h\ m^{-3}$)**

1983

1985

1996

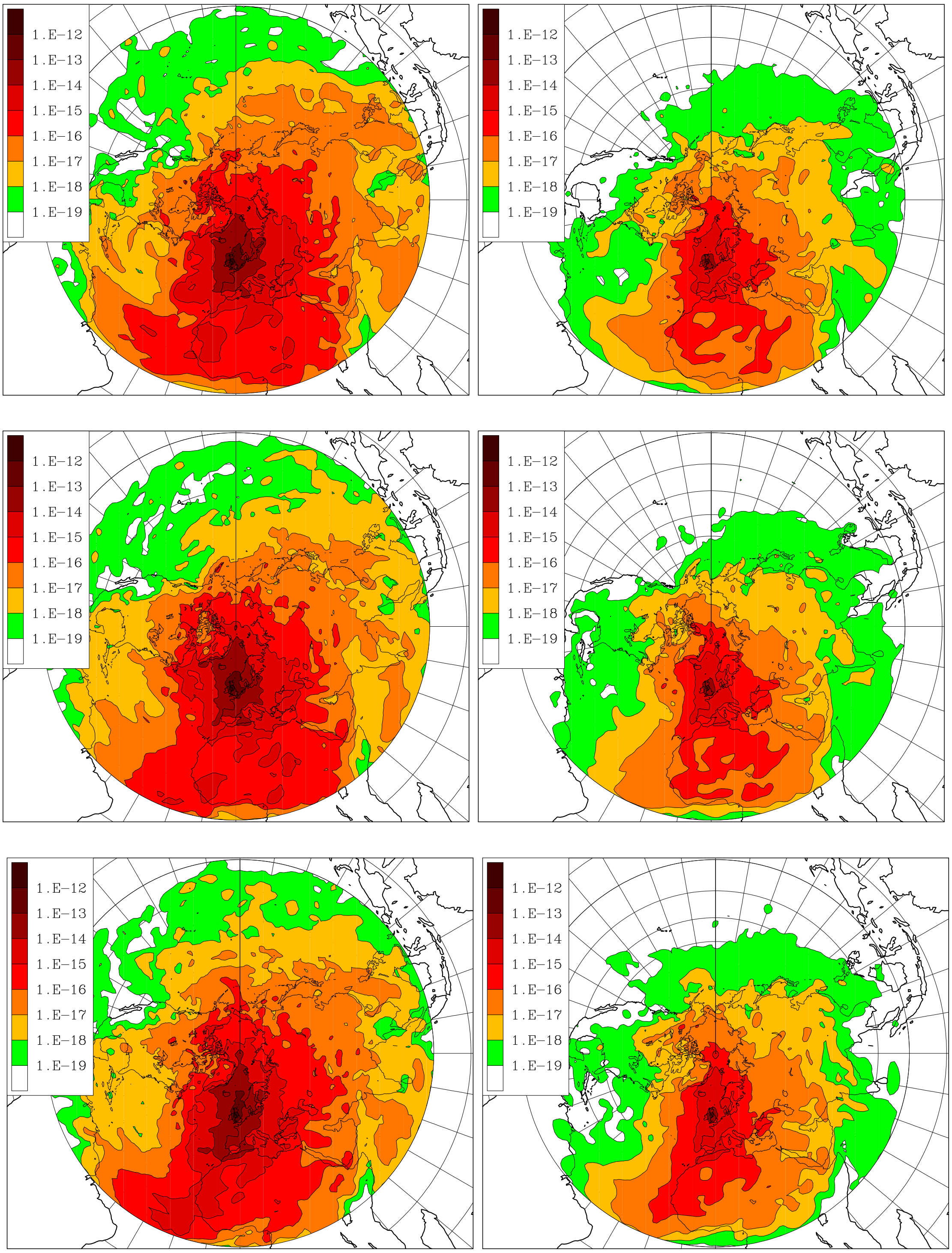

Plate 40 Nuclear power plant: **Sinpo**; Nuclide: **Caesium-137 aerosol**

Total deposition (m^{-2}) **Time integrated conc. ($h\ m^{-3}$)**

1983

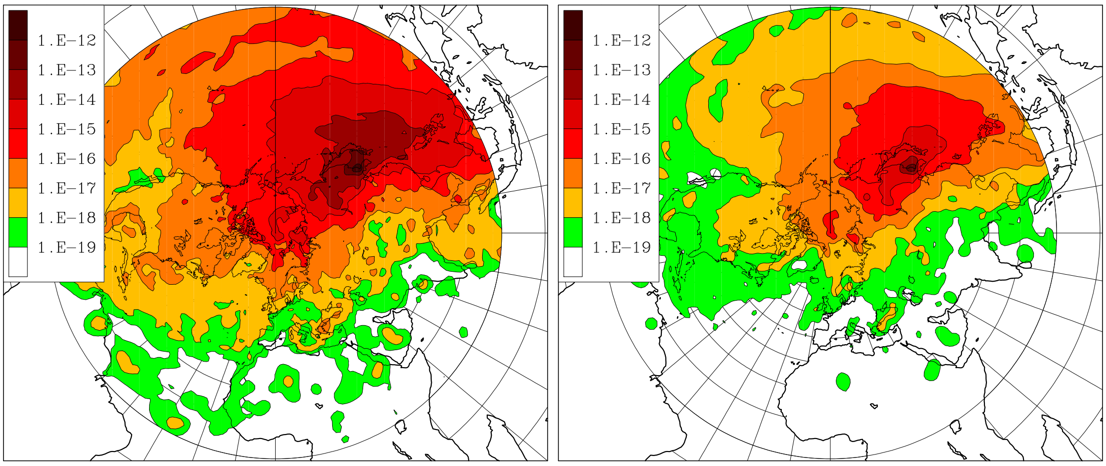

1985

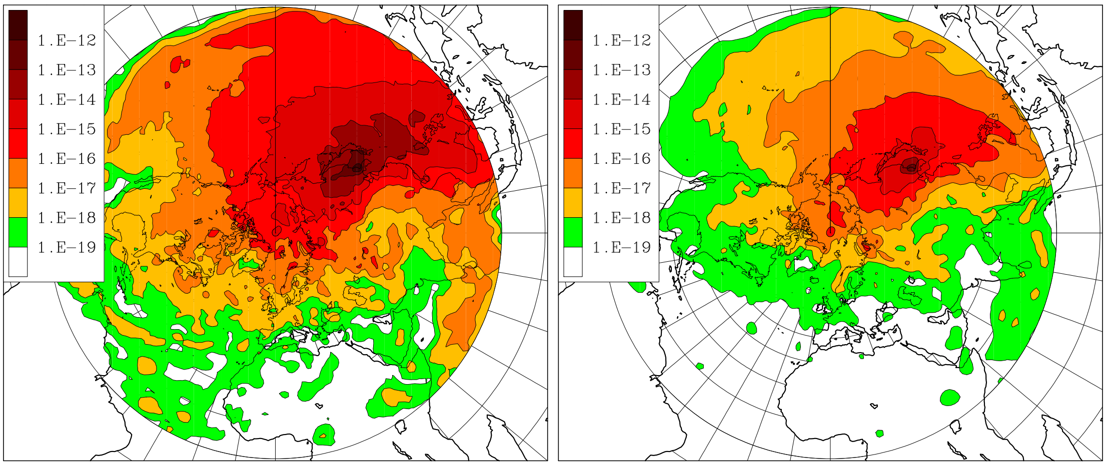

1996

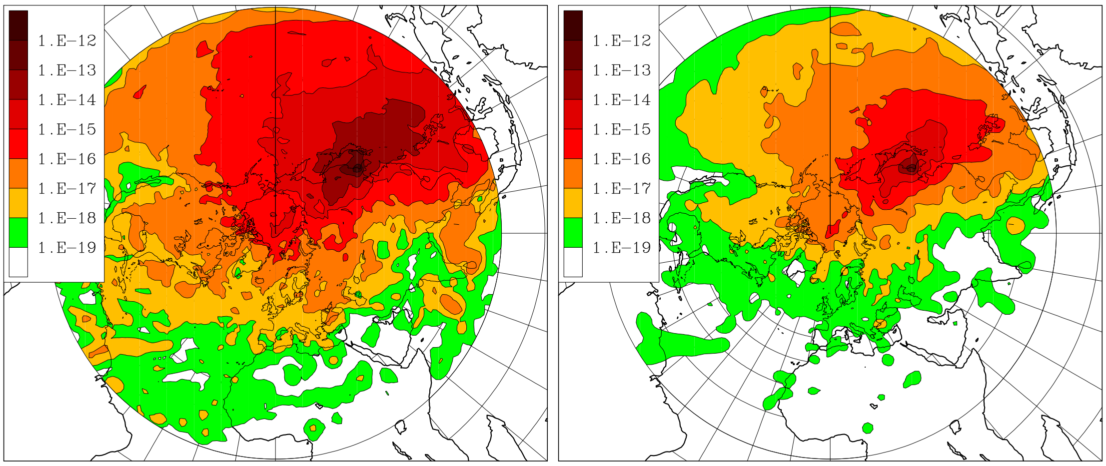

Plate 41 Nuclear power plant: **Sinpo**; Nuclide: **Iodine-131 gas**

Total deposition (m^{-2}) **Time integrated conc. ($h\ m^{-3}$)**

1983

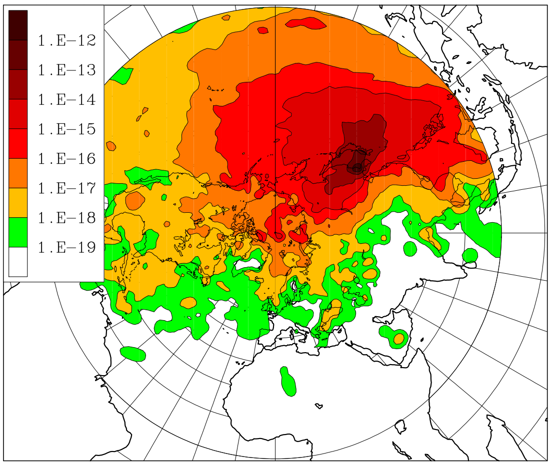

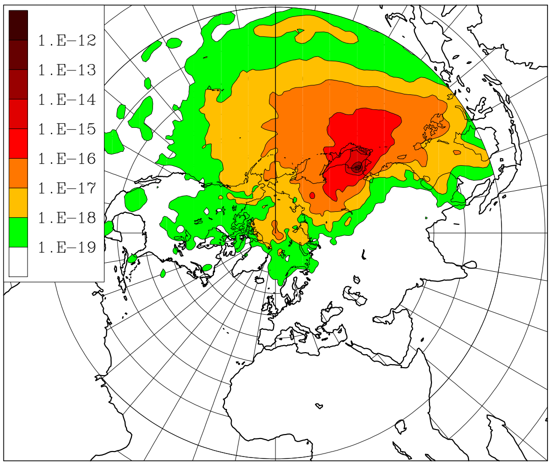

1985

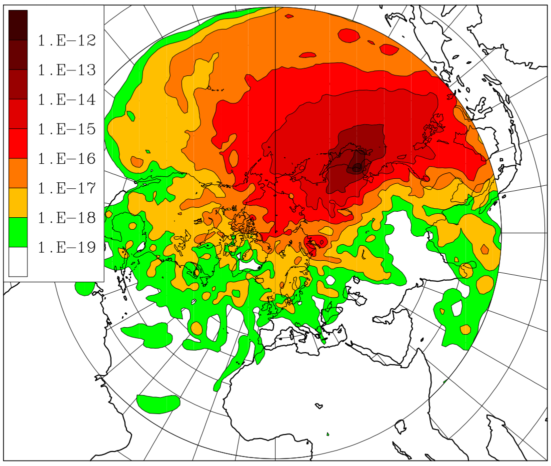

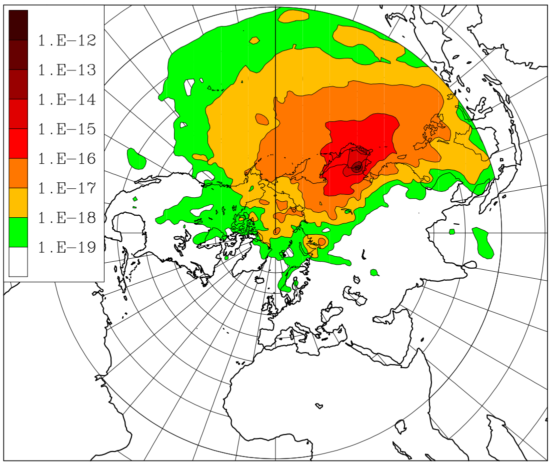

1996

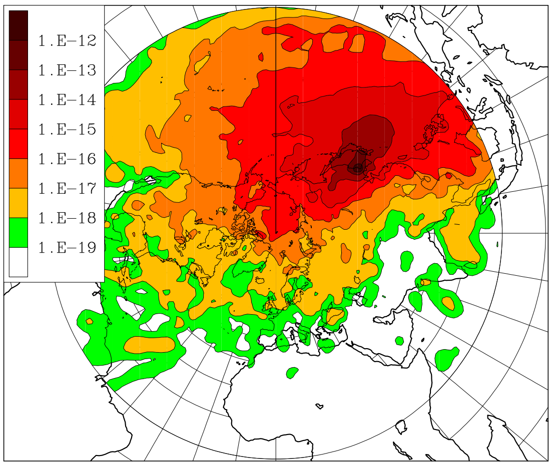

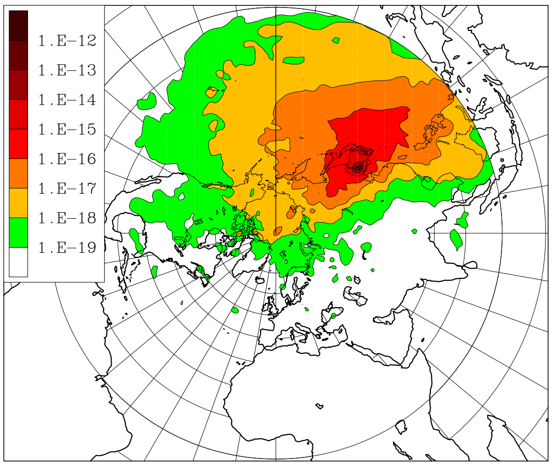

Plate 42 Nuclear power plant: **Sinpo**; Nuclide: **Iodine-131 aerosol**

Total deposition (m^{-2}) **Time integrated conc. ($h\ m^{-3}$)**

1983

1985

1996

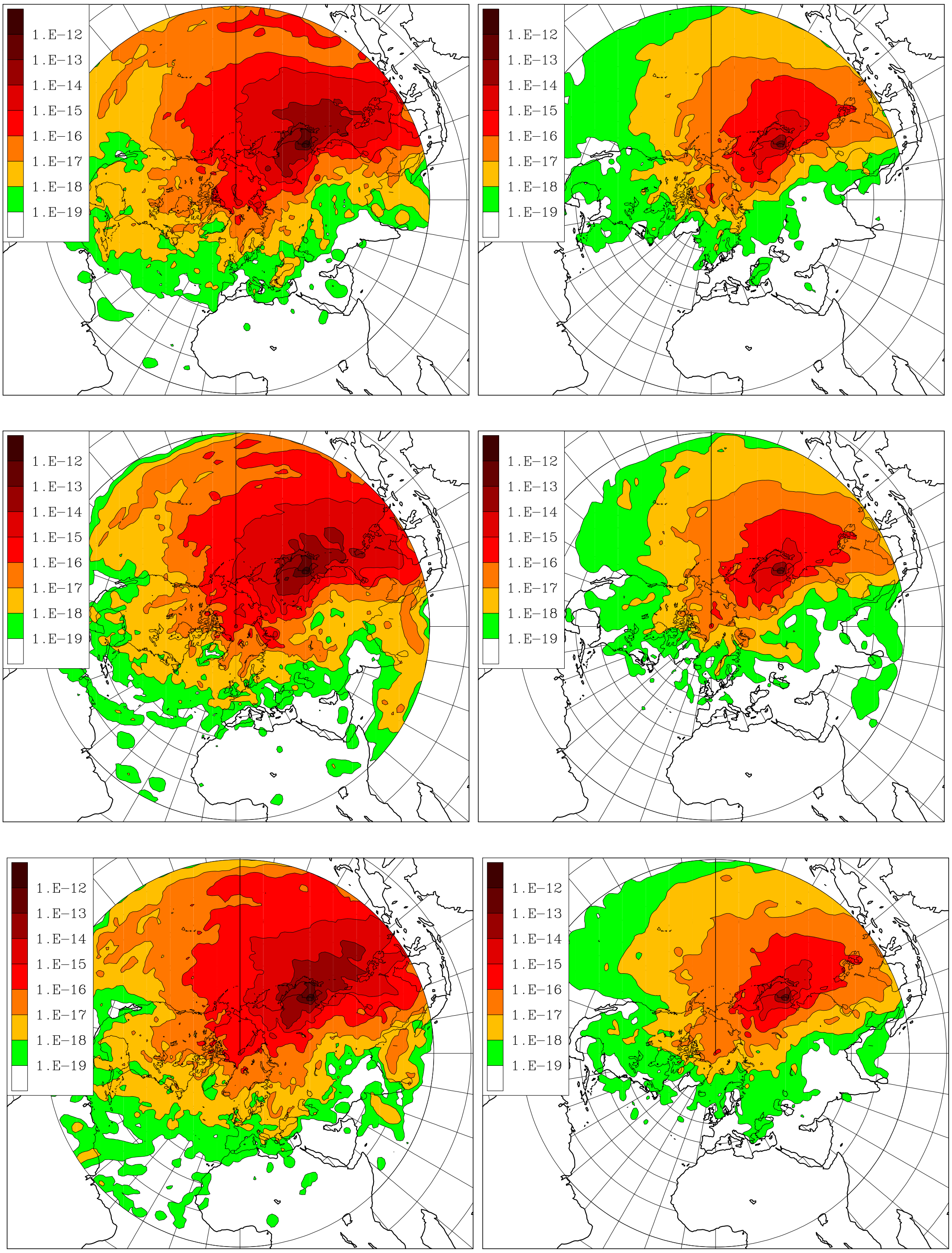

Plate 43 Nuclear power plant: **Savannah River**; Nuclide: **Caesium-137 aerosol**

Total deposition (m^{-2}) **Time integrated conc. ($h\ m^{-3}$)**

1983

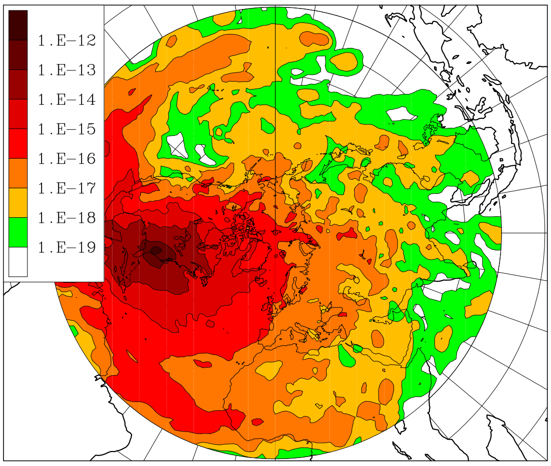

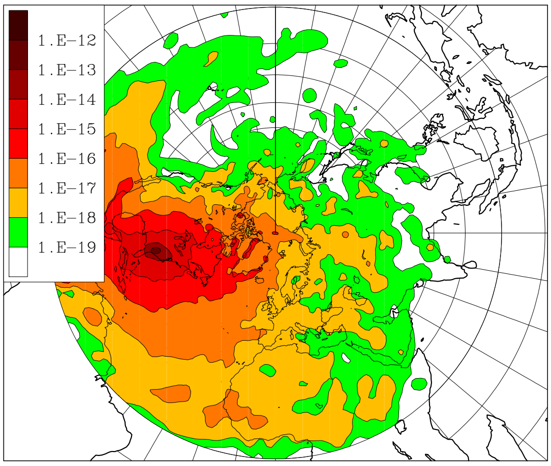

1985

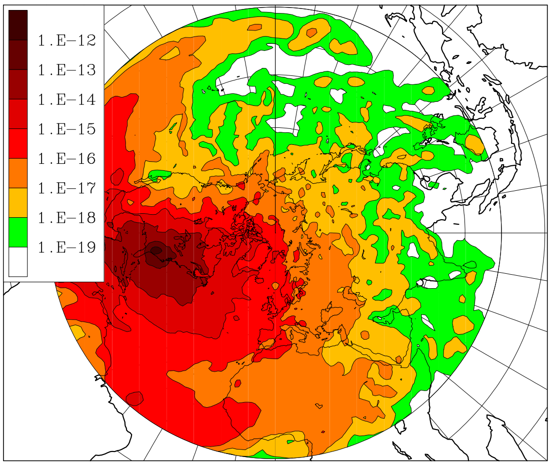

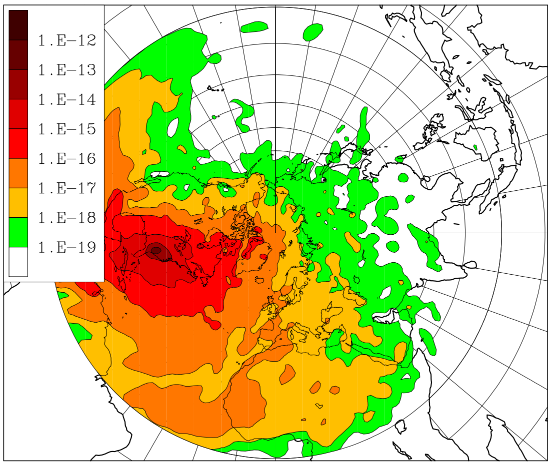

1996

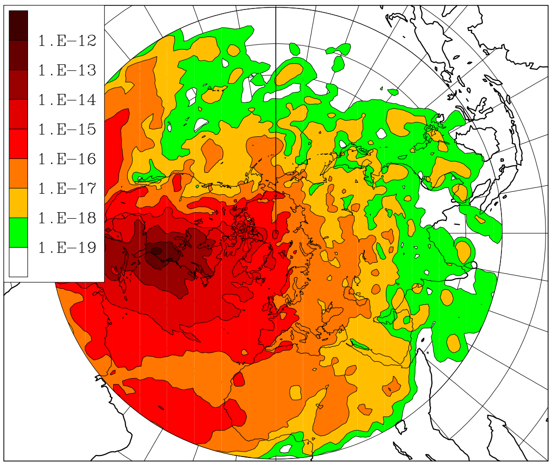

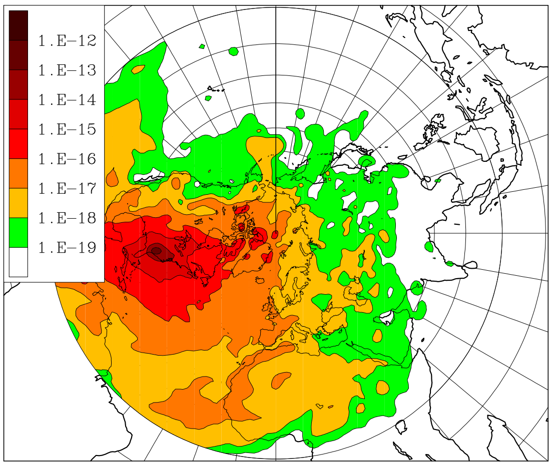

Plate 44 Nuclear power plant: **Savannah River**; Nuclide: **Iodine-131 gas**

Total deposition (m^{-2}) **Time integrated conc. ($h\ m^{-3}$)**

1983

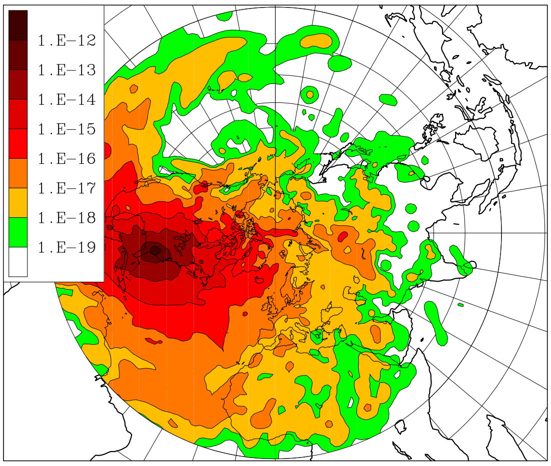

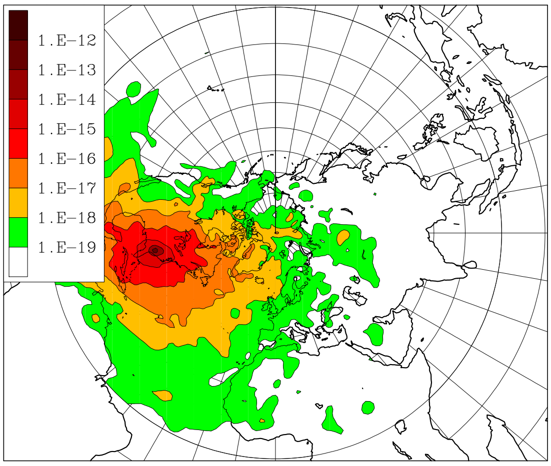

1985

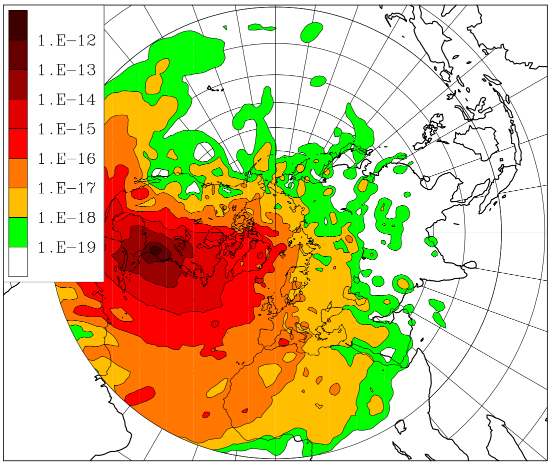

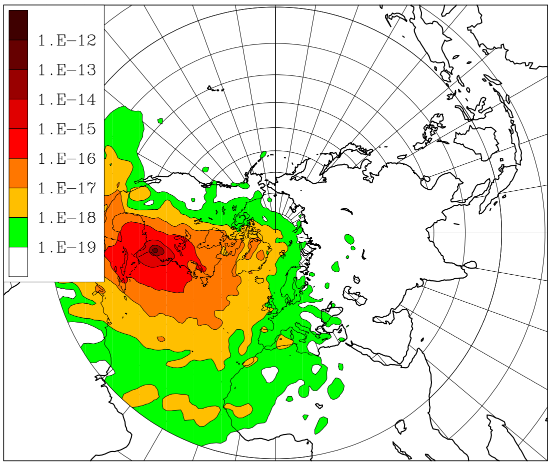

1996

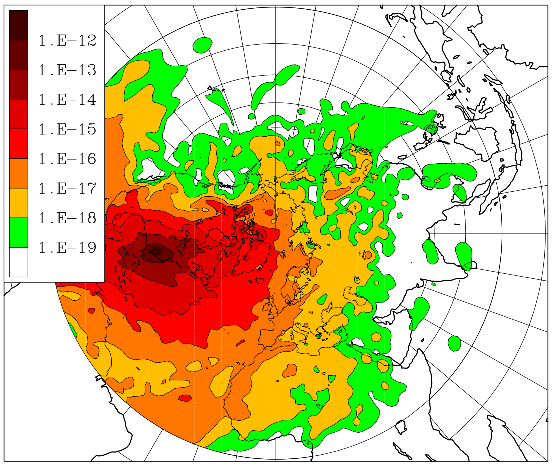

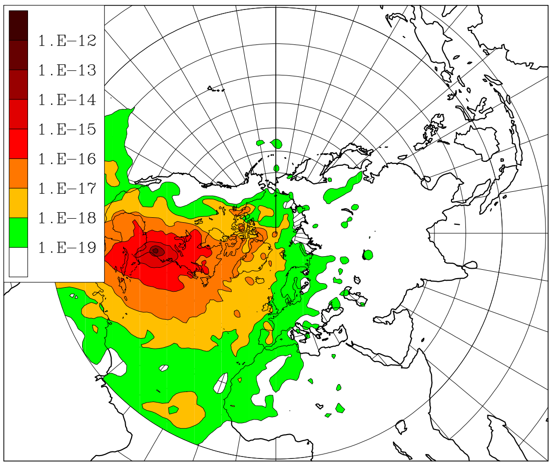

Plate 45 Nuclear power plant: **Savannah River**; Nuclide: **Iodine-131 aerosol**

Total deposition (m^{-2}) **Time integrated conc. ($h\ m^{-3}$)**

1983

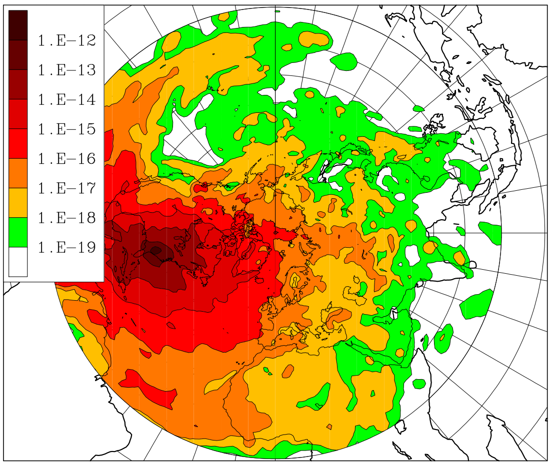

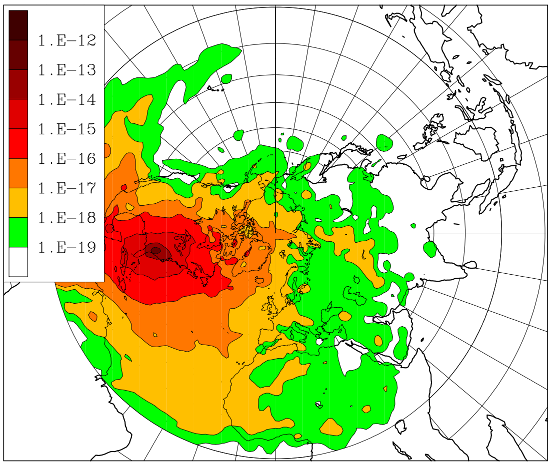

1985

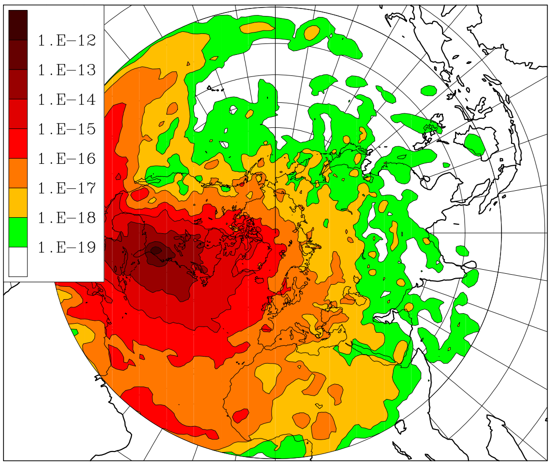

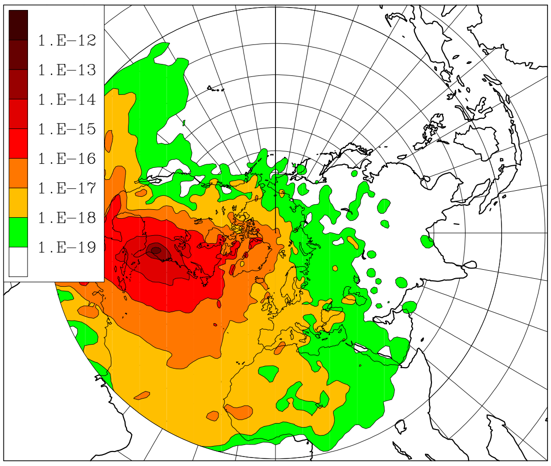

1996

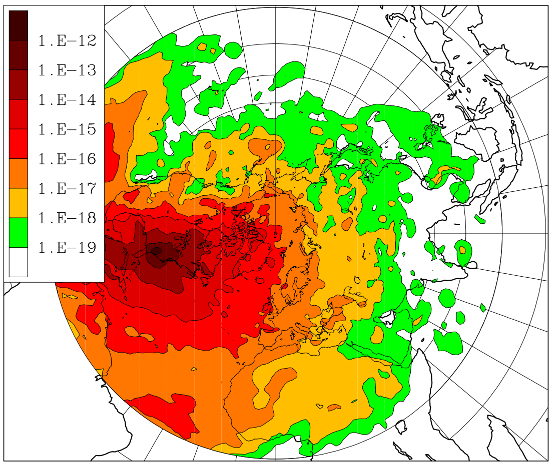

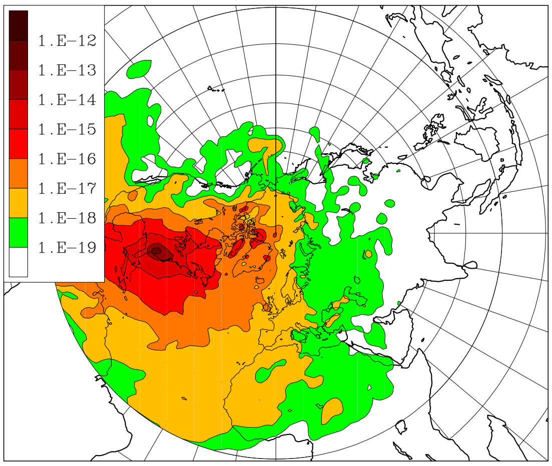

Plate 46 Nuclear power plant: **Tricastin**; Nuclide: **Caesium-137 aerosol**

Total deposition (m^{-2}) **Time integrated conc. ($h\ m^{-3}$)**

1983

1985

1996

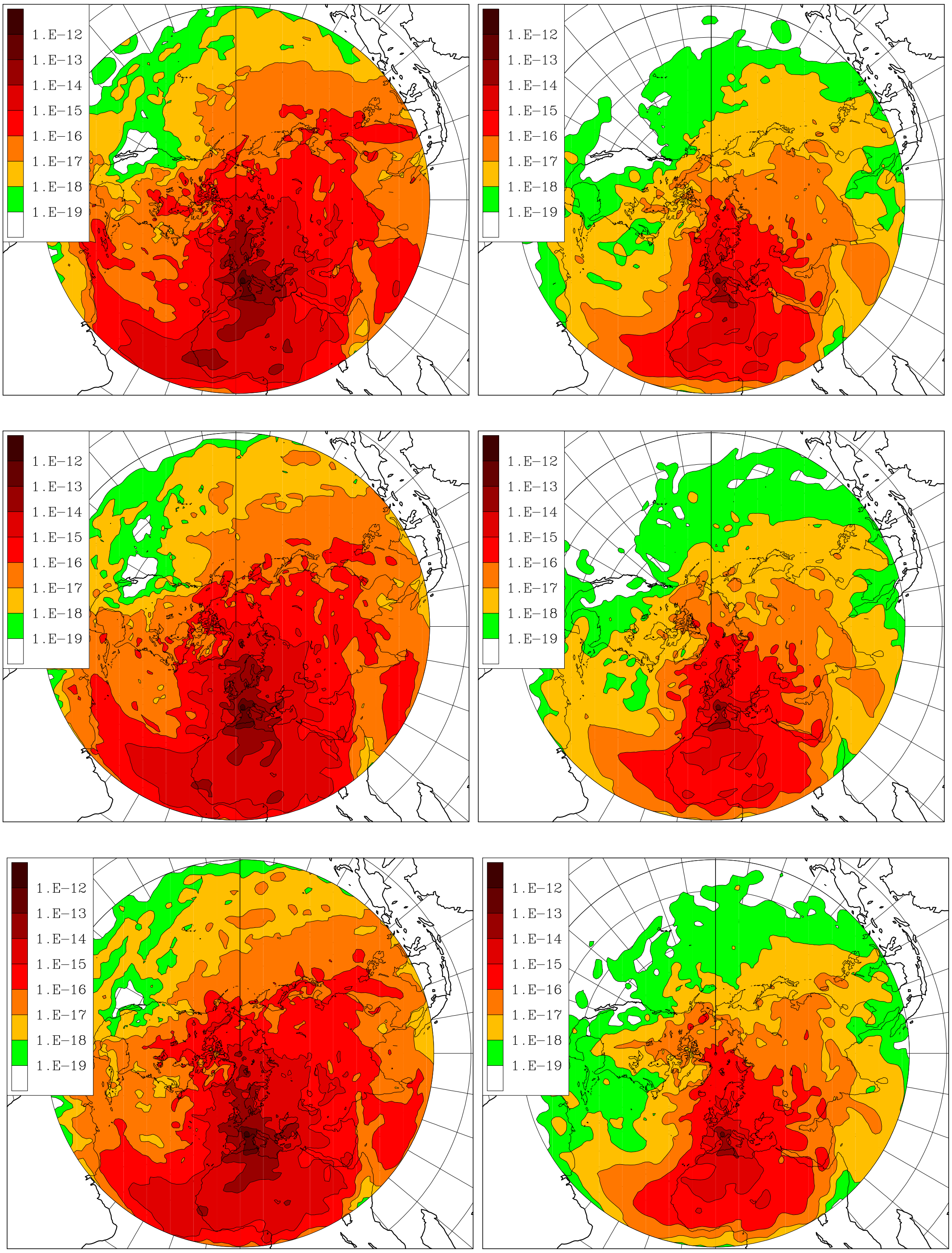

Plate 47 Nuclear power plant: **Tricastin**; Nuclide: **Iodine-131 gas**

Total deposition (m^{-2}) **Time integrated conc. ($h\ m^{-3}$)**

1983

1985

1996

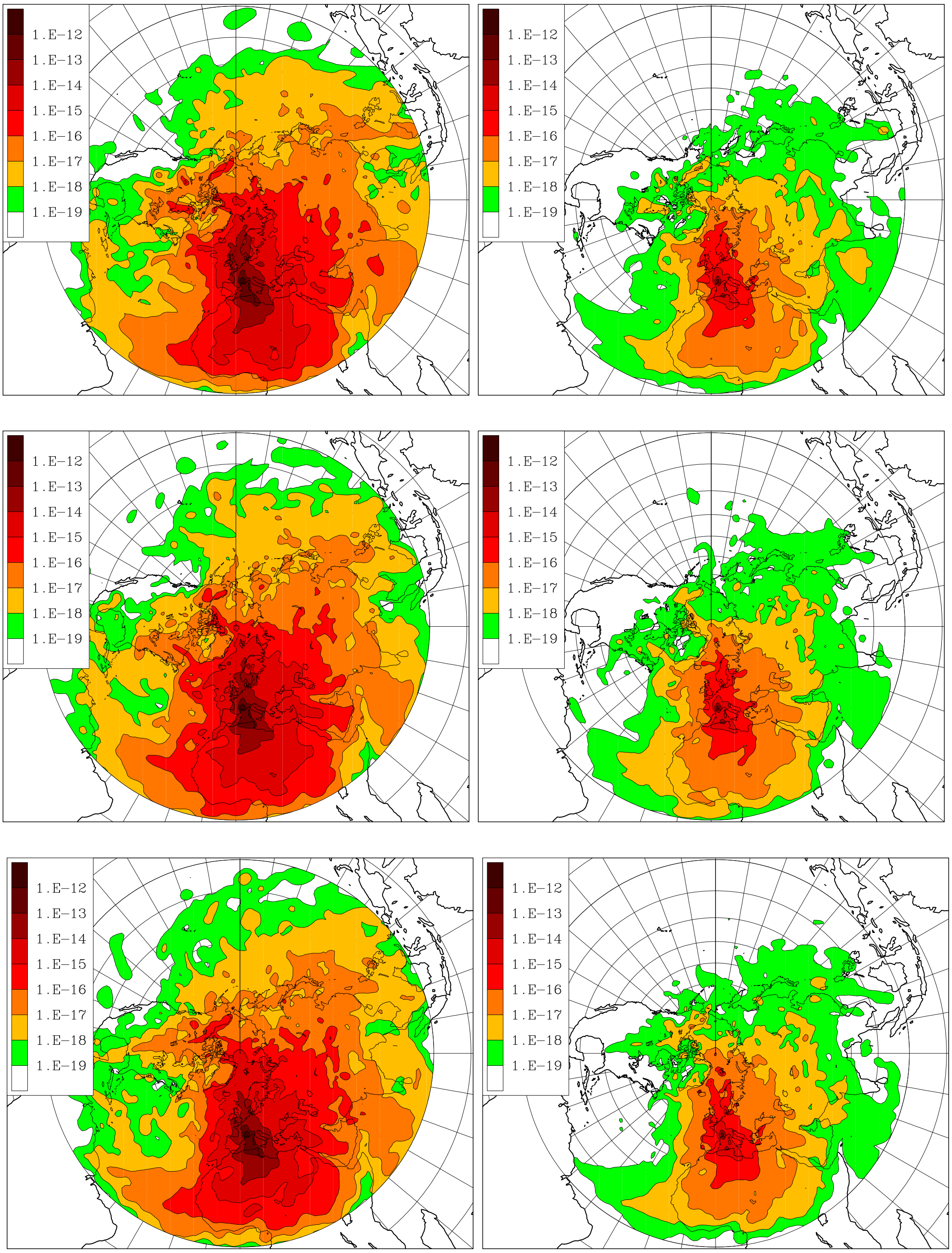

Plate 48 Nuclear power plant: **Tricastin**; Nuclide: **Iodine-131 aerosol**

Total deposition (m^{-2}) | **Time integrated conc. ($h\ m^{-3}$)**

1983

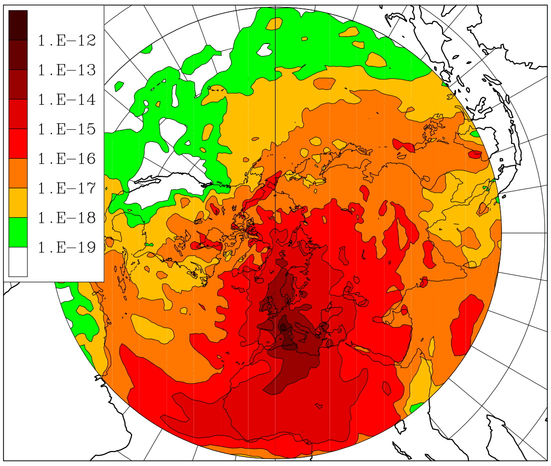

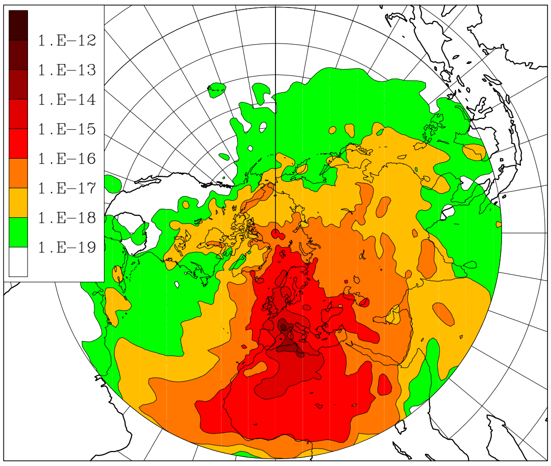

1985

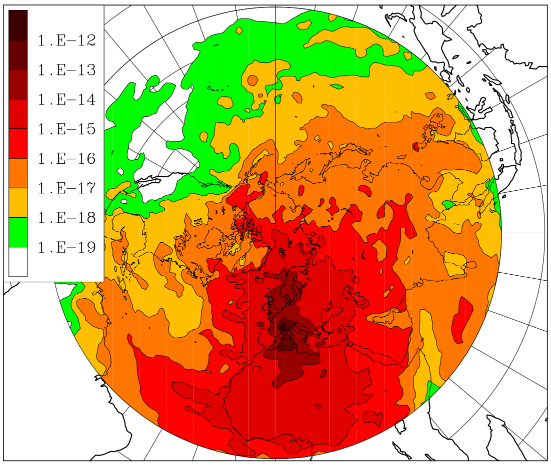

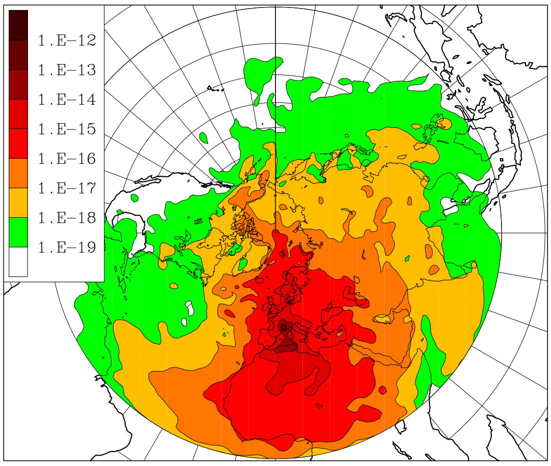

1996

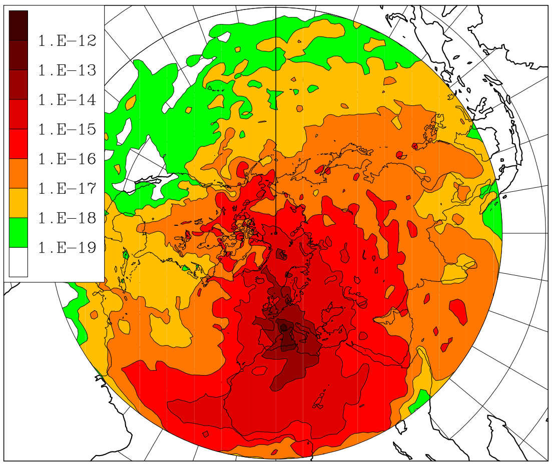

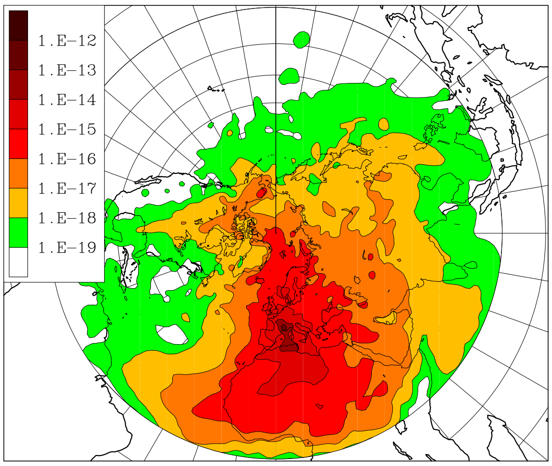

Bibliography

Baklanov, A. and J. H. Sørensen. Parameterisation of Radionuclide Deposition in Atmospheric Long-Range Transport Modelling. Phys. Chem. Earth (B), 26 (2001) 787-799

Baklanov, A., A. Mahura and J. H. Sørensen. Methodology for Prediction and Estimation of Consequences of Possible Atmospheric Releases of Hazardous Matter: Kursk Submarine Study. Atmos. Phys. Chem. 3 (2003) 747-762

Baklanov, A., Sørensen J. H., Mahura A. Long-Term Dispersion Modelling: Part 1: Methodology for Probabilistic Atmospheric Studies. Journal of Computational Technologies, 11 (2006) 136-156

Baklanov, A., J. H. Sørensen and A. Mahura. Methodology for Probabilistic Atmospheric Studies using Long-Term Dispersion Modelling. Environmental Modeling and Assessment, DOI 10.1007/s10666-007-9124-4 (2007)

Galmarini, S., R. Bianconi, W. Klug, T. Mikkelsen, R. Addis, S. Andronopoulos, P. Astrup, A. Baklanov, J. Bartnicki, J. C. Bartzis, R. Bellasio, F. Bompay, R. Buckley, M. Bouzom, H. Champion, R. DAmours, E. Davakis, H. Eleveld, G. T. Geertsema, H. Glaab, M. Kollax, M. Ilvonen, A. Manning, U. Pechinger, C. Persson, E. Polreich, S. Potemski, M. Prodanova, J. Saltbones, H. Slaper, M. A. Sofiev, D. Syrakov, J. H. Sørensen, L. Van der Auwera, I. Valkama, R. Zelazny. Can the Confidence in Long Range Atmospheric Transport Models Be Increased? The Pan-European Experience of ENSEMBLE. Radiat. Prot. Dosim. 109 (2004a) 19-24

Galmarini, S., R. Bianconi, W. Klug, T. Mikkelsen, R. Addis, S. Andronopoulos, P. Astrup, A. Baklanov, J. Bartniki, J. C. Bartzis, R. Bellasio, F. Bompay, R. Buckley, M. Bouzom, H. Champion, R. DAmours, E. Davakis, H. Eleveld, G. T. Geertsema, H. Glaab, M. Kollax, M. Ilvonen, A. Manning, U. Pechinger, C. Persson, E. Polreich, S. Potemski, M. Prodanova, J. Saltbones, H. Slaper, M. A. Sofiev, D. Syrakov, J. H. Sørensen, L. Van der Auwera, I. Valkama, R. Zelazny. Ensemble Dispersion Forecasting, Part I: Concept, Approach and Indicators. Atmos. Environ. 38 (2004b) 4607-4617

Hoe, S., H. Mller, F. Gering, S. Thykier-Nielsen and J. H. Sørensen. ARGOS 2001 a Decision Support System for Nuclear Emergencies. In: Proceedings of the Radiation Protection and Shielding Division Topical Meeting, April 14-17, 2002, Santa Fe, New Mexico, USA

Lauritzen, B., A. Baklanov, A. Mahura, T. Mikkelsen, and J. H. Sørensen. Risk assessment for long-range atmospheric transport of radionuclides. The 2nd International Conference on Radioactivity in the Environment & the 6th International Conference on Environmental Radioactivity in the Arctic and the Antarctic, 26 October 2005, Nice, France (Eds. P. Strand, P. Børretzen, and T. Jølle) 427-430

Lauritzen, B., A. Baklanov, A. Mahura, T. Mikkelsen and J. H. Sørensen. K-model description of probabilistic long-range atmospheric transport in the Northern Hemisphere. Atmos. Environ. 40 (2006) 4352-4369

Lauritzen, B., A. Baklanov, A. Mahura, T. Mikkelsen and J. H. Sørensen. Probabilistic risk assessment for long-range atmospheric transport of radionuclides. J. Envir. Radioactivity 96 (2007) 110-115

Mahura, A., A. Baklanov and J. H. Sørensen. Methodology for evaluation of possible consequences of accidental atmospheric releases of hazardous matter. Rat. Prot. Dos. 103 (2003) 131-139

Mahura, A., A. Baklanov, J. H. Sørensen. Long-Term Dispersion Modelling: Assessment of Atmospheric Transport and Deposition Patterns from Nuclear Risk Sites in Euro-Arctic Region. Journal of Computational Technologies 10 (2005a) 112-134

Mahura, A.G., A. Baklanov, J. H. Sørensen, F. L. Parker, V. Novikov, K. Brown, K. L. Compton, 2005b: Assessment of potential atmospheric transport and deposition patterns due to Russian Pacific fleet operations. Environmental Monitoring and Assessment 101 (2005b) 261-287

Mikkelsen, T., S. Alexandersen, H. Champion, P. Astrup, A. I. Donaldson, F. N. Dunkerley, J. Gloster, J. H. Sørensen and S. Thykier-Nielsen. Investigation of Airborne Foot-and-Mouth Disease Virus Transmission during Low-Wind Conditions in the Early Phase of the UK 2001 Epidemic. Atmos. Chem. Phys. 3 (2003) 2101-2110

Sørensen, J. H. Sensitivity of the DERMA Long-Range Gaussian Dispersion Model to Meteorological Input and Diffusion Parameters. Atmos. Environ. 32 (1998a) 4195-4206

Sørensen, J. H., A. Rasmussen, T. Ellermann and E. Lyck. Mesoscale Influence on Long-range Transport; Evidence from ETEX Modelling and Observations. Atmos. Environ. 32 (1998b) 4207-4217

Sørensen, J. H., D. K. J. Mackay, C. Ø. Jensen and A. I. Donaldson. An integrated model to predict the atmospheric spread of foot-and-mouth disease virus. Epidemiol. Infect. (2000) 124 577-590

Sørensen, J. H., C. Ø. Jensen, T. Mikkelsen, D. Mackay and A. I. Donaldson. Modelling the atmospheric spread of foot-and-mouth disease virus for emergency preparedness. Phys. Chem. Earth 26 (2001) 9397

Sørensen, J. H., A. Baklanov and S. Hoe. The Danish Emergency Response Model of the Atmosphere. J. Envir. Radioactivity 96 (2007) 122-129

Title	NKS NordRisk II: Atlas of long-range atmospheric dispersion and deposition of radionuclides from selected risk sites in the Northern Hemisphere
Author(s)	Ulrik Smith Korsholm[1)], Poul Astrup[2)], Bent Lauritzen[2)], Jens Havskov Sørensen[1)]
Affiliation(s)	[1)]Danish Meteorological Institute, Denmark [2)]Risø DTU, Technical University of Denmark, Denmark
ISBN	978-87-7893-314-0
Date	April 2011
Project	NKS-B / NordRisk II
No. of pages	60
No. of tables	2
No. of illustrations	55
No. of references	19

Abstract

The present atlas has been developed within the NKS/NordRisk-II project "Nuclear risk from atmospheric dispersion in Northern Europe". The atlas describes risks from hypothetical long-range dispersion and deposition of radionuclides from 16 nuclear risk sites on the Northern Hemisphere. The atmospheric dispersion model calculations cover a period of 30 days following each release to ensure almost complete deposition of the dispersed material. The atlas contains maps showing the total deposition and time-integrated air concentration of Cs-137 and I-131 based on three years of meteorological data spanning the climate variability associated with the North Atlantic Oscillation, and corresponding time evolution of the ensemble mean atmospheric dispersion.

Key words Risk assessment; long-range transport; radionuclide; pollutants; deposition

Available on request from the NKS Secretariat, P.O.Box 49, DK-4000 Roskilde, Denmark.
Phone (+45) 4677 4045, fax (+45) 4677 4046, e-mail nks@nks.org, www.nks.org